

Parash Mani Mishra

ASSESSMENT AND STABILITY ANALYSIS OF THE HEADRACE TUNNEL SHAFT SYSTEM OF SOLU DUDHKOSHI PROJECT, NEPAL

Master's thesis in Hydropower Development

Supervisor: Krishna Kanta Panthi

July 2019

Parash Mani Mishra

**ASSESSMENT AND STABILITY ANALYSIS
OF THE HEADRACE TUNNEL SHAFT
SYSTEM OF
SOLU DUDHKOSHI PROJECT, NEPAL**

Master's thesis in Hydropower Development
Supervisor: Krishna Kanta Panthi
July 2019

Norwegian University of Science and Technology
Faculty of Engineering
Department of Geoscience and Petroleum

 **NTNU**
Norwegian University of
Science and Technology

Acknowledgement

Firstly, I would like to offer my sincere gratitude to my esteemed supervisor Professor Dr. Krishna Kanta Panthi for his constant effort, suggestions and guidelines for bringing this report in this final stage. His attempt was to let this report be my own work but steered me in the right direction whenever needed.

Similarly, I would like to extend my heartfelt gratitude to my co-supervisor, Er. Bibek Neupane (Ph.D. candidate) for his persistent encouragement and constructive advice throughout this report. I would like to thank Hydro-consult Engineering Pvt. Ltd. Kathmandu Nepal, Sahas Urja Ltd. and Geophysical Research & Consultancy Service (P) Ltd Bagdole, Lalitpur for providing original drawings, geological report and other relevant data for this thesis project upon his request.

Likewise, I am highly obliged to my Hydropower Department, and Department of Geoscience and Petroleum for letting me choose this topic as my thesis work, all my batchmates (HPD, 2017) esp. Dipesh Nepal for his positive suggestions for bringing this report in this format. Also, my special thanks goes to Jeevan Maharjan for his kind proofreading.

On a personal note, I am indebted to my parents, my sisters and younger brothers who gave me the strength and supported my family back home during my abroad stay. I owe a big thanks to Indira Pokharel for encouraging me to apply for Hydropower Development as a second Masters.

Last but not the least, I am beholden to all my friends and well-wishers for their inspirations and blessings and specifically to those who have directly or indirectly co-operated with me in bringing this report at this stage.

Parash Mani Mishra

July 2019

ABSTRACT

The presence of thousands of rivers and rivulets has produced a golden opportunity to be independence in the energy sector of Nepal. The development of hydropower projects by governmental and private bodies has increased by large number recently. Solu Khola (Dudhkoshi) Hydro Electric Project (SKDKHEP) (86 MW) is one of the ongoing projects in the Solukhumbu District of Eastern Development Region of Nepal. The Solu Khola Dudhkoshi Hydroelectric project lies in the Lesser Himalaya of Okhaldhunga Window based on the Nepal Geological Map Compiled by Department of Mines & Geology 1996, which is the tectonically active zone which consists one of the intact rock gneiss and comparatively very weak rock phyllite and combination of both in its headworks, powerhouse and underground waterway system respectively. The layout planning of SKDKHEP has been studied and alternative possibilities of the tunnel section and underground powerhouse have been pointed out. Powerhouse has been suggested to be in the surface. The main purpose of this thesis is to conduct a stability analysis for the newly proposed underground waterway system.

The literature review related to the design and construction of underground openings has been studied during this thesis and some empirical, analytical and numerical approaches are included. The empirical method has been used to estimate the probable support required and the adequacy of the support has been checked and suggested in inadequate using the numerical modeling approach. The uncertainties in the rock masses has been addressed using the different data set values in analyzed section to that of actual condition as suggested by project reports. The drilling, laboratory testing, geophysical reports of the project and literature of similar works of other authors in similar geological conditions have been studied to imply the best possible rock mass parameter's value during the analysis. The Phase² software of Rocscience has been used to understand the in-situ stress regime before the excavation. The three chainages 1+900 m, 4+400 m and 5+000 m has been selected for the analysis as the representative sections with regards to varying geological condition and overburden height. No stability problems and less support requirement were observed in the first chainage analyzed due to presence of comparatively good rock type whereas the latter two chainages were observed to have more displacement and requirement of more support to obtain the desired factor of safety due to presence of weak rock.

Two alternate alignments for the penstock tunnel has been proposed considering the geological conditions to obtain the best possible alignment against the stability problems that may be encountered due to presence of sheared and weakness zones. Also, reduction of drop shafts from two to one in number is a major approach taken.

Contents

1	INTRODUCTION.....	1
1.1	BACKGROUND.....	1
1.2	OBJECTIVE AND SCOPE OF THE STUDY.....	2
1.3	METHODOLOGY OF THE STUDY.....	2
1.3.1	<i>Literature study</i>	2
1.3.2	<i>Study of Solu Dudhkoshi Hydropower Project</i>	2
1.3.3	<i>Alternative possibility</i>	3
1.4	STABILITY ANALYSIS.....	3
1.5	LIMITATION OF THE STUDY.....	3
2	ROCK MASS PROPERTIES AND DESIGN ASPECTS.....	4
2.1	ROCK MASS PROPERTIES.....	4
2.1.1	<i>Estimation of rock mass strength</i>	5
2.1.2	<i>Estimation of rock mass deformability</i>	6
2.1.3	<i>Strength Anisotropy</i>	7
2.1.4	<i>Discontinuity</i>	9
2.1.5	<i>Weakness Zones and faults</i>	10
2.1.6	<i>Weathering and alteration</i>	11
2.2	FAILURE CRITERIA.....	13
2.3	ROCK STRESSES.....	16
2.3.1	<i>Origin of rock stresses</i>	16
2.3.2	<i>Redistribution of rock stress</i>	18
2.3.3	<i>Stability problem of tunnel</i>	20
2.3.4	<i>Factors affecting the squeezing phenomenon</i>	21
2.3.5	<i>Squeezing Analysis</i>	22
2.3.6	<i>Empirical Method</i>	25
2.3.7	<i>Analytical Method</i>	26
2.3.8	<i>Assumptions of rock support interaction analysis</i>	26
2.3.9	<i>Convergent Confinement Method</i>	27
2.4	EXAMPLES FROM NEPAL :.....	31

2.4.1	<i>Kaligandaki “A” Hydroelectric Project</i>	31
2.4.2	<i>Modi Khola Hydroelectric Project</i>	32
2.4.3	<i>Chameliya Hydroelectric Project</i>	32
2.5	GROUND WATER.....	34
2.5.1	<i>Hydraulic conductivity of the rock mass</i>	34
2.5.2	<i>Problem associated with leakage and inflow and its estimation</i>	35
2.6	DESIGN ASPECTS.....	36
2.6.1	<i>General aspects</i>	36
2.7	NUMERICAL MODELING	37
2.7.1	<i>The Phase² Program</i>	37
2.7.2	<i>3D tunnel simulation using the core replacement technique in Phase2</i>	39
2.7.3	<i>Stability analysis</i>	40
3	PLANNING AND DESIGN ASPECT OF WATERWAYS	41
3.1	BACKGROUND.....	41
3.2	LINED TUNNELS:	42
3.3	UNLINED / SHOTCRETE LINED TUNNELS	42
3.3.1	<i>Prerequisite for unlined tunnels</i>	43
3.4	PLANNING AND DESIGN REQUIREMENTS.....	43
3.4.1	<i>Site Selection</i>	43
3.4.2	<i>Orientation of alignment and length axis</i>	44
3.4.3	<i>Shaping</i>	44
3.4.4	<i>Dimensioning</i>	45
3.5	DESIGN PRINCIPLES	46
3.5.1	<i>Confinement Criteria:</i>	46
3.5.2	<i>Leakage Analysis:</i>	49
4	SOLU KHOLA (DUDHKOSHI) HYDRO ELECTRIC PROJECT.....	51
4.1	GENERAL	51
4.2	PROJECT INFORMATION.....	51
4.3	GEOLOGY OF STUDY AREA	52
4.3.1	<i>Stratigraphy</i>	53

4.4 ASSESSMENT ON ROCK ENGINEERING ASPECTS.....55

 4.4.1 *Rock types and their character:*55

 4.4.2 *Joints*57

 4.4.3 *Rock mass condition along penstock alignment and powerhouse*58

4.5 ENGINEERING GEOLOGICAL CONDITIONS58

 4.5.1 *Weir Site:*.....58

 4.5.2 *Settling Basin*59

 4.5.3 *Surge Tank*59

 4.5.4 *Adit Portal*.....59

 4.5.5 *Headrace Tunnel:*.....59

 4.5.6 *Powerhouse*.....60

4.6 PRESENT DESIGN REVIEW60

 4.6.1 *Diversion Weir*61

 4.6.2 *Surface Settling Basin*61

 4.6.3 *Headrace Tunnel*.....61

 4.6.4 *Surge Shaft/Surge Tunnel*.....61

 4.6.5 *Penstock*62

 4.6.6 *Surface Powerhouse*.....62

 4.6.7 *Tailrace Canal*63

4.7 CRITICAL COMMENTS63

5 ALTERNATIVE DESIGN OF WATERWAY65

5.1 LAYOUT DESIGN65

5.2 COMPARISON67

5.3 COST COMPARISON:67

5.4 CONCLUSION.....68

6 SQUEEZING ANALYSIS AND NUMERICAL MODELING69

6.1 SQUEEZING ANALYSIS69

 6.1.1 *Empirical approach for squeezing*.....69

 6.1.2 *Semi empirical approach for squeezing*.....69

6.2 NUMERICAL MODELING.....70

6.2.1 *Elastic parameters*70

6.2.2 *Hoek-Brown parameters*70

6.2.3 *Dilation Parameter*71

6.3 ESTIMATION OF IN-SITU STRESS AT DIFFERENT SECTIONS.....71

 6.3.1 *Model setup*71

6.4 STABILITY ANALYSIS OF TUNNEL AT DIFFERENT SECTIONS71

 6.4.1 *Selection of tunnel sections for stability analysis*71

 6.4.2 *Model setup*72

 6.4.3 *Chainage 1+900 m*.....73

 6.4.4 *Chainage 4+400m*.....78

 6.4.5 *Chainage 5+000m*.....84

7 DISSCUSION91

8 CONCLUSION AND RECOMMENDATION96

8.1 CONCLUSION.....96

8.2 RECOMMENDATION.....97

APPENDIX 1.....104

APPENDIX 2.....109

APPENDIX 3.....114

List of Figures

Figure 2-1 Factors affecting tunnel stability (Panthi 2006)	4
Figure 2-2 Uniaxial Compressive Strength at different angle of schistosity plane (Panthi 2006).....	8
Figure 2-3 Discontinuity characteristics in rock mass (Panthi 2006)	10
Figure 2-4 Anderson’s classification of faults (after Braathen and Gabrielsen, 2000 and Rowland and Duebendorfer,1994) in (Panthi 2006)	11
Figure 2-5 Compressive strength of rock (left) and strength reduction in percentage (right) as a function of weathering grade (Panthi 2006)	12
Figure 2-6 Axial and Lateral normal strain with increasing deviatoric axial stress (Goodman 1989)	13
Figure 2-7 Mohr-Coulomb failure criterion with a tension cutoff (Goodman 1989)	15
Figure 2-8 Relationships between major and minor principal stresses for Hoek-Brown and equivalent Mohr-Coulomb criteria (Hoek, Carranza-Torres et al. 2002)	16
Figure 2-9 Plot of vertical stresses against depth below surface (left) and variation of ratio of average horizontal stress to vertical stress with depth below surface (right) (Hoek and Brown 1980).....	17
Figure 2-10 Stress trajectories in rock mass surrounding a circular opening (left) and tangential and radial stress distribution in elastic and non-elastic conditions (right) (Panthi 2006)	19
Figure 2-11 An illustration of squeezing in a circular tunnel (Panthi 2006)	21
Figure 2-12 Criteria for predicting squeezing ground (Singh and Singh 2006).....	23
Figure 2-13: Criteria for predicting squeezing ground conditions using rock mass number N (Goel 1994)	24
Figure 2-14 Schematic representation of Longitudinal Displacement Profile (LDP), Ground Reaction Curve (GRC) and Support Characteristics Curve (Carranza-Torres and Fairhurst 2000).....	28
Figure 2-15 Geological environment of Kaligandaki “A” and Modi Khola (Panthi 2006)	31
Figure 2-16 Rock mass condition at different chainage along headrace tunnel of Chameliya Hydroelectric Project (Basnet 2013).....	33
Figure 2-17 Squeezing in headrace tunnel of CHEP: Floor heave (left) and wall closure (right) (Basnet 2013) ...	33
Figure 2-18 Hydraulic conductivity of rock and soil (Freeze and Cherry 1979)	35
Figure 2-19 Schematics showing the interaction happening between three modes (Rocscience 2018).....	38
Figure 2-20 LDP templates to be used as an alternative to equations of LDP (Vlachopoulos and Diederichs 2009).....	40
Figure 3-1 Typical layout of underground hydropower scheme with unlined pressure shaft and tunnel (Basnet 2018)	41
Figure 3-2 Minimum rock cover for shallow seated underground opening (left) and stress situation in valley side with fault zone (right) (Broch 1984)	44
Figure 3-3 Design principles for underground openings with varying stress and directions (Nilsen and Thidemann 1993); (Broch 1984)	45
Figure 3-4 Dimensioning of two adjacent caverns (Panthi 2006)	46
Figure 3-5 Different parameters for different design criteria for unlined pressure tunnels/shafts (Note: S1 and S3 are major and minor principal stress and HWL is head water level) (Basnet 2018)	47
Figure 3-6 Design chart for finite element model. The curves run through points where the internal water pressure equals the minor principal stress in the rock mass. The pressure shaft is placed with sufficient overburden for H/d=0.7 (Broch 1984)	48
Figure 4-1 Map of Nepal showing project site	51
Figure 4-2 Google map showing different proposed components of SKDKHEP	52
Figure 4-3 Regional Geological map showing project site (Compiled by Department of Mines & Geology, 1996)	53

Figure 4-4 Outcrops and close view of Augen gnesiss at headwork (Hydro-Consult 2016) 55

Figure 4-5 Outcrop and close view of green phyllite with quartzite intercalation at Powerhouse (Hydro-Consult 2016) 56

Figure 4-6 a) Layout and b) Longitudinal section of existing Headrace Tunnel (Original), Not to scale 60

Figure 5-1 Penstock alignment (a) Layout; (b) Longitudinal section along X-X (Alternative 1) 65

Figure 5-2 Penstock alignment a) Layout; b) Longitudinal section along X-X (Alternative 2) 66

Figure 6-1 Strength factor at chainage 1+900 m (Elastic analysis). 74

Figure 6-2 Result showing displacement of 5 mm and radius of plastic zone 4 m in unsupported tunnel in chainage 1+900 m. 75

Figure 6-3 Major principal stress distribution before and after support installation at chainage 1+900 m (plastic analysis). 75

Figure 6-4 Total displacement before and after support installation for chainage 1+900 m (plastic analysis). 76

Figure 6-5 Support capacity plot for chainage 1+900 m (mean values) with obtained factor of safety. 76

Figure 6-6 Support capacity plot for chainage 1+900 m (minimum values) with obtained factor of safety. 78

Figure 6-7 Strength factor at chainage 4+400 m (Elastic analysis). 79

Figure 6-8 Result showing displacement of 36 mm and radius of plastic zone throughout the external boundary in unsupported tunnel in chainage 4+400 m. 80

Figure 6-9 Major principal stress distribution before and after support installation at chainage 4+400 m (plastic analysis). 80

Figure 6-10 Total displacement before and after support installation for chainage 4+400 m (plastic analysis). 81

Figure 6-11 Support capacity plot for chainage 4+400 m (mean values) with obtained factor of safety. 81

Figure 6-12 Support capacity plot for chainage 4+400 m (maximum values) with obtained factor of safety. 83

Figure 6-13 Support capacity plot for chainage 4+400 m (minimum values) with obtained factor of safety. 84

Figure 6-14 Strength factor at chainage 5+000 m (Elastic analysis). 85

Figure 6-15 Result showing displacement of 11.04 mm and radius of plastic zone throughout the external boundary in unsupported tunnel in chainage 5+000 m. 86

Figure 6-16 Major principal stress distribution before and after support installation at chainage 5+000 m (plastic analysis). 86

Figure 6-17 Total displacement before and after support installation for chainage 5+000 m (plastic analysis). 87

Figure 6-18 Support capacity plot for chainage 5+500 m (mean values) with obtained factor of safety. 87

Figure 6-19 Support capacity plot for chainage 4+400 m (maximum values) with obtained factor of safety. 89

Figure 6-20 Support capacity plot for chainage 5+000 m (minimum values) with obtained factor of safety. 90

Figure 7-1 Comparisons of maximum total displacement values according to the changing rock mass parameters at chainage 1+900 m. 91

Figure 7-2 Comparisons of maximum total displacement values according to the changing rock mass parameters at chainage 4+400 m. 92

Figure 7-3 Comparisons of maximum total displacement values according to the changing rock mass parameters at chainage 5+000 m. 93

Figure 7-4 Comparisons of required thickness of concrete to obtained factor of safety 1.4 at different chainages. 94

List of Tables

Table 2-1 Indirect estimation of Rock Mass strength.....	6
Table 2-2 Indirect Estimation of deformation modulus	7
Table 2-3 Classification of rock strength anisotropy (Panthi 2006).....	8
Table 2-4 Weathering classification according to (ISRM 1978) in (Panthi 2006).....	12
Table 2-5 Squeezing behavior (Jethwa, Singh et al. 1984).	25
Table 3-1 Recommended factor of safety against hydraulic jacking or uplift (Benson 1989)	50
Table 4-1 Litho-stratigraphical sequence of the project area.....	54
Table 4-2 Summary of second phase Uniaxial Compression test near powerhouse location	56
Table 4-3 Properties of joints in Phyllite near powerhouse.....	57
Table 4-4 Properties and location of expected shear zones.....	63
Table 4-5 Rock Mass distribution in headrace tunnel (Hydro-Consult 2016).....	64
Table 5-1 Comparison of salient features of original design with new alternatives.....	67
Table 6-1 Assessment of squeezing using empirical approach.....	69
Table 6-2 Assessment of squeezing using semi empirical approach.	69
Table 6-3 Input parameters for Phase2 analysis for each tunnel sections for elastic and plastic analysis.	72
Table 6-4 The average rock mass parameter value set for analysis of chainage 1+900 m.....	73
Table 6-5 The taken rock mass parameter value for further analysis according to the decrement of rock mass properties value.....	77
Table 6-6 The average rock mass parameter value set for analysis of chainage 4+400 m.....	78
Table 6-7 The taken rock mass parameter value for further analysis according to the increment and decrement of rock mass properties value.....	82
Table 6-8 The average rock mass parameter value set for analysis of chainage 5+000 m.....	84
Table 6-9 The taken rock mass parameter value for further analysis according to the increment and decrement of rock mass properties value.....	88
Table 7-1 Total displacement values of different data set along with displacement percentage of chainage 1+900 m.	91
Table 7-2 Total displacement values of different data set along with displacement percentage of chainage 4+400 m.	92
Table 7-3 Total displacement values of different data set along with displacement percentage of chainage 5+000 m.	93
Table 7-4 Comparisons of required thickness of concrete to obtained factor of safety 1.4 at different chainages.	93
Table 7-5 Possible support requirement at different section of tunnel alignment.	94

List of Abbreviation

BH	Bore Holes
CCM	Convergence-Confinement Method
CHEP	Chameliya Hydroelectric Project
CHP	Chilime Hydroelectric Project
CSIR	Council of Scientific and Industrial Research
DDERT	2D Electrical Resistivity Tomography
DK	Dware Khola Formation
DPR	Detailed Project Report
ERT	Electric Resistivity Tomography
FEM	Finite Element Method
Gp	Ghan pokhara Formation
GRC	Ground Reaction Curve
GSI	Geological Strength Index
GWh	Giga Watt Hour
Hg	Himal Gneiss
HRT	Headrace Tunnel
HWL	Highest Water Level
ISRM	International Society for Rock Mechanics
KHP	Khimti I Hydropower Project
kWh	Kilo Watt Hour
LDP	Longitudinal Displacement Profile
MASW	Multi-Channel Analysis of Surface Waves
MBT	Main Boundary Thrust
MCT	Main Central Thrust
MFT	Main Frontal Thrust
MKHP	Modi Khola Hydroelectric Project
MPa	Mega Pascal
MW	Mega Watt
NEA	Nepal Electricity Authority

Pg	Panglema Quartzite
RMR	Rock Mass Rating
RoR	Run of River
RQD	Rock Quality Designation
SCC	Support Characteristics Curve
SKDKHEP	Solu Khola (Dudhkoshi) Hydro Electric Project
SRF	Strength Reduction Factor
SRT	Seismic Refraction Tomography
St	Seti Formation
STDS	South Tibetan Detachment System
UCS	Uniaxial Compressive Strength
Ul	Ulleri Formation
UTHP	Upper Tamakoshi Hydroelectric Project
V.D.C	Village development Committee

1 INTRODUCTION

1.1 Background

Nepal is a mountainous landlocked country with over 6000 rivers (including rivulets and tributaries) flowing from higher Himalayas towards the Indian ocean (WEPA 2019). The presence of those continuous flowing rivers create enormous opportunities for private and government sector of Nepal for development of various hydroelectric projects. The knowledge is clear cut that the development rate of a country like Nepal can be geared up with adequacy of renewable source of energy which can be produced in cheaper rate as to maintain the balanced economic flow. The presence of steep topography in the Northern reign of Nepal provides the good head helping in the production of higher capacity projects even with the less discharge of the rivers which has been luring private sectors for hydropower development in revolutionary numbers.

Despite being attractive scheme for the development of the hydropower there are many challenges during the construction of such projects. The rugged slope of the Nepal Himalaya, the presence of jointed rock mass, sheared and weakness zones formed due to the collision of Indian Plate with the Eurasian Plate make the process of planning safer and economic project a complex task to deal with. Despite the presence of fragile geology, more construction period and a bit high cost, the investors are convinced about the long-term stability of underground waterway system, settling basin and powerhouse. Though the design and supervision during construction needs higher degree of consciousness, knowledge and prompt decision making capacity, underground space is being more used while the development of hydropower in Nepal.

For this thesis, Solu Khola (Dudhkoshi) Hydro Electric Project (SKDKHEP) has been taken for the study. The project lies in Solukhumbu district of Sagarmatha zone in Eastern Development Region of Nepal. It is an 86 MW Run of River (RoR) type hydroelectric project located at Dudhkaushika and Necha-Salyan Rural Municipalities (former Tingla, Kangel and Panchan V.D.Cs). This project has a design discharge of $17.05 \text{ m}^3/\text{s}$ and utilizes gross head of 613.2 m and net head of 598.09 m between proposed intake at Solu Khola and Powerhouse at Dudhkoshi River. Gravity type weir is being proposed having total length of 31.8m. Four bays are proposed for surface settling basin with dimensions 85.0 m x 9.5 m x 4.5 m. The headrace tunnel has a total length of 4259.0 m among which the penstock pipe is 2085 m which includes drop shaft 1 with length 224.18 m horizontal section 1 of length 715.65, drop shaft 2 of length 199.61 m and horizontal section 2 of length 926.94 m. In this thesis, the study of the waterway system is carried out as the title suggest “ASSESSMENT AND STABILITY ANALYSIS OF THE HEADRACE TUNNEL SHAFT SYSTEM OF SOLU DUDHKOSHI PROJECT, NEPAL”.

1.2 Objective and scope of the study

The main objective of this study is:

1. Planning, optimization, and analysis of the waterway system of SKDKHEP.

This thesis also covers the following aspects:

1. Literature review on the planning and design aspects of the waterway system for hydropower project.
2. Literature review on the engineering geological and mechanical properties of the rock mass, prevailing design aspects of tunnels and shafts.
3. Describe the existing features of the Solu Dudhkoshi Hydropower Project and highlight the engineering geological conditions along the waterway system.
4. Carry out alternative layout design of a waterway system with reduced penstock length by introducing new alignments for penstock tunnel and shafts.
5. Compare the alternative design with the existing one and discuss.
6. Carry out stability assessment of the penstock tunnel, penstock shaft and headrace tunnel using empirical, analytical and numerical modeling methods.
7. Discuss and conclude the work.

1.3 Methodology of the study

The following methodology has been followed in this thesis:

1.3.1 Literature study

Different search engines like google.scholar and Oria were used for the literature review. NTNU library, Hydropower book series, past master's thesis and Rocscience website were other places from where necessary literatures were obtained. The literature review was focused on the rock mass properties, Norwegian design principle for unlined waterway system, different types of stability problems encountered in underground waterway system and different approaches for designing the underground excavations.

1.3.2 Study of Solu Dudhkoshi Hydropower Project

Information regarding the project was obtained from the Detail geological report of SKDKHEP, geotechnical reports and geophysical report of the SKDKHEP conducted by Hydro-consult Engineering. Additional information has been gathered from ICRS report of drilling and material testing along with literatures from previous works along the Nepal Himalaya for similar rock types and geological conditions to determine the properties of the rock.

1.3.3 Alternative possibility

Two alternative designs have been proposed for the penstock tunnel with regard to the available geological information. The placement of the powerhouse cavern has been varied by those alternatives.

Option 1:

The alignment is designed to cross all the sheared zones by the vertical shaft and so that the penstock alignment is not being affected by any weak zones. The powerhouse is proposed underground, and tailrace tunnel is introduced.

Option 2:

The total length of vertical shaft is decreased as compared to that of original one and it crosses all the weak zones in the shaft. The slope of penstock tunnel is increased, and powerhouse is kept at its original place.

1.4 Stability analysis

The proposed headrace tunnel and penstock tunnel's stability has been checked using the numerical modeling. The used of different software such as Phase2, RocData1 has been used to analyze the stability of waterway system.

1.5 Limitation of the study

This study is carried out depending on the literature provided and software generated rock mass parameters for stability analysis with discussion with supervisor and co-supervisor on those data. Those input parameters may have some uncertainty due to lack of field verification which were tried to incorporate by using different data set combination during the analysis. Further, the field stresses developed around the underground location was not found to be more reliable due to lack of instrumentation and thus was generated by using rock mass parameters and developed using modeling. Moreover, any data related to ground water flow could not be found on those provided reports. It would have been far better to have at least one field visit to the project site to test the rock strength and rock stresses but was not possible because of time and money constraints. However, best attempt has been made for the pure academic study purpose.

2 ROCK MASS PROPERTIES AND DESIGN ASPECTS

2.1 Rock mass properties

Introduction

In engineering field, it is very crucial to know the difference between rock and rock mass. Rock by definition is, a naturally composed aggregate of one or more minerals, and the properties of the rock will depend of the mineral composition, size, shape, orientation and binding forces between the minerals (Nilsen and Thidemann 1993). However, rock mass is a heterogeneous construction material consisting of the intact rock, all joints and other discontinuities. The presence of these structures will therefore have influence on the properties of the material which is being excavated and in which the tunnel or cavern is located (Nilsen and Palmström 2000). For the analysis of underground opening, reliable estimate of strength and deformation characteristic of rock masses are required (Hoek 2007).

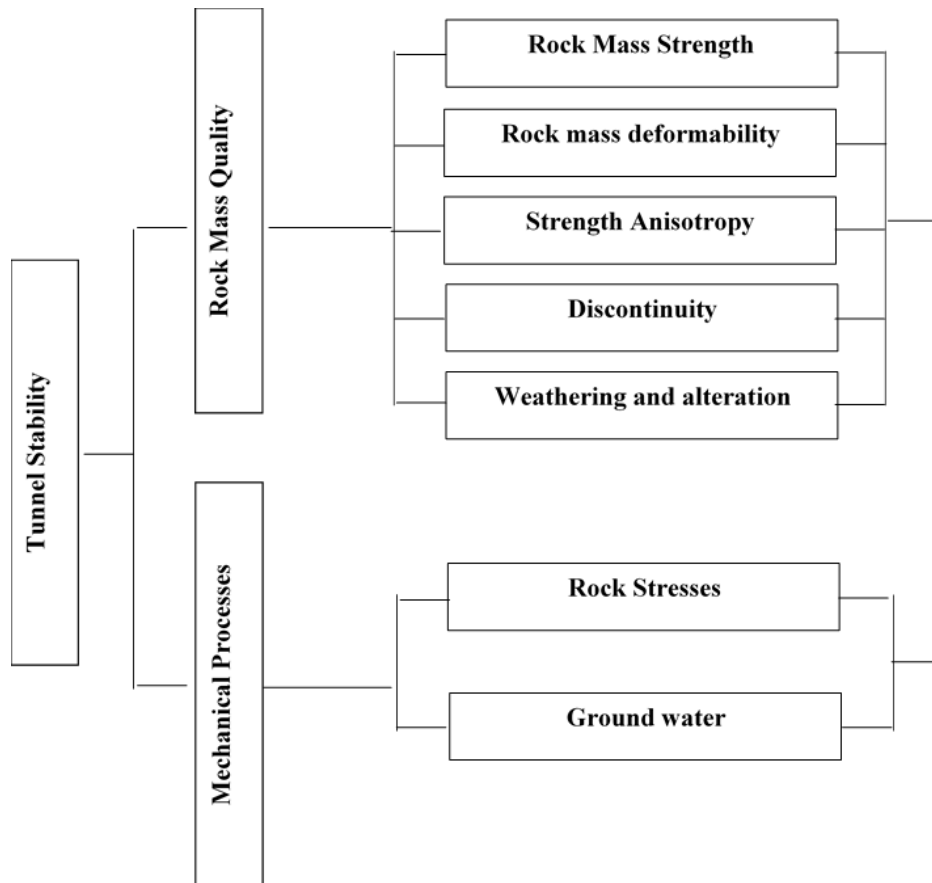


Figure 2-1 Factors affecting tunnel stability (Panthi 2006)

(Panthi 2006) emphasizes that the rock mass quality along with mechanical processes will have a final effect in the stability of underground excavations. Besides, the tunnel stability is influenced by project specific characteristics such as size, shape, location and its orientation. So, it is very crucial to revise the main properties of rock mass as well as the stability factors stated by (Panthi 2006).

(Nilsen and Thidemann 1993) defines rock properties for the following specifications:

Physical properties

Physical nature of the rock will be determined by the physical features of the rock mass like hardness, density and porosity. Apart from these, sonic wave velocity also helps to determinate the rock quality.

- Weathering of rocks

It involves physical breakdown and/or chemical alteration of rock at or near earth's surface. Physical weathering is the result of four important processes undergone known as frost wedging, expansion due to a change in stress regime, thermal expansion and dynamic activity. Chemical weathering results due decomposition and dissolution. Both acts together but the intensity may vary depending upon the environment and climatic regime. (Thapa 2018)

- Jointing in rock masses

The location of joints and discontinuities have a great influence on in situ rock mass. Joints do not transfer tension forces like compressive and shear forces. Along with the identification of behavior of rock mass the type and pattern of the joints is necessary.

- Weakness Zones and Faults

Weakness zones typically observed in trenches and gorges on the surface has its extension deep into the bedrocks. So, it is hard to avoid such weakness zones but the study of their orientation and extent into the bedrock will give us the idea to locate the tunnel depth and position.

2.1.1 Estimation of rock mass strength

The rock mass strength can be defined as an ability of rock mass to withstand stress and deformation (Panthi 2006). The strength and deformation of an intact rock sample are different from the strength and deformation of the rock mass. Discontinuities, foliation or schistosity planes, and the orientation of these features relative to the direction in which the strength is assessed, often influences the rock mass strength. The intact rock specimen is usually strong and homogeneous, with few discontinuities, and therefore does not represent the strength of the total rock mass (Panthi 2006). Estimation of the rock mass strength is essential in almost any type of analysis used for the design of underground excavations (Hoek 2007).

A few attempts have been made to test the strength of the intact rock in the field. A few cases involved the use of special equipment designed for that purpose; even triaxial testing was possible according to (Hoek and Hudson 1993). Mostly, the intact rock strength is estimated through testing of rock samples collected in field. Common test methods are the uniaxial

compressive test, triaxial test and point load strength test (Nilsen and Thidemann 1993). However, the strength of the rock mass is difficult to estimate directly in field or by laboratory tests. So, many authors have suggested empirical relationships for the estimation of rock mass strength (σ_{cm}), which is presented in Table 2-1.

Typically, these methods include the intact rock strength (σ_{ci}) and a rock mass characterization parameter, such as the Q-value or RMR (Rock Mass Rating).

Table 2-1 Indirect estimation of Rock Mass strength

Proposed by	Rock mass strength and its relationship with rock mass classifications
Beiniawski (1993)	$\sigma_{cm} = \sigma_{ci} * \exp\left(\frac{RMR - 100}{18.75}\right)$
Palmström (1995)	$\sigma_{cm} = RMi = \sigma_{ci} * JP$
Aydan et al. (1997)	$\sigma_{cm} = 0.0016RMR^{2.5}$
Hoek et al. (2002)	$\sigma_{cm} = \sigma_{ci}s^a = \sigma_{ci} * \left[\exp\left(\frac{GSI - 100}{9 - 3D}\right)\right]^a$
Barton (2002)	$\sigma_{cm} = 5\gamma * \left[\frac{\sigma_{ci}}{100} * Q\right]^{\frac{1}{3}}$
(Panthi 2017)	$\sigma_{cm} = \frac{\sigma_{ci}^{1.5}}{60} \text{ for schistose rock mass}$
(Panthi 2017)	$\sigma_{cm} = \frac{\sigma_{ci}^{1.6}}{60} \text{ for brittle rock mass}$

where JP is the joint parameter in the RMi system, s and a are material constants related to the Hoek-Brown failure criteria and γ is the rock density (g/cm^3)

2.1.2 Estimation of rock mass deformability

Rock mass tends to deform on application of load. The load applied results in deformation on the rock mass which can be characterized by a modulus. The Commission of Terminology of (ISRM 1975b) defines modulus of deformation (E_m) as the ratio of stress to corresponding strain during loading of rock mass including elastic and inelastic behavior and the modulus of elasticity, E_{ci} as the ratio between applied stress and corresponding strain with in the elastic limit. Since jointed rock mass does not have elastic behavior, the use of modulus of deformation is more relevant than the use of modulus of elasticity.

The measurement of modulus of deformation can be done in field by different methods, such as plate loading test (PLT), Flat Jack Test (FJT), Dilatometer Test (DT), Goodman Jack Test (GJT) Radial Jack Test (RJT) etc. (Palmström and Singh 2001). But the major drawbacks of these in situ methods are being costly and demanding (Panthi 2006). In addition to this, different tests may give different values (Nilsen and Palmström 2000). Thus, different empirical formulations were proposed by several authors presented in Table 2-2 where the modulus is estimated from the relevant parameters.

Table 2-2 Indirect Estimation of deformation modulus

Proposed by	Empirical relationship
Beiniawski (1978)	$E_m = 2RMR - 100$
Palmström (1995)	$E_m = 5.6RMI^{0.375}$
Hoek et al. (2002)	$E_m = \left(1 - \frac{D}{2}\right) \sqrt{\frac{\sigma_{ci}}{100}} 10^{\frac{GSI-10}{40}}$
Barton (2002)	$E_m = 10 * Q_c^{\frac{1}{3}} = 10 * \left[\frac{Q \cdot \sigma_{ci}}{100}\right]^{\frac{1}{3}}$
Hoek and Diederichs (2006)	$E_m = E_{ci} * \left[0.02 + \frac{(1 - \frac{D}{2})}{1 + e^{(60+15D-GSI)/11}} * Q\right]^{\frac{1}{3}}$
(Panthi 2006)	$E_m = E_{ci} * \frac{\sigma_{cm}}{\sigma_{ci}}$

2.1.3 Strength Anisotropy

Strength anisotropy is the variation of compressive strength according to the direction of loading, (Goodman 1989). He also explained that sedimentary and metamorphic rocks commonly show strength anisotropy because of bedding, foliation and schistosity. (Panthi 2006), claims that the rocks of Himalaya are highly directional in strength and deformability. It is more likely that the thin bands of very weak, highly sheared and thinly foliated rocks such as slate, phyllite and schist are intercalated within the bands of relatively strong and brittle rocks such as gneiss, quartzite and dolomite. This ultimately cause several stability problems during tunneling. Figure 2-2 shows the effect of anisotropy on the uniaxial compressive

strength of different rock types in Himalayas and other part of world. The figure indicates that the rock strength is smallest when the schistosity plane is inclined with an angle at around 30 degrees from the direction of loading and is highest when the schistosity plane is oriented perpendicular to the direction of loading. So, false impression of an isotropic material can occur if the compressive strength is measured on core drilled parallel and normal to the schistosity (Panthi 2006).

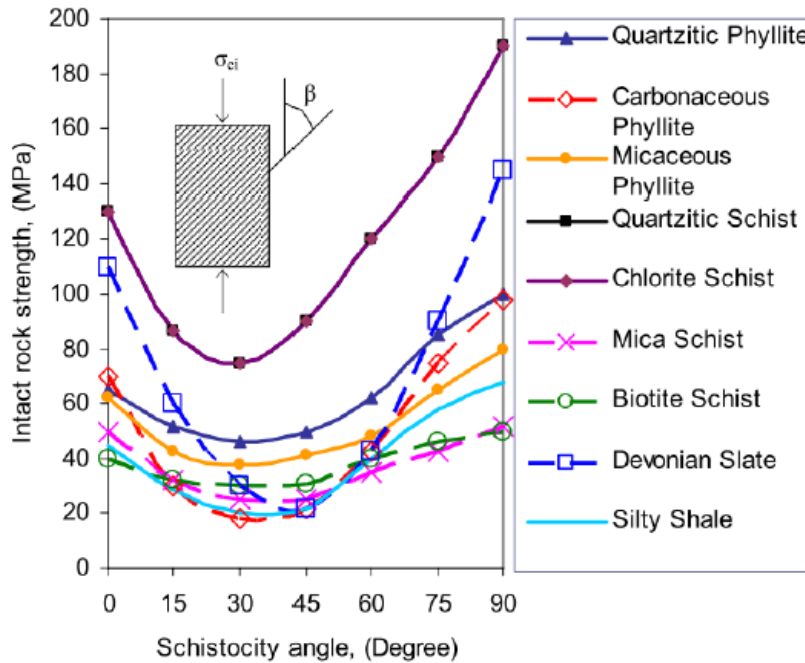


Figure 2-2 Uniaxial Compressive Strength at different angle of schistosity plane (Panthi 2006)

Furthermore, it may not always be possible to determine the compressive strength of anisotropic rocks, as it is not always feasible to drill cores of rock samples oblique to the schistosity plane. As an overcome to this, point load test could be a reliable method to determine the grade of strength anisotropy, because in this method point load strength is tested both normal to and parallel with the schistosity plane. (Panthi 2006) classifies the strength anisotropy of rock mass in five categories based on maximum and minimum anisotropy index as shown in Table 2-3.

Table 2-3 Classification of rock strength anisotropy (Panthi 2006)

Classification	Strength anisotropy index I_a	Description
Isotropic rock	1-1.2	< 10 % platy/prismatic minerals, may be randomly orientated <i>Rock types: Igneous rocks and very high-grade metamorphic rocks (diomite, granite, gabbro, quartzite, granitic gneiss, granulite, etc.)</i>

Slightly anisotropic	1.2-1.5	10-20% platy/prismatic minerals, showing compositional layering. <i>Rock types: High grade metamorphic rocks and some strong sedimentary rock (quartz-feldspatic gneiss, mylonite, marble, migmatite, sandstone, limestone etc.)</i>
Moderately anisotropic	1.5-2.5	20-40% platy/prismatic minerals, with distinctly visible foliation plane. <i>Rock Types: Medium-high grade metamorphic rocks (mica gneiss, quartzitic schist, mica schist, biotite, schist, etc.)</i>
Highly anisotropic	2.5-4.0	40-60% platy/prismatic minerals, very closely foliated. <i>Rock Types: Low-medium grade metamorphic rocks (phyllite, silty alate, etc.)</i>
Extremely anisotropic	> 4.0	>40-60% platy/prismatic minerals, very closely foliated. <i>Rock Types: Low grade metamorphic and argillaceous sedimentary rock (slate, carbonaceous phyllite, shale, etc.)</i>

2.1.4 Discontinuity

The term discontinuity is used as a collective term for all fractures and structural features. According to (ISRM 1978) discontinuity is a general term for any mechanical discontinuity in the rock mass that has zero or low tensile strength. (Nilsen and Palmström 2000) defines discontinuity as a structural or geological feature that alters the homogeneity of the rock mass. It is a collective term for most types of joints, weak bedding planes, weak schistosity planes, weakness zones and faults. In an engineering context the discontinuities are possibly the single most important factor governing the mechanical properties of the rockmass (Halseth 2018).

The properties of rock mass are largely influenced by the presence of structural features which could be different from intact rock. Some of the structural features are described below.

Bedding Plane

Bedding planes are the highly persistence features that divide the rock into bed or strata basically in sedimentary rocks. It may contain parting material of different grain size from sediment forming the rock mass or may have been partly healed by low-order metamorphism. In either of these two cases, there would be cohesion between the beds; otherwise, shear resistance on bedding planes would be purely frictional. Arising from the depositional process, there may be a preferred orientation of particles in the rock, giving rise to planes of weakness parallel to bedding (Basnet 2013).

Jointing of rock mass

They frequently form parallel to bedding planes, foliations or slaty cleavage, where they may be termed bedding joints, foliation joints or cleavage joints. Joints are the most common discontinuities in the rock mass and are of different types. The terms used for the different joint types generally depends on the size and composition (crack, fracture, seam etc.) or their origin (tectonic joints, exfoliation joints, bedding joints, foliation joints etc.) (Nilsen and Palmström, 2000). Joint of a certain preferred orientation are called a joint set, and two or more joint sets in an area form a joint pattern or joint system. Sedimentary rocks often contain two sets of joints approximately orthogonal to each other and to the bedding planes (Brady and Brown, 2007). Figure 2-3 shows the different characteristics of the joints that can be identified during the field mapping. Joint orientation can be presented with the help of joint rosette and stereographic projection after the field mapping are done.

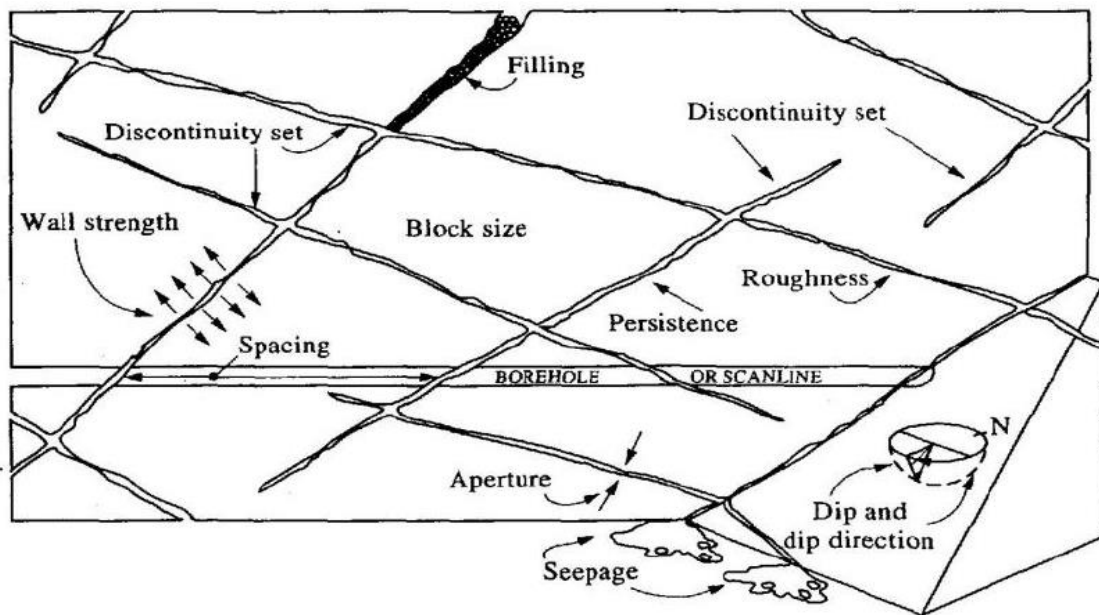


Figure 2-3 Discontinuity characteristics in rock mass (Panthi 2006)

The most influencing joint characteristics regarding underground stability are:

- Surface Roughness
- Alteration and Filling
- Wall Strength
- Spacing and block size (Panthi 2006)

2.1.5 Weakness Zones and faults

The lineaments in the bed rock that could be noticed even from far are the weakness zone. The distance between parallel lineaments can be in the order of hundreds and thousands of meters. (Nilsen and Palmström 2000) define a weakness zone as, "a part of the rock mass where the mechanical properties are significantly lower than those of the surrounding rock mass". This includes structures such as faults, shear and shear zones, thrust zones, weak mineral layers etc.

Such zones require special attention as they can have a major impact on the tunnel stability as well as the excavation process (Panthi 2006). Problems connected to such zones are for instance flowing and running ground, swelling pressure and highwater inflow (Nilsen and Palmström 2000). There are mainly two types of weakness zones (Nilsen and Thidemann 1993);

- beds or layers of particularly weak rock in a series of sedimentary or metamorphic rocks,
- a zone of crushed and/or altered rock formed by faulting or other tectonic movements

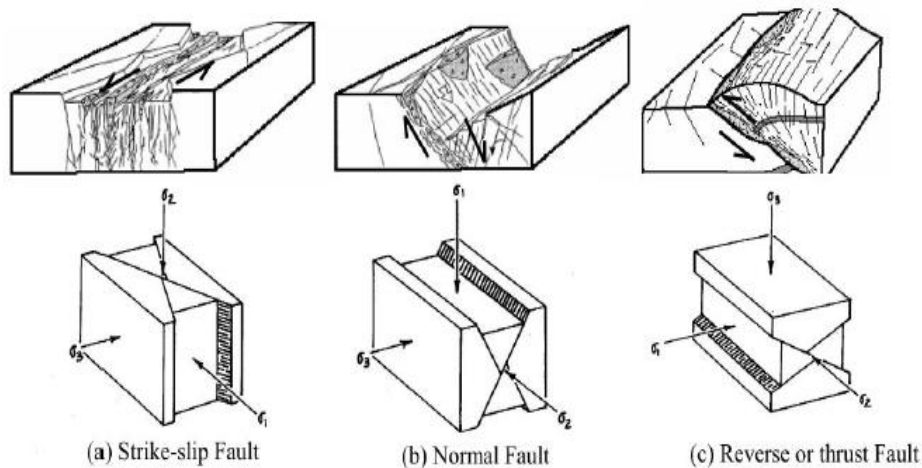


Figure 2-4 Anderson's classification of faults (after Braathen and Gabrielsen, 2000 and Rowland and Duebendorfer, 1994) in (Panthi 2006)

Many of the zones of weak material are regarded as weakness zones only if they are surrounded by other, stronger rock masses. (Nilsen and Palmström 2000) Fault is also a weakness zone where identifiable shear displacement has taken place. They may be identified by the relative displacement of the rock on opposite side of the fault plane. The direction of these displacements is often used to classify faults.

The filling materials within weakness zones are called gouge materials. The main gouge materials are often coarse rock fragments. But some minerals may be altered or changed into new minerals and form clay minerals. Some clay minerals, e.g. smectites, have a swelling capacity when exposed to water. Faults containing swelling clay are a major risk to tunneling, especially for hydropower tunnels. The reason is that during the tunneling works, existing clay may gradually dry out. The potential stability problem can then be seriously underestimated as the dry clay often has relatively high strength and it is often nearly impossible to distinguish swelling materials from non-swelling materials. (Nilsen and Thidemann 1993); (Nilsen and Palmström 2000).

2.1.6 Weathering and alteration

Weathering refers to the various processes of physical disintegration and chemical decomposition of the rock material because of exposure to the atmosphere and hydrosphere (Halseth 2018). The physical disintegration involves mechanical breakdown of the rock mass, leading to fragmentation, opening of joints, formation of new joint surfaces and fracturing of

individual mineral grains (Nilsen and Palmström 2000). Generally, weathering process in the rock mass starts from its discontinuities and migrates to the rock minerals. The degree of weathering usually decreases with depth below the surface. Weathering can eventually cause decomposition of rock minerals into clay minerals. Weathering reduces properties such as rock mass strength, deformability, slaking durability (resistance against disintegration when hydrated) and frictional resistance. At the same time, it may increase permeability considerably (Panthi 2006). (Panthi 2006) presented the six categories of weathering grades that are defined by ISRM (1978) which are shown in Table 2-4 below:

Table 2-4 Weathering classification according to (ISRM 1978) in (Panthi 2006)

Term	Description of rock mass conditions	Weathering grade
Fresh rock	No visible sign of rock material weathering; perhaps slight discolouration on major discontinuity surfaces.	I
Slightly weathered	Discoloration indicates weathering of rock material and discontinuity surfaces. All the rock material may be discoloured by weathering and may be somewhat weaker externally than in its fresh conditions.	II
Moderately weathered	Less than half of the material is decomposed and/or disintegrated to a soil. Fresh or discoloured rock is present either as a continuous framework or as corestones.	III
Highly weathered	More than half of the rock material is decomposed and/or disintegrated to a soil. Fresh or discoloured rock is present either as a discontinuous framework or as corestones.	IV
Completely weathered	All rock material is decomposed and/or disintegrated to soil. The original mass structure is still largely intact.	V
Residual soil	All rock material is converted to soil. The mass structure and material fabric are destroyed. There is a large change in volume, but the soil has not been significantly transported.	VI

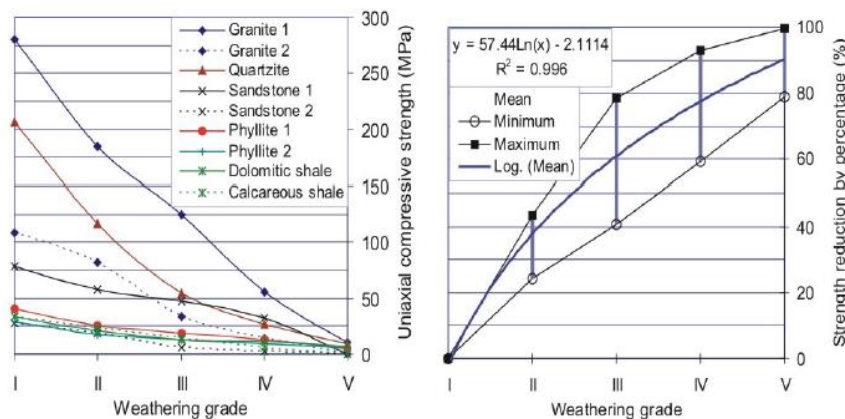


Figure 2-5 Compressive strength of rock (left) and strength reduction in percentage (right) as a function of weathering grade (Panthi 2006)

2.2 Failure Criteria

The term failure, when used in engineering context indicates to the loss of ability to perform the intended function, but in general failure implies to complete loss of integrity in a rock sample. For the engineering design purpose, it is useful to record the peak stress values which is point D seen in Figure 2-6. In addition, the compression tests don't have to end in rupture at that point and could proceed to point E (Figure 2-6) or beyond, depending if the loading system is very stiff or not. When tested on a stiff system the rock will exhibit a complete stress-strain curve because the system responds to a gradual deterioration in load carrying capacity through an automatic reduction in the applied load (Goodman 1989). Several failure criteria have been developed over the years. Among them widely used theoretical failure criteria are 'Mohr-Coulomb' and 'Hoek-Brown' (Ulusay and Hudson 2012). In both criteria only major and minor principal stresses are taken into consideration while intermediate stresses are neglected. It is remarkable that, failure criterion is limited to intact rock material because stability in tunneling is also result of natural joints and cracks due to blasting. (Nilsen and Thidemann 1993).

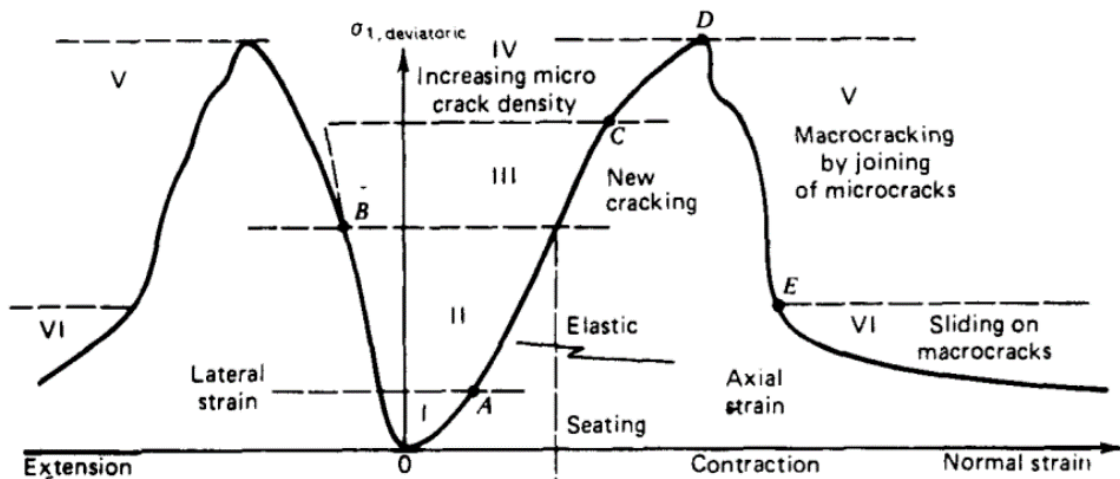


Figure 2-6 Axial and Lateral normal strain with increasing deviatoric axial stress (Goodman 1989)

Hoek-Brown Failure Criteria:

This criterion was developed as an attempt for providing the input data in the analysis of the underground excavations in hard rock. It was derived from the results of the research into the brittle failure of the intact rock by Hoek and on model studies of jointed rock mass by Brown. (Hoek, Carranza-Torres et al. 2002) In terms of principal stress relationship, the original Hoek-Brown criterion is given as equation:

$$\sigma'_1 = \sigma'_3 + \sigma_{ci} \left(m \frac{\sigma'_3}{\sigma_{ci}} + s \right)^{0.5} \quad 2.1$$

Where σ'_1 and σ'_3 are the major and minor effective principal stresses at failure, σ_{ci} is the uniaxial compressive strength of the intact rock material and m and s are material constants, where $s = 1$ for intact rock.

(Hoek 1990) discussed the derivation of equivalent friction angles and cohesive strengths based on the tangents to the Mohr envelope derived by Bray. The shape of principal plot or the Mohr envelop could be adjusted by inserting a variable 'a' in place of the square root term in above equation and thus concept of Generalized Hoek- Brown criterion was developed and is expressed as (Hoek, Carranza-Torres et al. 2002);

$$\sigma'_1 = \sigma'_3 + \sigma_{ci} \left(m_b \frac{\sigma'_3}{\sigma_{ci}} + s \right)^a \quad 2.2$$

where m_b is a reduced value of the material constant given by m_i and is related as;

$$m_b = m_i \exp \left(\frac{GSI - 100}{28 - 14D} \right) \quad 2.3$$

s and a are constants for the rock and given by;

$$s = \exp \left(\frac{GSI - 100}{9 - 3D} \right) \quad 2.4$$

$$a = \frac{1}{2} + \frac{1}{6} \left(e^{-\frac{GSI}{15}} - e^{-\frac{20}{3}} \right) \quad 2.5$$

Where 'D' is the factor that depends upon the degree of disturbance to which the rock mass has been subjected by blast damage and stress relaxation, varying from 0 (for undisturbed in situ rock masses) to 1 (for very disturbed rock masses as shown in Appendix 2-3). (Hoek, Carranza-Torres et al. 2002)

Mohr-Coulomb Failure Criteria

Mohr-Coulomb criterion is the simplest and best-known criterion of failure for rocks. It consists of a linear envelope tangent to all Mohr's circles representing critical combinations of principal stresses. The ultimate stress σ_1 and the confining pressure σ_3 can be represented by Mohr's circle in a $\sigma - \tau$ diagram (Li 2015). It is expressed in terms of normal and shear stresses on the plane represented by the point of tangency of a Mohr circle with the envelop and is expressed as;

$$\tau_p = c + \sigma_n \tan \phi \quad 2.6$$

where, ϕ is called the angle of internal friction which describes the rate of increase of peak strength with normal stress (σ_n). τ_p is the peak shear stress, or shear strength and c is cohesion or residual shear strength (Goodman 1989).

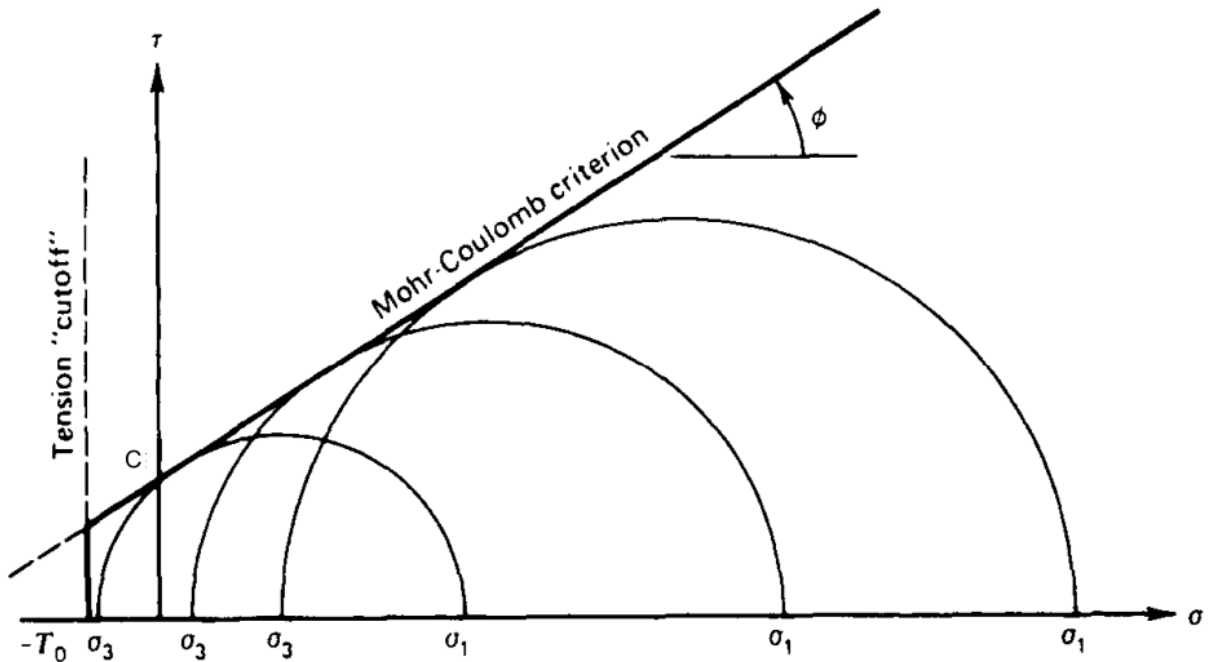


Figure 2-7 Mohr-Coulomb failure criterion with a tension cutoff (Goodman 1989)

Failure occurs when the applied shear stress less the frictional resistance associated with the normal stress on the failure plane becomes equal to a constant of the rock, c . However, this equation loses its physical significance when the value of σ_n crosses into tensile region as it would not be rational to consider the frictional resistance linked with tensile stress. As a simplified solution to that, it could be used by extrapolating the Mohr-Coulomb line into the tensile region to the point where minor principle stress (σ_3) becomes equal to the uniaxial tensile strength $-T_0$, and σ_3 can never be less than $-T_0$ which is shown in Figure 2-7 (Goodman 1989)

Relation between Hoek-Brown and Mohr-Coulomb Failure Criteria

Most of the available geotechnical software are still designed in terms of Mohr-Coulomb failure criteria so it is necessary to determine equivalent friction angles and cohesive strengths for each rock mass and stress range. For this purpose, an average linear relationship is fitted to the curve generated by solving equation 2.2 for a range of minor principle stress values defined by $\sigma_t < \sigma_3 < \sigma'_{3max}$, as shown in Figure 2-8 and fitted by balancing the areas above and below the Mohr-Coulomb plot. σ_t is the tensile strength and σ'_{3max} is the maximum confining stress over which the relationship is considered and has to be determined for each case (Hoek, Carranza-Torres et al. 2002). While selection is done among these two methods, it is worthy to note that Mohr-Coulomb failure criteria is applicable only for rock mass having one or two joint sets while Hoek-Brown criterion is applied for the other cases.

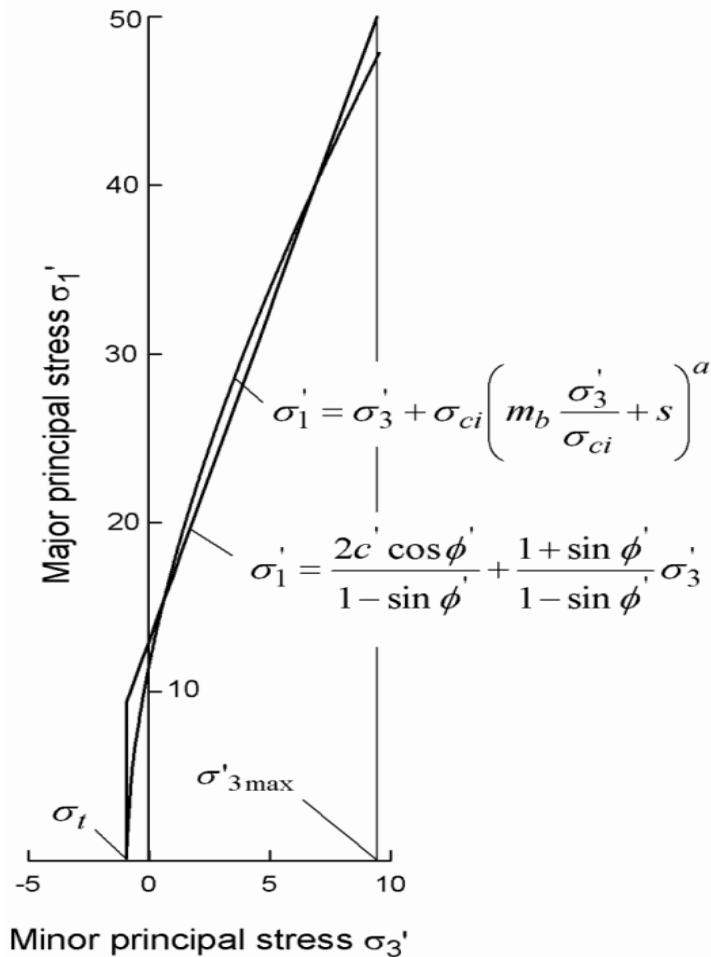


Figure 2-8 Relationships between major and minor principal stresses for Hoek-Brown and equivalent Mohr-Coulomb criteria (Hoek, Carranza-Torres et al. 2002)

2.3 Rock Stresses

The design of an underground structure in rock mass differs from other types of structural design in the nature of loads operating in the system. For an underground rock structure, the rock medium is subject to initial stress prior to excavation. The final, post-excavation state of stress is the result of initial state of stress and stresses induced by excavation. Since induced stresses are directly related to the initial stresses, specification and determination of the pre-excavation state of stress is a key to any design analysis (Basnet 2013).

The stability of an underground excavation will depend on the rocks ability to sustain failure induced by the stresses around the opening. Tunnels passing through areas of high rock cover (overburden) may be subject to instabilities related to induced rock stresses. (Panthi 2012)

2.3.1 Origin of rock stresses

According to (Nilsen and Thidemann 1993) virgin rock stress have following components

- Gravitational stresses
- Topographic stresses

- Tectonic stresses
- Residual stresses

Gravitational stresses

Rock stresses originated from the effect of gravity is termed as gravitational stresses. Due to gravity, there are two components of the gravitational stresses i.e. horizontal and vertical components. When surface is horizontal, the vertical gravitational stress at a depth z is expressed as:

$$\sigma_v = \sigma_z = \gamma \times H \tag{2.7}$$

But, if the rock mass is elastic, and having a Poisson’s ratio ν , the horizontal stresses induced by gravity are expressed as;

$$\sigma_h = \sigma_x = \sigma_y = \frac{\nu}{1 - \nu} \times \gamma \times H \tag{2.8}$$

Furthermore, the total horizontal stress is expressed as (Basnet 2013);

$$\sigma_h = \frac{\nu}{1 - \nu} \times \gamma \times H + \sigma_{tec} \tag{2.9}$$

Where, σ_v and σ_h are the vertical and horizontal stresses in MPa, σ_{tec} is the tectonic stresses due to plate tectonic movement, γ is the specific weight of rock mass in MN/m^3 and H is overburden depth in meters.

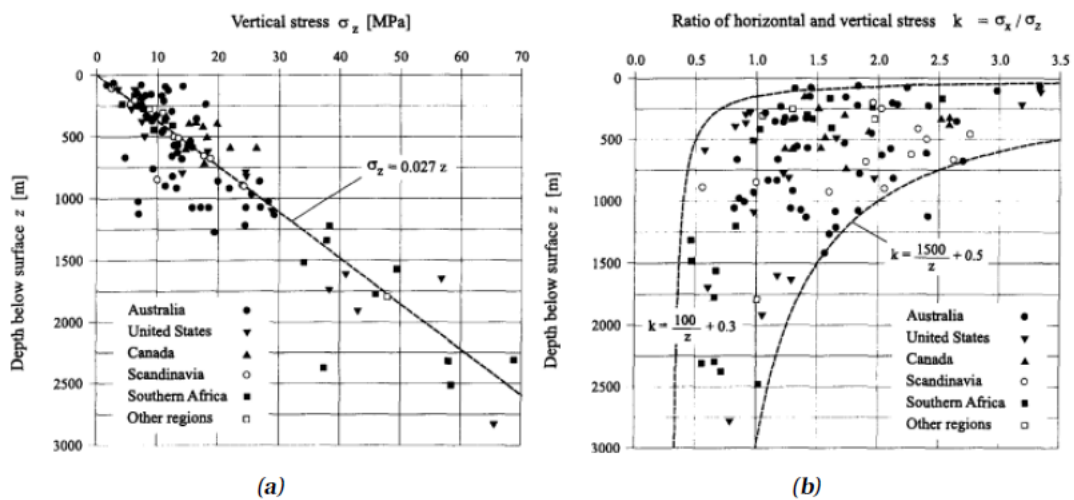


Figure 2-9 Plot of vertical stresses against depth below surface (left) and variation of ratio of average horizontal stress to vertical stress with depth below surface (right) (Hoek and Brown 1980)

Figure 2-9(left) shows that the measured vertical stresses almost are in vicinity with the simple prediction given by calculating the vertical stress due to the overlying weight of rock at a particular depth from the equation 2.7. It can be noticed that at shallow depths, there is a

considerable amount of scatter. This scattering may be associated with the fact that these stress values are often close to the limit of the measuring accuracy of most stress measuring tools. On the other hand, the possibility of existence of high vertical stress cannot be discounted, particularly where some unusual geological or topographic feature may have influenced the entire stress field (Hoek and Brown 1980).

Figure 2-9 (right) gives a plot of k , which is the ratio of average horizontal to vertical stress, below the surface (depth). For most of values plotted, it is seen that the value of k lies within the limits defined by;

$$\frac{100}{z} + 0.3 < k < \frac{1500}{z} + 1.5 \quad 2.10$$

At depths of less than 500 meters, horizontal stresses significantly exceed the vertical stresses, which is clearly noticed in the plot. For depths in excess of 1 kilometer (3280 feet), the average horizontal stress and the vertical stress tend to equalize, as suggested by Heim's rule (Hoek and Brown 1980). If very high horizontal stresses existed at depths more than one kilometer, these would have induced fracturing, plastic flow and time-dependent deformation in the rock, and all of these processes would tend to reduce the difference between horizontal and vertical stresses (Hoek and Brown 1980).

Topographic stresses

When the surface is not horizontal the topography will influence the rock stresses situation. In high valley sides, where hydropower is often located, the stresses situations are totally dominated by topographic effects. In such cases the major principle stress (σ_1) near the surface will be more or less parallel to the slope of the valley, and the minor principle stress (σ_3) will be approximately perpendicular to the slope of the valley (Nilsen and Thidemann 1993).

Tectonic stresses

Action of plate tectonics results in tectonic stress as well as occurrence of faulting and folding. The magnitude of horizontal stress induced by tectonic stress is noticeably greater than horizontal stress induced by gravity alone. This is particularly the case of the shallow and moderate depth. Tectonic stresses vary according to the extent of tectonic movement, its movement direction and degree of schistosity and shearing. Orientation of the tectonic stress in the central part of the Himalaya is very close to North-South. Thus, tunnels-oriented North-South will have least effect of the tectonic stress across its section. Under such circumstances, the total in-plane horizontal stress in a tunnel at high depth can be well low, resulting to high degree of stress anisotropy (KC 2016).

2.3.2 Redistribution of rock stress

After the underground excavation in a rock mass, the stresses which previously existed in the rock are disturbed, and new stresses are induced in the rock in the immediate vicinity of the opening. One way to represent this new stress field is by means of principal stress trajectories

which are imaginary lines in a stressed elastic body along which principal stresses act (Hoek and Brown 1980).

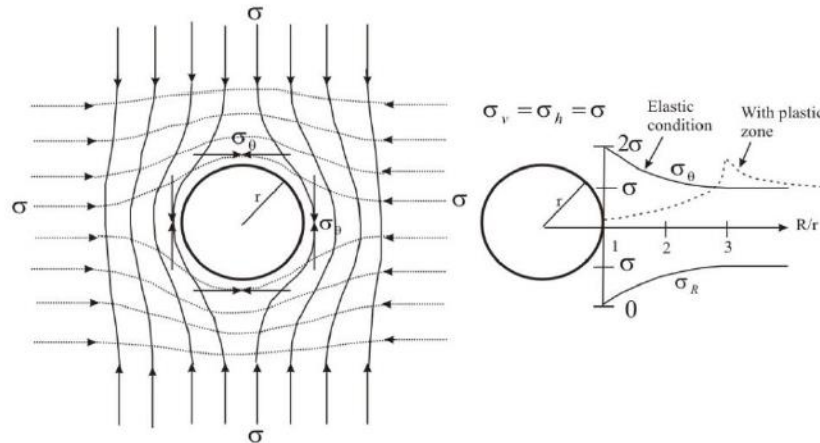


Figure 2-10 Stress trajectories in rock mass surrounding a circular opening (left) and tangential and radial stress distribution in elastic and non-elastic conditions (right) (Panthi 2006)

As shown in Figure 2-10, if the radius of the opening is r , the tangential stresses (σ_θ) and the radial stress σ_R at the periphery of a circular opening in fully isostatic stress condition and for elastic rock material will be twice and zero times the isostatic stress respectively. Stresses become normalized as the ratio between radial distance (R) and opening radius (r) increases (Panthi 2006). The magnitudes of σ_θ and σ_R are expressed as follow:

$$\sigma_\theta = \sigma \times \left(1 + \frac{r^2}{R^2}\right) \quad 2.11$$

$$\sigma_R = \sigma \times \left(1 - \frac{r^2}{R^2}\right) \quad 2.12$$

However, the stress conditions are seldom isostatic. Due to highly anisotropic stress condition the tangential stress will vary around the periphery of a circular opening. For anisotropic condition Kirsch's equation are used for the evaluation of tangential stresses. According to Kirsch the tangential stress will reach its maximum value ($\sigma_{\theta\max}$) when the σ_1 direction is a tangent to the contour, and its minimum value ($\sigma_{\theta\min}$) when the σ_3 direction is a tangent with its values:

$$\sigma_{\theta\max} = 3\sigma_1 - \sigma_3 \quad 2.13$$

$$\sigma_{\theta\min} = 3\sigma_3 - \sigma_1 \quad 2.14$$

Non-symmetric geometry and sharp corner will affect the magnitude of the tangential stress (Nilsen and Thidemann 1993).

2.3.3 Stability problem of tunnel

Induced stability problems in the tunnel occurs when the stress around the tunnel periphery exceeds the rock stress. There are mainly two reasons for the instability of tunnel caused by the induced stress.

2.3.3.1 Problems due to tensile stress

If the minimum value of tangential stress given by the equation 2.14 is negative i.e. the region is in tensile stress field, there will be radial jointing of the rock mass in that area. In most cases a tensile jointing will not have much influence on the rock stability. For high pressure tunnels it is more important that secondary jointing and opening of existing joints may increase the water leakage out of the tunnel (Nilsen and Thidemann 1993).

2.3.3.2 Problems due to high compressive stress

If the compressive tangential stress, given by the equation 2.13, exceeds the strength of the rock instability problems will occur. Basically, they are of two types depending upon the rock mass characteristics.

- Rock burst
- Rock squeezing

Rock burst

If the compressive tangential stress ($\sigma_{\theta_{max}}$) exceeds the rock mass strength (σ_{cm}) in hard and brittle rock, fracture parallel to the tunnel contour with loud noise occurs which is commonly referred as rock burst. At moderate stress levels the fracturing will result in a loosening of thin slabs, often referred to as rock spalling. When the rock stresses are very high, rock burst may be a major threat to safety.in absence of right support at right time. Rock burst activity is most intensive at the working face immediately after excavation (Nilsen and Thidemann 1993). According to the Norwegian rule of thumb, rock spalling/ rock burst is likely to occur when overburden above the rock exceed 500m. The extent of this type of failure is likely to be severe, even if the tunnel runs parallel to the valley side with a slope angle exceeding 25° (Panthi 2012).

Rock squeezing

When the strength is less than induced tangential stresses along the tunnel periphery, in soft rock, gradual formation of micro cracks along the schistosity or foliation plane will take place. As a result, a viscous-plastic zone of micro-fractured rock mass is formed deep into the walls, as shown in Figure 2-11. The induced maximum tangential stresses are moved beyond the plastic zone.

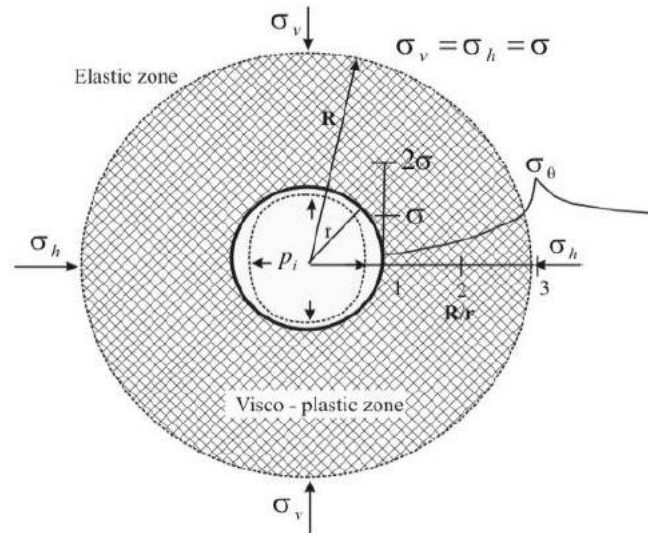


Figure 2-11 An illustration of squeezing in a circular tunnel (Panthi 2006).

Owing to this, a time dependent inward movement of rock material will take place and supports in the opening will experience gradual buildup of pressure which is known as squeezing of tunnel (Panthi 2006). In this figure, r is tunnel radius, R is radius of visco-plastic zone and p_i is the support pressure.

2.3.4 Factors affecting the squeezing phenomenon

According to (Shrestha 2006), squeezing ground conditions are influenced by many factors which contribute in different degrees. Based on analysis and case studies, many authors have identified and recognized those factors in various ways. All those factors are summarized as below:

- Stress condition
- Strength and deformability of the rock mass
- Rock type
- Water pressure and porosity of rock mass
- Orientation of the geological structures
- Construction procedures and support systems

The ratio of rock mass strength to in situ stress plays a major role. This signifies that weak or strongly foliated or crushed rock may lead to squeezing even for low overburden. It is obvious, that low rock mass strength gives low value for the ratio of rock mass strength to in situ stress which causes overstressing condition. In addition, high deformability causes large deformation. Thus, the rock mass strength and deformability could have direct contribution to the squeezing phenomenon.

Most common examples of squeezing rock types are phyllite, schist, serpentine, claystone, tuff, certain types of flysch, and weathered clayey and micaceous metamorphic rock. According to

(Basnet 2013), fault crushed zone is also a common location for squeezing problem, for example Lærdal tunnel in Norway.

Water presence also plays the most important effect as pore water pressure. When there is clay in a discontinuity plane which is in the vicinity of the tunnel, this may lead to increased pressure. Reduction of water pressure may result in the reduction of the squeezing potential with time (Shrestha 2006). On the other hand, increase in the porosity of rock reduces the mechanical strength of the rock, which will result more squeezing.

If the tunnel alignment is parallel to foliation or near to fault line, there will be more squeezing than for the tunnel axis perpendicular to those faults. The orientation of other structural features such as schistosity plane, joints etc. could also have great influence in squeezing. Over break due to buckling of schistose layers will occur mainly where the schistosity is parallel to the tunnel perimeter and for nearly vertically dipping layers a vertical sidewall is unfavorable.

2.3.5 Squeezing Analysis

According to ISRM in (Panthi 2006) squeezing of rock is the time dependent large deformation which occurs around a tunnel and other underground openings and is essentially associated with creep caused by exceeding shear strength (limiting shear stress). Deformation may terminate or continue over a long period of time.

Squeezing depends upon the factors as the rate of deformation, geological condition, in-situ stress relative to rock mass, ground water flow, pore water pressure and rock mass properties (Singh and Singh 2006).

2.3.5.1 Empirical Approach for squeezing

Empirical method implies the observation and experience rather than theory as they are based on overburden height, dimension of tunnel and UCS of rock mass. (Singh, Jethwa et al. 1992) and (Goel 1994) are used. Singh's approach (1992) method of analysis is based on the rock mass classification. Singh et al. (1992) developed an empirical relationship from the log-log plot between the tunnel depth (H) and the logarithmic mean of the rock mass quality, Q (Figure 2-12). Forty one tunnel sections data were used to plot this figure. A clear line of demarcation can be seen on the figure, which is in (Singh and Singh 2006) between the elastic and squeezing condition. The equation of this line is given as:

$$H = 350 \times Q^{1/3} \quad 2.15$$

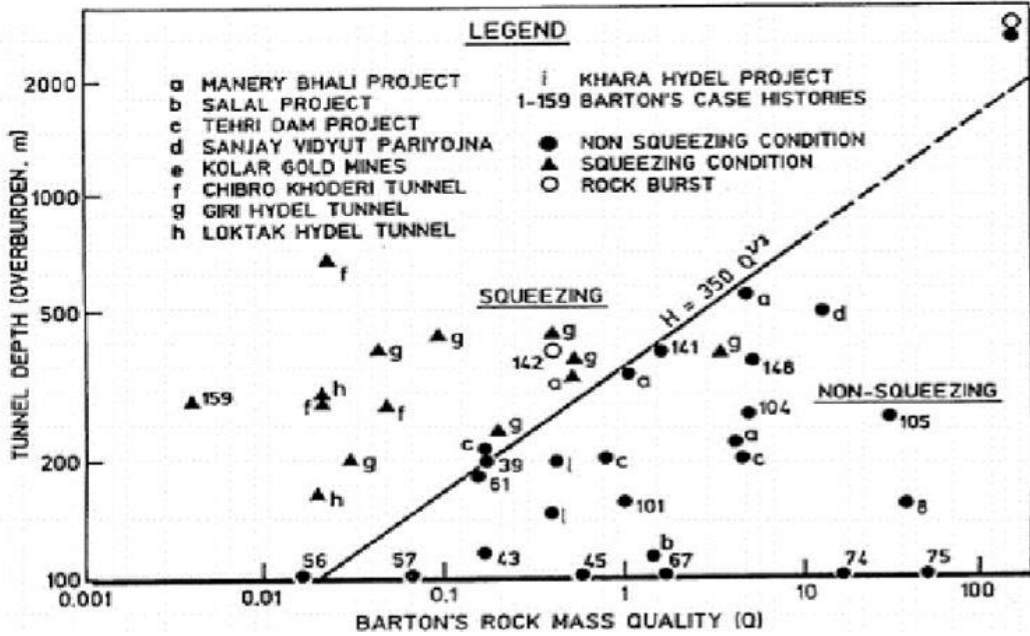


Figure 2-12 Criteria for predicting squeezing ground (Singh and Singh 2006).

Squeezing is likely to occur if the value of overburden exceeds $350 \cdot Q^{1/3}$ which alternatively can be said that the point on the graph lying above the line represents squeezing condition and point lying below represents non-squeezing condition. This relation presented by Singh is very easy and simple to use.

Goel’s approach (1994)

(Goel 1994) developed an empirical approach based on the rock mass number N which equals to Q-value with SRF = 1. ‘N’ value was used to avoid the problems and uncertainties in obtaining the correct rating of parameter SRF in Q method. With Consideration to the overburden depth H, the tunnel span or diameter B, and the rock mass number N from 99 tunnel sections, (Goel 1994) plotted the available data on log-log diagram (Figure 2-13) between N and $HB^{0.1}$. Out of 99 tunnel section data, 39 data were taken from Barton's case histories and 60 from projects in India. Out of those 60 data 38 data were from five projects in Himalayan region. All the 27 squeezing tunnel sections were observed in those five projects in Himalayan region. Other 72 data sets were from non-squeezing sections. As shown in the Figure 2-13, a line distinguishes the squeezing and non-squeezing cases.

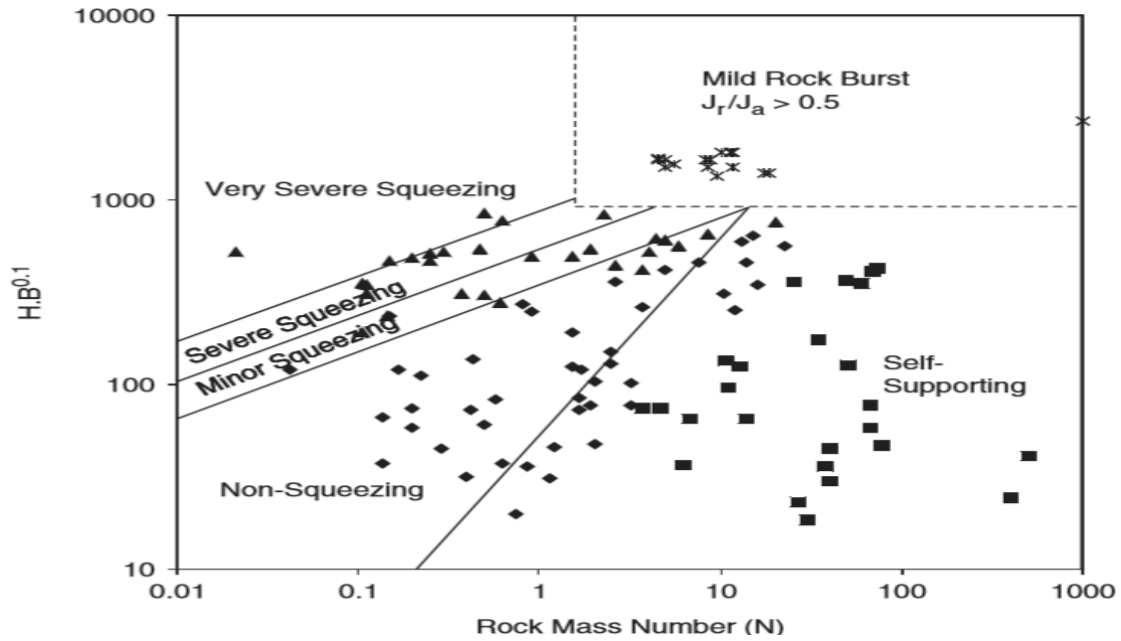


Figure 2-13: Criteria for predicting squeezing ground conditions using rock mass number N (Goel 1994)

The equation of the line is:

$$H > (275N^{0.33})B^{-0.1} \text{ meters} \quad 2.16$$

Where H is tunnel depth or overburden in meters and B is tunnel span or diameter in meter. The data point lying above the line in Figure 2-13 represents squeezing condition whereas points lying below the line represent non-squeezing condition.

2.3.5.2 Semi- Empirical Approach

Among various approaches the (Jethwa, Singh et al. 1984) approach has been discussed here:

Jethwa et al. approach (1984)

The degree of squeezing in this approach is described using coefficient N_c which is equal to the ratio of rock mass uniaxial compressive strength (UCS) to in-situ stress. Based on this value, type of behavior of tunnel can be estimated. (Jethwa, Singh et al. 1984) define the degree of squeezing based on following relation:

$$N_c = \frac{\sigma_{cm}}{P_o} \quad 2.17$$

Where, σ_{cm} is rock mass uniaxial compressive strength P_o is in-situ stress γ is Unit weight of rock mass and H is the tunnel depth below surface.

Table 2-5 Squeezing behavior (Jethwa, Singh et al. 1984).

N_c	Type of Behavior
< 0.4	Highly squeezing
0.4–0.8	Moderately squeezing
0.8–2.0	Mildly squeezing
> 2.0	Non-squeezing

2.3.6 Empirical Method

Among the various methods to predict tunnel support and excavation requirement have either empirical, analytical character or finite element modeling. The empirical method is based on prototype observations, and the analytical methods are based on first principle. A feature that both empirical and analytical method share is the characterization of the rock mass. This is accomplished by describing the rock mass in terms of parameters which are either empirical characterization or theoretical property.

The various physical parameters are determined in the empirical method. The empirically derived relationship between rock mass parameters and supports are then utilized to predict the support types and quantities and possibly the excavation procedure. Empirical method is generally applied during two circumstances when there might be limited geological information but relatively unlimited time and during construction when there is ample geological information, but time is critical.

2.3.6.1 Rock Mass Rating (RMR)

The geomechanics classification or the rock mass rating (RMR) system was initially developed at the South African Council of Scientific and Industrial Research (CSIR) by (Bieniawski 1993) on the basis of his experiences in shallow tunnels in sedimentary rocks (Kaiser, MacKay et al. 1986). The following six parameters are determined for each of the structural unit:

- Uniaxial compressive strength of intact rock material
- Rock quality designation (RQD)
- Joint or discontinuity spacing
- Joint condition
- Ground water condition
- Joint orientation

In applying the classification system, the rock mass is divided into a number of structural regions and each region is classified separately. The boundaries of the structural region must

coincide with a major structural feature such as a fault or with a change in rock type. In some cases, a significant change in discontinuity spacing or characteristics, within the same rock type, may necessitate the division of the rock mass into a number of small structural units.

2.3.6.2 Q-system

(Barton, Lien et al. 1974) Norwegian Geotechnical Institute (NGI) originally proposed the Q-system of rock mass classification based on about 200 case histories of tunnels and caverns.

$$Q = \frac{RQD}{J_n} \times \frac{J_r}{J_a} \times \frac{J_w}{SRF} \quad (0.001 \leq Q \leq 1000) \quad 2.18$$

Where,

RQD = Deere's Rock Quality Designation

J_n = Joint set number, J_r = Joint roughness number for critically oriented joint set, J_a = Joint alteration number for critically oriented joint set, J_w = Joint water reduction factor, SRF = Stress reduction factor to consider in situ stresses and J_v = Volumetric joint count.

The relation between Q and RMR system as proposed by (Barton 1995) is:

$$RMR = 15 \times \log Q + 50 \quad 2.19$$

2.3.7 Analytical Method

The Analytical solution is divided on the basis of in situ stress conditions. In low stress conditions, the support is designed to resist deformation induced by dead weight of loosened rock blocks or wedges locally. Limit equilibrium method is applicable to design the support for wedges or blocks or beams for local stability. On the other hand, in high stress condition, the deformation is induced by a redistribution of the stress field in the rock mass surrounding the excavation and the corresponding rock support is usually carried out in a systematic pattern. The development of the concept of interaction of load-deformation characteristics of rock mass and support system, results in the convergence confinement method (CCM), which is often used in design of support based on idealized uniform stress field and circular opening. Similarly, in terms of Mohr-Coulomb criteria, tangential stress σ_θ acts as the major principal stress σ_1 and radial stress σ_r acts as the minor principal stress σ_3 . At the tunnel contour, σ_r is zero so σ_3 indicates the required tunnel support pressure p_i (FAMA 1993). Thus, these two types of analytical solutions are discussed. The analytical methods discussed in the following sections are for general tunnel stability analysis.

2.3.8 Assumptions of rock support interaction analysis

The Basic Assumptions considered (Hoek and Brown 1980) are:

Tunnel geometry: The analysis assumes a circular tunnel of initial radius r_i . The length of the tunnel is such that the problem can be treated two-dimensional.

In situ stress field: The horizontal and vertical in situ stresses are assumed to be equal and to have a magnitude P_0 .

Support pressure: The installed support is assumed to exert a uniform radial support pressure p_i in the Walls of the tunnel.

Material properties of original rock mass: The original rock mass is assumed to be linear-elastic and to be characterized by a Young's modulus (E) and a Poisson's ratio (ν).

2.3.9 Convergent Confinement Method

This analysis method is based on the concept of a Ground reaction curve or Characteristic line, obtained from the analytical solution for a circular tunnel in an elasto-plastic rock mass under a hydrostatic stress field. The ground pressure acting on tunnel lining depends upon:

- Rock mass property
- Natural stress field
- Type and rigidity of the lining
- Time of installation of support

Fenner carried out the first major attempt to use elasto-plastic stress analysis for determining tunnel support pressure by using the Mohr-Coulomb yield criterion. He attempted to prove theoretically that any cylindrical opening can stand on its own without supports, provided that the plastic zone is allowed unhindered expansion (Goel 1994). He demonstrated, through numerical examples, that the extent of plastic zone required to ensure tunnel stability without supports was several times larger than the tunnel radius and concluded that it was desirable to install flexible supports rather than remove large volume of crushed zone. Goel was the first to recognize that the failed rock mass has low cohesion and friction as compared to an intact rock mass (Goel 1994). He concluded that supports were necessary for tunnel stability. He suggested further that radial displacements may continue even after the broken zone has stabilized.

The Convergence-Confinement method is based on the analytical solution for the elasto-plastic response of a circular cylindrical opening in isotropic material when subjected to isotropic or hydrostatic in- situ stresses and supported around the opening. CCM is the procedure that allows the load imposed on support installed behind the face of tunnel to be estimated. If the support is installed immediately in the vicinity of face, it does not carry out full load to which it is supposed to. The part of load is carried by face itself. As tunnel and face advance away from the support, face effect decreases, and support must carry more loads. When the tunnel moves well away from face, the support will be subjected to full design load.

CCM has three basic components viz. the Longitudinal Displacement Profile (LDP), the Ground Reaction Curve (GRC) and the Support Characteristics Curve (SCC) (Carranza-Torres and Fairhurst 2000).

2.3.9.1 Longitudinal Displacement Profile (LDP)

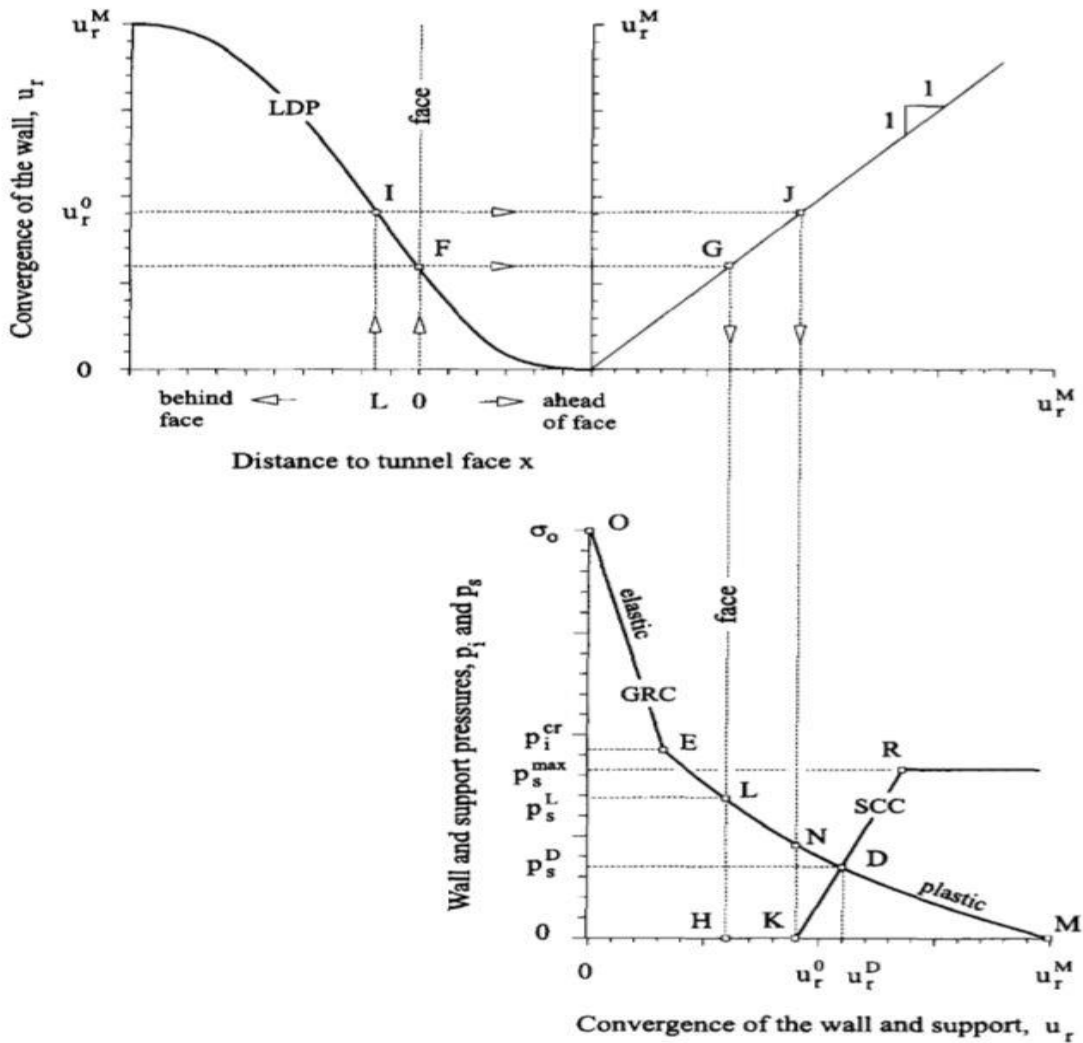


Figure 2-14 Schematic representation of Longitudinal Displacement Profile (LDP), Ground Reaction Curve (GRC) and Support Characteristics Curve (Carranza-Torres and Fairhurst 2000).

LDP is the graphical representation of radial displacement that occurs along the axis of unsupported cylindrical excavation i.e. for the sections located ahead of and behind tunnel face. The upper diagram in Figure 2-14 represents the typical LDP. The diagram indicates that at some distance behind tunnel face the effect of face is small so that beyond this distance the tunnel has converged by final value i.e. u_r^M . At some distance ahead of face, the tunnel excavation has no effect on the rock mass and the radial displacement is zero. Hence, it provides insight into how quickly the support.

The construction of LDP is very important task in CCM. According to (Vlachopoulos and Diederichs 2009), in order to facilitate to construct the LDP, (Panet 1996) derived the following equation based on plastic analysis.

$$u^* = \frac{u_r}{u_{max}} = \frac{1}{4} + \frac{3}{4} \left(1 - \left(\frac{3}{3+4X^*} \right)^2 \right) \quad 2.20$$

Where, $X^* = X/R_t$, u_r is the radial displacement and u_{max} is the maximum short-term radial displacement from distance from face. This formula is only used for positive value of x .

Similarly, based on the measured value of the convergence in the vicinity of the face for the tunnel in Mingtam power canal project by (Chern, Shiao et al. 1998), an empirical best fit relationship to these actual measured data was proposed by (Vlachopoulos and Diederichs 2009).

$$u^* = \frac{u_r}{u_{max}} = \left(1 + e^{\left(\frac{-X^*}{11} \right)} \right)^{-1.7} \quad 2.21$$

Both the relationship given above are responsible for plastic analysis provided that the radius of plastic zone does not exceed 2 tunnel radii. However, there is possibility of developing the plastic zone radius exceeding 2 tunnel radii. In order to account for the influence of increased overall yielding on the shape of the normalized LDP, the term normalized plastic zone radius, $R^* = R_p/R_T$ (where, R_p is plastic zone radius and R_T is the tunnel radius), is logical to use. Based on analysis using Phase² in plain strain cross section and axisymmetric models, (Vlachopoulos and Diederichs 2009) proposed a new set of best fit relationships which are shown in the following equations.

$$u_o^* = \frac{u_o}{u_{max}} = \frac{1}{3} e^{-0.15R^*} \quad 2.22$$

For $X^* \leq 0$ (in rock mass):

$$u_o = \frac{u_o}{u_{max}} = u_o^* e^{X^*} \quad 2.23$$

For $X^* \geq 0$ (in rock mass):

$$u^* = \frac{u}{u_{max}} = 1 - (1 - u_o^*) e^{\frac{-3X^*}{2R^*}} \quad 2.24$$

For 2D analysis, u_{max} and R_p need to be calculated prior to the sequenced analysis (Vlachopoulos and Diederichs 2009).

2.3.9.2 Ground Reaction Curve (GRC)

GRC is a relationship between decreasing internal pressure P_i and increasing radial displacement of the tunnel wall u_r . The relationship depends upon mechanical properties of rock mass and can be obtained from the elasto-plastic solution of rock deformation around an excavation (Carranza-Torres and Fairhurst 2000). The curve OEM in Figure 2-14 is the typical diagram of GRC.

According to (Carranza-Torres and Fairhurst 2000), the uniform internal pressure P_i and far field stress σ_o can be scaled to give the scaled internal pressure P_1 and scaled far field stress S_o respectively. Assuming that the rock mass satisfies Hoek-Brown failure criteria, P_i will be;

$$P_i = \frac{p_i}{m_b \sigma_{ci}} + \frac{s}{m_b^2} \quad 2.25$$

$$S_o = \frac{\sigma_o}{m_b \sigma_{ci}} + \frac{s}{m_b^2} \quad 2.26$$

The pressure p_{cr}^i defined by the point E in the GRC of the Figure 2-14, marks the transition from elastic to plastic behavior of the rock mass i.e. for an internal pressure $p_i \geq p_{cr}^i$, a plastic region of radius R_{pl} develops around a tunnel. The scaled critical pressure P_{cr}^i for which the elastic limit is achieved is given by the following expression:

$$P_{cr}^i = \frac{1}{16} \left[1 - \sqrt{1 + 16S_o} \right] \quad 2.27$$

The actual critical pressure is found from inverse of the equation

$$p_{cr}^i = \left[P_{cr}^i - \frac{s}{m_b^2} \right] m_b \sigma_{ci} \quad 2.28$$

In case of $p_i \geq p_{cr}^i$, the relationship between radial displacement u_r^{el} and internal pressure p_i elastic part of GRC is given by:

$$u_r^{el} = \frac{\sigma_o - p_i}{2G_{rm}} \quad 2.29$$

For the values of internal pressure $p_i \leq p_{cr}^i$, the extend of the plastic region R_{pl} that develops around the tunnel is :

$$R_{pl} = R \exp \left[2 \left(\sqrt{P_{cr}^i} - \sqrt{P_i} \right) \right] \quad 2.30$$

Where R is the radius of tunnel.

(Hoek and Brown 1997) suggest that in some cases the assumption of no plastic volume-change for the rock mass may be more appropriate. For the case of non-dilating rock masses is :

$$\frac{u_{pl}^r}{R} = \frac{2G_{rm}}{\sigma_o - p_{cr}^i} = \left[\frac{1-2\nu}{2} - \frac{\sqrt{P_{cr}^i}}{S_o - P_{cr}^i} + 1 \right] \left(\frac{R_{pl}}{R} \right)^2 + \frac{1-2\nu}{4(S_o - P_{cr}^i)} - \frac{1-2\nu}{2} \frac{\sqrt{P_{cr}^i}}{S_o - P_{cr}^i} \left[2 \ln \left(\frac{R_{pl}}{R} \right) + 1 \right] \quad 2.31$$

2.3.9.3 Support Characteristics Curve (SCC)

Support characteristic Curve is the plot between increasing pressure P_s on the support and increasing radial displacement u_r of the support. If the elastic stiffness of the support is denoted by K_s , the elastic part of the SCC - i.e., segment KR in Figure 2-14 can be computed from the expression:

$$P_s = K_s u_r \quad 2.32$$

The plastic part of the SCC i.e. horizontal segment starting at point R in Figure 2-14, is defined by the maximum pressure p_s^{\max} that support can accept before collapse. For different support system such as; concrete or shotcrete linings, ungrouted bolts and cables, steel ribs, lattice

girders etc., the main task is to find the maximum pressure and elastic stiffness for the construction of SCC.

2.4 Examples from Nepal :

Solu Khola (Dudhkoshi) Hydro Electric Project (SKDKHEP) lies in the Lesser Himalaya of Okhaldhunga Window based on the Nepal Geological Map Compiled by Department of Mines & Geology (1996). Augen gneiss of Paleozoic age and the Kuncha formation of green phyllite of Precambrian age are main rock types. Thus, the selection of cases to review is based on the similar geological conditions. Kaligandaki “A” Hydroelectric Project, Modi Khola Hydroelectric Project and Chameliya Hydroelectric project are the projects which lie in similar geological zones.

2.4.1 Kaligandaki “A” Hydroelectric Project

The Kaligandaki “A” Hydroelectric Project is located in the western part of Nepal about 200 km west of Kathmandu in the Lesser Himalaya.

The project is one of the largest RoR scheme project with installed capacity of 144 MW and is capable of generating 82 GWh electrical energy annually. Geologically, the project lies in the lesser Himalayan highly deformed rock formation and is relatively close to Main Boundary Thrust (MBT) with project area mainly comprising of Precambrian to lower Paleozoic shallow marine sediments. The dominant rock types are dark slate, graphitic and siliceous phyllite and siliceous dolomite and the HRT of the project mostly passes through highly deformed graphitic phyllite and phyllitic slate intercalation. The mineral composition of these rocks and the degree of metamorphism vary considerably (NEA 1992).

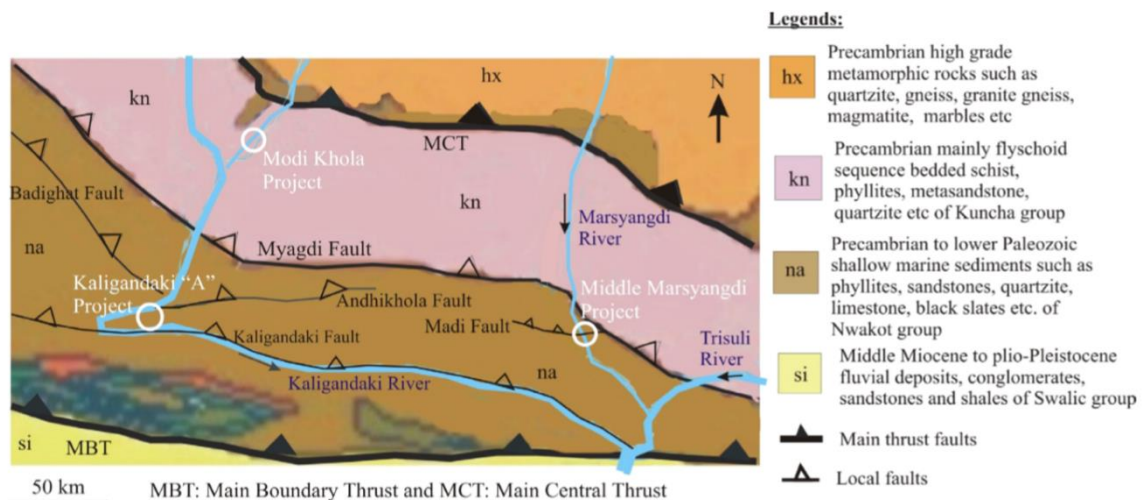


Figure 2-15 Geological environment of Kaligandaki “A” and Modi Khola (Panthi 2006)

The project area is very close to several local faults, namely Badighat, Andhikhola and Kaligandaki faults. The splay (branch) of Andhikhola fault crosses the headrace tunnel at about 700 meters from the intake.

The headrace tunnel was predicted to encounter heavy squeezing at the upstream one-kilometre section due to presence of small fault and weakness zone as predicted by planning phase investigation whereas the rest of tunnel alignment was assumed to have fair to good quality rock mass except for some sections with highly sheared and deformed rock mass. During the excavation of headrace tunnel the rock mass encountered was very weak, highly sheared, thinly foliated and intensely folded and the tunnel problems were mainly induced due to plastic deformation (squeezing), from few centimetres to nearly a meter (Shrestha 2014).

2.4.2 Modi Khola Hydroelectric Project

The Modi Khola Hydroelectric Project lies west of the Kathmandu and is located on the right bank of Modi river, a tributary of Kaligandaki river. The project has an installed capacity of 14.7 MW and can generate 91 GWh electrical energy annually. The project is a run-of-river scheme with a medium head of approximately 67 meters and a design discharge of 27.5 m³/s (Authority 2000).

The project includes the total underground waterway length of approximately two kilometers, includes a 1,503 meters long headrace tunnel with cross section area of approximately 15 square meters, a 50 meters deep vertical pressure shaft and a 430 meters long pressure tunnel.

The project are compromises of the rocks of Precambrian sequence of the lesser Himalayan meta-sedimentary rock formation. The area has many local faults and rock mass is fractured and deformed. The bedrock along the underground waterways of this project is mainly dominated by fractured but abrasive greenish quartzite (HH 2001). The upstream first 500 meters of headrace tunnel passes through a fracture zone which consists of highly fractured quartzite and highly sheared and deformed phyllitic green schist. The pressure tunnel also crosses a major shear fault consisting of decomposed quartzite fragments and highly sheared green schist (Paudel, Dangol et al. 1998).

Good quality greenish to white quartzite was observed during tunnel excavation along the headrace tunnel except the tunnel section passing through weakness and fracture zones. Three sets of joint plus random joints were present along the headrace tunnel alignment with slightly to moderately weathered with some degree of alteration due to presence of silty clay fragments in the discontinuities. The intercalation of decomposed green to dark grey mica schist within massive quartzite was present at some locations. Large deformation leading to immediate collapse occurred at locations where the groundwater initiated. Even after the initial stabilization and advancing further ahead, those affected sections started squeezing heavily up to 1.5 m and even buckling closely spaced steel ribs (Paudel, Dangol et al. 1998); (HH 2001).

2.4.3 Chameliya Hydroelectric Project

The Chameliya Hydroelectric Project is located has an installed capacity of 30 MW and is located in the Darchula district of far western region of Nepal 270 km north-west of Dhangadi. The project area is covered by meta-sedimentary rock of Surhet group and Midland group and the main rock types are siliceous dolomite, sandstone, calcareous slate, dolomite and dolomite intercalated with slate (Authority 1997). Main Boundary Trust (MBT) is 60 km south and Main

Central Thrust (MCT) is near to the project site causing high degree of folding and faulting. Two faults are inferred across the headrace tunnel alignment.

Most of the rock mass was supposed to be of fair quality but was found to be different during the tunnel excavation to that of predicted one.



Figure 2-16 Rock mass condition at different chainage along headrace tunnel of Chameliya Hydroelectric Project (Basnet 2013)

The presence of thinly foliated and fracture dolomite (left) of Figure 2-16 and highly sheared and fractured talcosic phyllite with some bands of dolomite (right) of Figure 2-16 caused the rock mass to be poor to exceptionally poor whereas the other sections of headrace tunnel encounter very less problems during the construction process.

2.4.3.1 Tunnel stability problems

The major stability problems in the headrace tunnels were due to the crossing of different rocks, weakness zones and faults.



Figure 2-17 Squeezing in headrace tunnel of CHEP: Floor heave (left) and wall closure (right) (Basnet 2013)

The first 3 kilometres of headrace tunnel faces problems of rock spalling, mud flow instances. The other kilometre of tunnel faced stability issues due to severe squeezing due to presence of extremely poor talcosic phyllite as shown in Figure 2-17.

Nepal has a typical geological formation with major faults known as South Tibetan Detachment System (STDS), main central thrust (MCT), main boundary thrust (MBT) and main frontal thrust (MFT). Most of the hydropower projects and especially the underground structures are situated in lesser Himalayan or lower part of higher Himalayan (Panthi 2006). Such complex geology makes the construction process of the hydropower projects difficult. The poor rock mass condition along with intersection of sheared and jointed rock mass, groundwater ingress and sufficient vertical cover above the tunnel causes the significant squeezing in the tunnel. These three cases studied could be good examples for the tunneling cases in weak rock mass.

2.5 Ground Water

The rock mass is a jointed aquifer, having capacity to hold water and water can move through the most permeable discontinuities or through open channels along them. In general, the rock mass close to the surface is more jointed and the joints are more open than in the rock mass at deeper depth. Visual observations in many un-grouted tunnels indicate that most water leakage occurs in the part of the tunnel which is closest to the surface and that it is mainly confined in fractures, faults and weathered zones (Nilsen and Thidemann 1993) and (Karlsrud and Kvelsvik 2002) in (Panthi 2006). The presence of water in the rock alters its strength and other properties.

2.5.1 Hydraulic conductivity of the rock mass

Hydraulic conductivity, also known as the coefficient of permeability, is the most common parameter for characterizing hydrogeological conditions. The conductivity of rock masses is mainly controlled by the degree of jointing and the character of the joints. If joint sets in the rock mass are interlinked to each other and have wide aperture and are open or filled with permeable materials, the hydraulic conductivity is high which can be seen in Figure 2-18.

In general, the degree of jointing, spacing between joints and wideness of aperture in the rock mass differs along the depth. With the increase in depth, joints become tighter with reduced aperture, and often there is an increase in joint spacing and reduction in the joint set numbers. As a result, the hydraulic conductivity of the rock mass decreases with increased depth (Panthi 2006) Different rocks types have different value of hydraulic conductivity. As shown in Figure 2-18, different rock types; jointed but strong and brittle rocks such as granite, quartzite and gneiss may have a corresponding value of hydraulic conductivity as of clean sand.

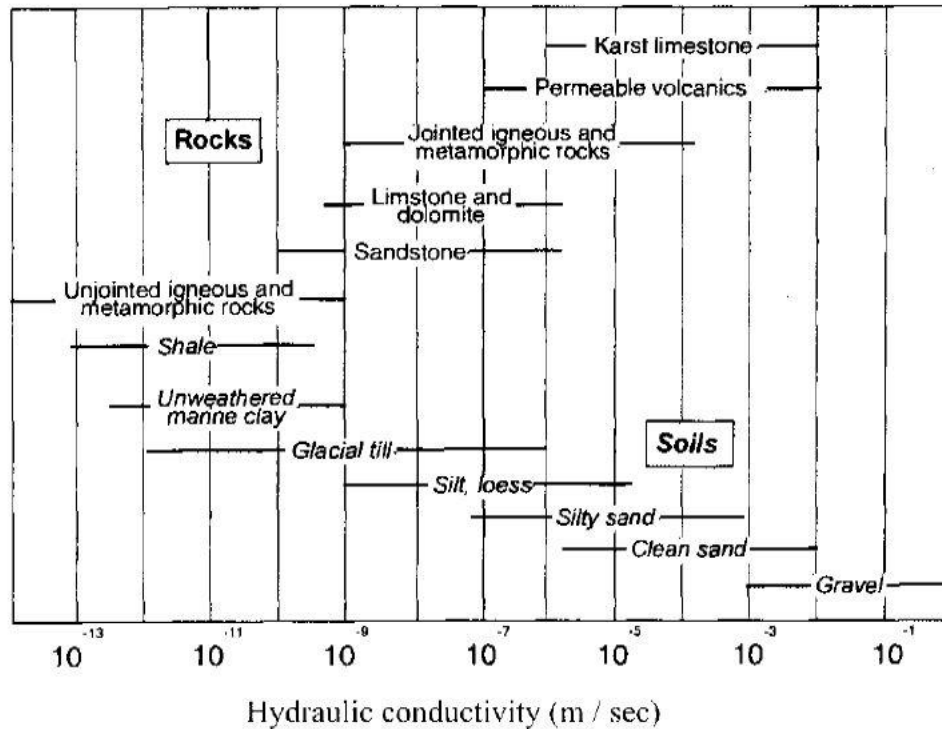


Figure 2-18 Hydraulic conductivity of rock and soil (Freeze and Cherry 1979)

On the other hand, unjointed rocks of similar category may have permeability lower than that of marine clay. Similarly, very weak, highly folded and highly sheared rocks such as shale, phyllite and schist have low hydraulic conductivity. Rocks such as limestone and marble, with calcite as the mineral, have a tendency of dissolution when in contact with acid water which may result in large water inflow as well as leakage through karst channels (Panthi 2006). Therefore, problems related to ground water differs from geology to geology. It mainly depends upon the type of rocks, jointing characteristics in the rock mass, and depth from the surface.

2.5.2 Problem associated with leakage and inflow and its estimation

In underground excavations safety and stability are the main concerns. Tunnels thus have to be water tight in this regard. Water leakage problems in unlined or shotcrete lined water tunnels are persistent issues. Severe water inflow as well as leakage problems have been faced many times that not only reduced stability of the rock mass surrounding the tunnel, but also valuable water has been lost from it. In the Himalaya region, the tectonics are active resulting in the rock masses to be highly fractured, folded, sheared and deeply weathered. Thus, tunnel has to pass through numerous weakness zones, fractures and faults. Moreover, the majority of these zones are in general highly conductive, representing potential sources of ground water aquifer as well as possible sources of water leakage from the completed unlined or shotcrete lined water tunnels. Thus, the degree of uncertainty and risk associated with water leakage is extremely high. (Panthi and Nilsen 2008).

According to (Kassana and Nilsen 2003) in (Panthi 2006) some notable projects, which have suffered excessive water leakage problems are Khimti I Hydropower Project in Nepal

Himalaya, Chivor II (Columbia), Whatshan (Canada), Askora and Bjerka (Norway) and Kihansi (Tanzania). High pressure grouting techniques can be one of the solutions to control the water inflow during excavation through difficult ground conditions. The systematic pre injection grouting not only improves the hydraulic conductivity of the rock mass closest to the tunnel periphery by many folds, but also considerably improves the quality of the rock mass (Panthi and Nilsen 2005).

Thus, water leakage control in the tunnels is most important not only in improving the rock mass quality, but also in increasing the safety as well as saving economic loss caused by large leakages. The real challenge however is prediction and quantification of possible water leakage accurately prior to tunnel excavation.

2.6 Design Aspects

The optimum use of engineering geological information to minimize the risk of instability is the goal of planning underground excavations for hydropower projects. Aspects related to optimum location, alignment orientation, and the shape and size are to be analyzed carefully during the planning stage of hydropower projects (Edvardsson and Broch 2002). Key to successful tunneling is reflected from cost-effectiveness, selection of appropriate tunneling method and managing geological uncertainties (Panthi 2017).

2.6.1 General aspects

Preferable locations for underground tunnels and caverns are zones with favorable rock mass conditions, avoiding young sedimentary rocks, jointed rock with clay seams and fissures. To avoid the stress induced instabilities relatively distressed joints are preferred.

Particularly, the weakness zones due to presence of high stress anisotropy should be avoided. For excavations with spans less than 20 m, a minimum rock cover of 5 m in un-weathered rock must be satisfied to provide the necessary arching effect (Nilsen and Thidemann 1993). Eventually, hydropower may require the use of access tunnels that are seated in weak rocks and face instability such as cave-ins (Encalada 2018). Alignments of excavations in relation to major joint sets must be defined based on the maximum angle between the joint sets. Thus, the bisecting angle between major joint sets is the rule. However, in some cases the orientation must be adjusted such as in clay filled joints and strong dipping joints. ‘Design as you go’ principal has to be adopted when uncertainties in the rock mass occurs. Change in the orientation of caverns during construction can happen and this may require changes in the orientation of the surrounding tunnels. In such cases the priority should be given to the caverns if the purpose is to increase stability (Encalada 2018). Excavation alignments are recommended to be oriented between 15 and 30 degrees from the horizontal projection of the maximum principal stress with respect to stresses (Nilsen and Thidemann 1993). In cases, when stress-induced instabilities cannot be avoided, a shape that concentrates stress problems in a limited space may help to minimize the cost of support (Nilsen and Thidemann 1993); (Edvardsson and Broch 2002).

For the shape of the caverns the case study of the Mingtan power house in Taiwan, probably could be an example. Three different shapes were analyzed to overcome problems that had been observed in nearby caverns. The first choice consisted of a mushroom shape with a concrete arch at the roof, but this design was disregarded due to the failure in the concrete. The second option was horseshoe shaped geometry that too resulted in failure at the roof and walls. However, it seemed controllable with the application of extensive support. The third option was an elliptical geometry. This option also presented problems at the roof and walls that needed extensive support, but less than the second option. In general, the difference in support required between the elliptical (the most efficient shape) and the standard section was marginal (Encalada 2018). Yet, due to construction reason second option was chosen.

So, it is very crucial to carry out the characterization of the rock mass in advance according to the choice of size and shape of a cavern. For the analysis of instantaneous deformation, parameters such as the quality of the rock mass, uniaxial compressive strength and deformation modulus are most important. For instance, the modulus of deformation, can be taken from in situ measurements. In case of in situ stress, measurements at only one location would not be enough to cover the uncertainty associated with stress measurement. For this reason, it is recommended to compare stress ratios between the new project and nearby existing projects. (Encalada 2018) states, that this has proven to be a good way to solve the uncertainty related to stresses. For, tunnels in weak rock (Encalada 2018) recommended to carry out 3D numerical modelling to account for face stability problems.

2.7 Numerical Modeling

The hydropower tunnels pass through the various kind of valleys depending on the topography so to incorporate all the stress acting on the tunnel it is very important to include the topographical and tectonic stress during the analysis. The empirical and analytical method for stress evaluation will be thus conservative.

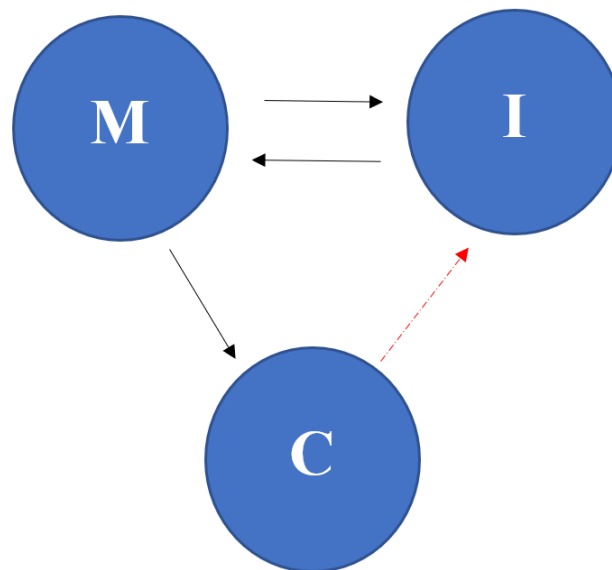
The numerical modeling is being very famous amongst the personals working in geo-technical field. The modeling helps to generate the discontinuous and continuous models where the discontinuous class models the rock mass as a single block only whereas the continuous class discretize the rock mass as many individual elements and are checked individually for rock stresses and deformation (Nilsen and Thidemann 1993). The use of RS² (Phase²) is done for 2D finite element programming and uses Finite Element Method (FEM) to define a geological model with actual site rock properties and boundary conditions. This program is very famous to perform stress state analysis and stability analysis.

2.7.1 The Phase² Program

The Phase² is a 2D windows-based program. This program is very famous amongst geotechnical engineering projects and incorporates the analysis of difficult tunnelling problems in very weak rocks, tunnel design, stress analysis, support design for tunnels and slope, slope stability and groundwater seepage analysis. Some basic and user-friendly features in the Phase² program are:

- Elastic or plastic materials
- Staged excavation
- Multiple materials
- Bolt/Liner support estimation
- Constant or gravity field stress
- Jointed rock
- Plain strain or axis symmetry
- Groundwater (including pore pressure in analysis).

RS² (Phase²) is 2D finite element program used in wide range of projects that include excavation design, slope stability, groundwater seepage, probabilistic analysis, consolidation and dynamic capabilities (Broch 1984) . As shown in Figure 2-19, the program includes three modes i.e. Model (M), Compute (C) and Interpret (I). The black arrows indicate the workability within model whereas the red arrow indicates that the Compute should be done before Interpret. The three individual modes are described briefly below



M: Model, C: Compute, I: Interpret

Figure 2-19 Schematics showing the interaction happening between three modes (Rocscience 2018).

2.7.1.1 Model Generation

The generation of model starts with the project setting window. Different information such as project name, stages of analysis, groundwater condition can be included along with the staged excavation. The selection between plain strain or axisymmetric analysis can also be done in this window. The next step is to define the boundaries which can be added manually, importing dxf file or from predefined tunnel shape. The model incorporates an area which is to undergo excavation for which external boundary must be fixed. The model can be staged, with or without joints, structural interface and piezometric line. The meshing and discretization are

done after boundaries are fixed which is eased by Phase² based on triangular or quadrilateral finite elements. The loading window is used after that to input the in-situ stress condition before the excavation. Two loading conditions i.e. Constant field stress and Gravity field stress can be chosen according the necessity of incorporating varying topography or not. The gravity field stress addresses the consideration of ground surface elevation. Different material properties are required for the modeling such as Unconfined Compressive Strength of intact rock (σ_{ci}), Hoek-Brown constant (m_i), Geological strength index (GSI), Young's Modulus of intact rock (E_i), Poisson's ratio (ν), density of the rock mass (γ) of the rock mass as an input as material properties in Phase². The most suitable support system required option is available in Phase². The mostly used support systems bolts and liner (standard beam, reinforced concrete, geosynthetic, cable truss) options are available in Phase² and the properties of those support system can also be defined in the support window.

2.7.1.2 Compute (C)

After the model setup, input of rock properties and stress situation, the finite element analysis of model can be done using the compute command using either parallel or sequential model. Thus, computed files are stored in a compressed file format by default in Phase². All the output files after analysis are saved in a single compressed file with extension *.fez.

2.7.1.3 Interpret (I)

Interpret window helps to visualize and interpret the post-processed module of the Phase² analysis result. The contours of different data such as stress, displacement, strength factor and their results can be viewed on this window. The stress level at particular location can be analyzed. The strength factor of the rock mass around the tunnel can be displayed with contours and option of either performing plastic analysis or not can be confirmed. If the strength factor is less than 1 it becomes compulsory to perform the plastic analysis.

2.7.2 3D tunnel simulation using the core replacement technique in Phase2

The simulation of 3-dimensional excavation of tunnel is possible in Phase² program. The tunnel face provides support, but the support of face will be reduced eventually as the face advances. The core replacement technique helps to determine the deformation prior to support installation.

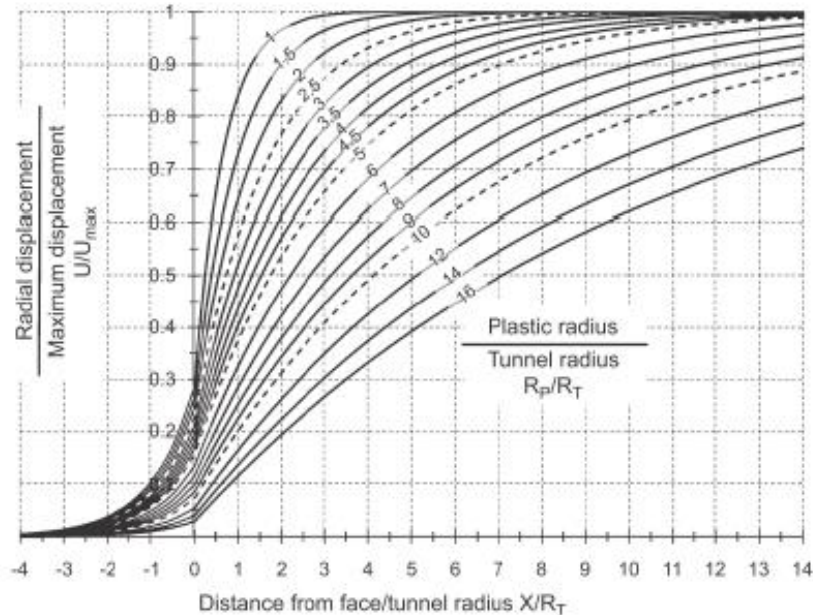


Figure 2-20 LDP templates to be used as an alternative to equations of LDP (Vlachopoulos and Diederichs 2009).

The graph given in Figure 2-20 can be used after the two pieces of information i.e. the maximum tunnel wall deformation u_{\max} , far from tunnel face and the radius of plastic zone far from tunnel face are obtained from finite-element analysis. These values can be calculated using the plain stain analysis with zero internal pressure inside the excavation and thus the displacement if wall at the point of support application can be found using Figure 2-20. Further step is to determine the core modulus that yield a displacement equal to that at the same point of support application and the same location should be used to determine the u_{\max} , as the location of maximum displacement can change depending upon the magnitude of internal pressure. The internal pressure that yields displacement equal to that at the point of support application can be determined by plotting the displacement versus stage for a point on the tunnel under consideration of the excavation.

2.7.3 Stability analysis

The in-situ stress condition of the ground can be found out using the valley slope model, the section will be analysed for exaction then after. Thus, analysing the stress situation around the tunnel periphery, the proposed geometrical confinement and hydraulic properties are known to be satisfied or not. The installation of proper support system to overcome the instability or total collapse is chosen based on the presence of the rock type and its properties.

3 PLANNING AND DESIGN ASPECT OF WATERWAYS

3.1 Background

Especially in the run-of-the-river plants, construction of the waterway tunnel is significant in terms of cost. Therefore, in order to make a hydropower project financially attractive, reduction and optimization of the cost of waterway is a major issue. One of the possible solutions is to use unlined or shotcrete lined pressure tunnel / shaft or combination of both for the waterway system if the rock mass and applied shotcrete and/or systematic bolting guarantee long-term stability and safety (Basnet 2018). A typical layout of an underground hydropower scheme with the possible locations of unlined / shotcrete lined pressure shaft and tunnel in the waterway system is shown in Figure 3-1.

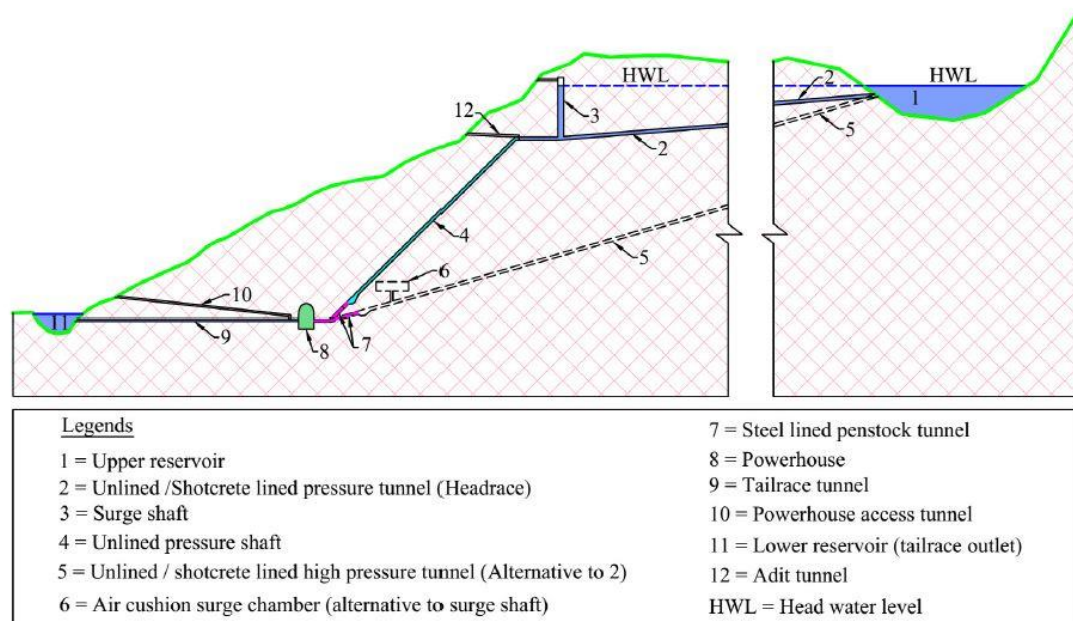


Figure 3-1 Typical layout of underground hydropower scheme with unlined pressure shaft and tunnel (Basnet 2018)

In Norway more than 200 underground powerhouses and 4200 km-long hydropower tunnels in the past 100 years (Broch 2013). It is estimated that over 95% of total length of shafts and tunnels of Norwegian hydropower schemes are left unlined. Apart from Norway, the practice of using shotcrete lined pressure tunnel in the headrace system of hydropower waterways could be seen in Nepal Himalaya. As an earliest attempt in 2000, Khimti I Hydropower Project (KHP) used a low-pressure shotcrete lined tunnel with a maximum water head of about 40 m at its headrace tunnel system (Basnet 2018).

Similarly, the shotcrete lined tunnels in Modi Khola Hydroelectric Project (MKHP) with maximum water head of about 30 m and in Chilime Hydroelectric Project (CHP) with

maximum water head of about 20 m have been in successful operation since the start of commercial operation of the project in 2000 and 2003, respectively (Basnet 2018).

The topographical, geological and tectonic environment of the Scandinavia and the Himalaya are quite different (Panthi 2014). The experience of planning, design and construction of the pressure tunnel in the Upper Tamakoshi Hydroelectric Project (UTHP) indicates that the existing conditions of the Himalaya makes it challenging for the use of unlined or shotcrete lined tunnel. Periodic earthquakes that occur in this region releasing the stress accumulated and de-stressing the rock mass.

The magnitude of major tectonic principal stress in the Himalayan region has been influenced by the compressional tectonic deformation and active reverse faulting mechanism (Panthi 2006). Thus, we can conclude that geology of Himalaya is complex in nature.

3.2 Lined tunnels:

Conventional lined tunnels have an extra layer of lining over the excavated surface. Lining types may vary from case to case. According to (Benson 1989), purpose of lining system in the tunnel is aimed to fulfil following.

- Minimize or acceptable head loss in the conduit
- Protection against excessive leakage by factors like seepage or hydraulic fracturing
- Long-term stability of the tunnel in case of watering up, operation and dewatering

However, to achieve such purpose with lining additional time and cost is required. Moreover, young sedimentary rock types should be avoided to be safe from unfavourable conditions that will occur during construction. Another factor that should be known beforehand is the orientation of major weakness zone. Designer must be sure to decide the location of the opening where those weakness is not intersecting (Nilsen and Thidemann 1993).

3.3 Unlined / Shotcrete lined tunnels

Unlined means that no steel or continuous concrete lining is installed in the shaft or tunnel, with the result that the rock itself is under direct pressure from the water (Broch 1984).

In other words, principle behind unlined pressure tunnel concept is that the rock mass itself works as a natural concrete against the pressure exerted by water column in the tunnel (Basnet 2018). Due to shortage of steel for penstock during and after First World War, application of unlined tunnels in Norway came into practice. And recent development in unlined tunnels has been marked in Nepal as well. (Basnet 2018) has already conducted his Ph.D. research into possibilities of applicability of such tunnels in Nepal Himalayas.

In general, if the tectonic and geological conditions seem favourable, unlined pressure could be economical, simple, and takes less design time. In unlined tunnel some acceptable leakage is always anticipated but within acceptable range. Moreover, minimum principal stress should always be greater than the hydrostatic pressure. In addition to that critical locations should be taken proper care for instance, connection of unlined and steel lining, and penstock connection

to the powerhouse. Restricting the use of steel and concrete lining results in a reduction of construction time which enables early production, and this ultimately reduces capital cost.

3.3.1 Prerequisite for unlined tunnels

There are certain conditions that need to be fulfilled, before unlined tunnelling is executed. According to (Nilsen and Thidemann 1993), following locations are not favourable for orientation of unlined tunnels.

1. High porosity rocks that may include some volcanic mass and sandstones
2. karstic areas
3. Heavily jointed rock masses and open, intercommunication joints
4. The unfavourable orientation of faults and weakness zones
5. Impermeable rock layers or clay zones that may create a pressure in critical locations.

3.4 Planning and design requirements

Safe design of tunnels and cavern throughout the alignment depends mainly on the geological conditions and the results of the geological investigation carried out on the project site. It is a key factor to decide the cost for overall underground construction. According to (Panthi 2017), key to successful tunnelling is reflected from cost-effectiveness, selection of appropriate tunnelling method and managing geological uncertainties. Thus, careful attention is a primary need in design.

(Nilsen and Thidemann 1993) has pointed four such primary areas for good design of underground openings which are explained below.

3.4.1 Site Selection

The type of rock that is to be encountered affects the choice of location. In addition, it will govern the stability and feasibility of the project. The proper location will ease the decision maker during the construction and operation of the project. For instance, in shallow seated openings decisions regarding the minimum rock cover is a challenge because the designer should firstly have knowledge on the depth of weathering (Figure 3-2 left) and secondly investigate for probable over break above the opening. 5 m of rock cover is accepted in hard rock for span limit of 20m (Nilsen and Thidemann 1993). In such openings small rock stresses result in weak interlocking of the blocks. Whereas, in deep-seated openings because of high stresses and anisotropic nature stability problems like squeezing, rock bursting and other stress-induced problems are anticipated. In deep-seated opening (Figure 3-2 right) the challenge for designer, is to locate a position that is distressed as in deep valleys, so that more rock stress problems could be avoided.

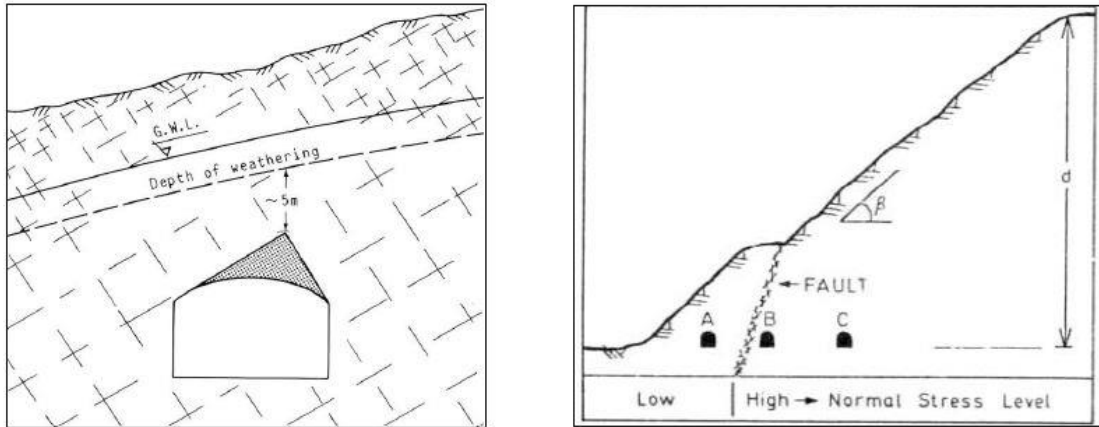


Figure 3-2 Minimum rock cover for shallow seated underground opening (left) and stress situation in valley side with fault zone (right) (Broch 1984)

Another important point to be taken into consideration is to make sure that opening is far away from the weakness zone. Whenever, the crossing is needed it is important to choose with smallest one and as short as possible. So, while selecting the location for the underground complex intermediate position is advantageous.

3.4.2 Orientation of alignment and length axis

Optimization of the opening is more appropriate and effective when comprehensive joint mapping and its location is selected. Orientation is proposed in such a way to keep the stability problems and over break as minimum as possible. For this purpose, major discontinuities in the rock mass is identified and it is made sure that it has less or no effect on the orientation of the opening. In case of shallow opening, it is basic rule to orient the alignment of opening at the maximum intersection angle between two predominant joint directions. However, if there are high rock stresses, the direction of principal stress also plays a role and thus, must be considered. It is therefore important to avoid the parallel orientation of tunnel alignment and length axis of the cavern with a major joint. When the tangential stress is oriented favourably with major joint sets it results in less over break, so it should be a major concern.

3.4.3 Shaping

The main design philosophy for underground opening is to distribute the compressive stresses evenly along the periphery. However, generally the rock is discontinuous having low ability to withstand tensile stress and largely depend on the shear strength of the discontinuities. So, the only way to overpass such difficulty is a simple design with an arched roof, avoiding sharp intruding corners (Figure 3-3 bottom left). Shape of opening, in case of shallow-seated openings is determined by number of character of joints and foliation, orientation, and bedding partings. In case of deep-seated openings where tensile strength might exceed the strength of rock, it is better to avoid small curvature radii. Furthermore, shape of the opening is designed in such a way that stress will concentrate locally which helps in reducing the areas that need support and special attention can be given to locally concentrated zone (Figure 3-3top). In

Figure 3-3 summary of the principles for design shape depending on their location and stress situation is given.

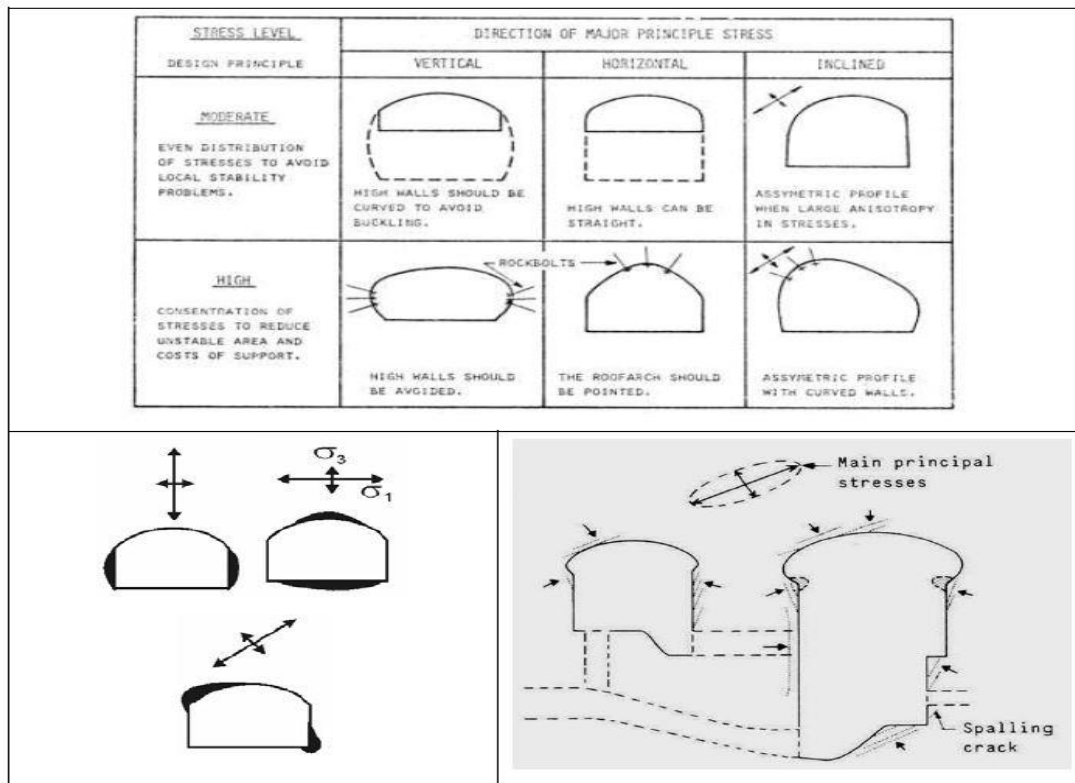


Figure 3-3 Design principles for underground openings with varying stress and directions (Nilsen and Thidemann 1993); (Broch 1984)

3.4.4 Dimensioning

Self-supporting capacity of every rock mass varies and has their own limits. Tunnelling is known as negative construction method and therefore it is hard to limit the size of underground openings as it largely depends on geological and other factors as mentioned above. Depending on the size of the power plant some approachable limits has been set from experience. Constant increase in span would bring more stability problems had not that been the case. For instance, it is more reasonable to fulfil the demand of needed volume by increasing the opening along length axis. If span is increased, curvature has to be maintained the same for stability reasons, which is only possible with increased arch height with every increase in span. But, new challenges arise with extra space thus created. On the other hand, besides the rock mass condition and local stress situation, the thickness between the adjacent openings is governed by height of underground openings (caverns). From general rule of thumb, in good quality rock types with simple design walls between two cavern(s) should be equal to the height of cavern (H) as shown in Figure 3-4 (Nilsen and Thidemann 1993).

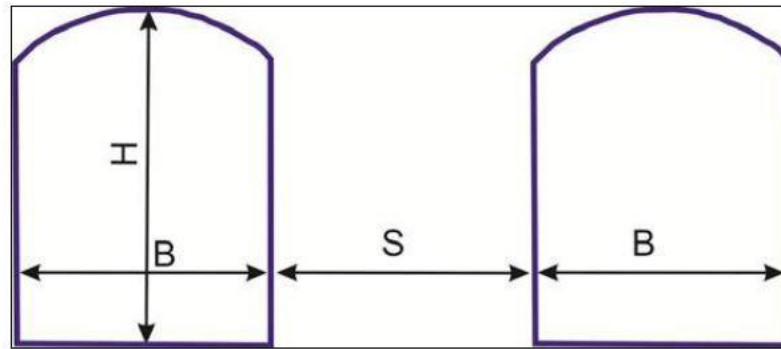


Figure 3-4 Dimensioning of two adjacent caverns (Panthi 2006)

But for complex design use of analytical and numerical model is often carried out for better understanding of the situation. With these above-mentioned requirements both fully lined tunnel also known as conventional tunnel and unlined tunnel opening can be executed. The choice among these two types may vary according to the available geological features and need of project. In case of hydropower, tunnels can vary from low pressure to high pressure. If good rock conditions are available, it is not always mandatory to go for intensive protection except for local regions near weakness zones and faults, in case of free flowing to low pressure tunnels. Regarding the factors mentioned above (section 3.4), in any case rock types with unfavourable characteristics should be avoided as far as possible. In case of medium to high pressure tunnels including pressure shafts, in hydropower it should be made sure that hydrostatic pressure in the section does not exceed minor principal stress. If it happens then this may lead to failure like hydraulic fracturing, lifting etc. where concrete or fully steel linings are considered as better options to safeguard such situations.

3.5 Design Principles

The stability of tunnels and shafts are highly influenced by the mechanical properties of the surrounding rock and the stress situation and distribution of stresses around the excavation (Panthi 2014). Meticulous geological and technical investigation is required before we proceed to design underground openings mostly in case of unlined tunnels and caverns. Prior knowledge of unfavourable conditions and their positions will help in preparing for uncertainties. It not only helps the designer to fulfil the necessary requirement of structural resistance, durability, and serviceability (Basnet 2018) but also to be safe from the surrounding rock mass deformation that could arise when dealing with high water pressure. Two major issues that should be addressed during such underground openings are briefly described below.

3.5.1 Confinement Criteria:

The sufficient confinement criterion is highly influenced by topography and the distribution of stresses in the valley side. The tunnel or shaft should be placed in such a way that the water pressure acting on the excavation wall does not exceed the lowest principal stress in the rock mass. If the internal pressure is too high, this could result in hydraulic splitting and deformations in the surrounding rocks (Halseth 2018). In order to fulfil this requirement several

design criteria have been suggested over the years. With increasing experience gained from completed projects, the criteria have continuously revised and improved (Nilsen and Thidemann 1993).

3.5.1.1 First Criteria:

This design criterion is used for unlined high-pressure shafts and tunnels. First design criteria are based on equilibrium considerations. According to (Broch 1984) the rule of thumb that was in Norway before 1968, being used for planning of unlined pressure shafts is expressed as:

$$h > c \cdot H \tag{3.1}$$

Where,

$h =$ vertical depth of point studied

$H =$ static water head (m) at point studied

$c =$ Constant with a value between 0.6 to 1.0 for valley sides with inclination from 35° to 60° respectively

Later, after failure of shaft at Byrte, in 1968 having inclination of 60°, this rule of thumb was revised by (Selmer-Olsen 1969), with a concept that the ground pressure given by vertical rock cover is sufficient to resist the water pressure so that jacking is avoided. Inclination above 45° were rather uncommon and thus, this revised rule took inclination into consideration as;

$$h > \frac{\rho_w \cdot H}{\rho_r \cdot \cos \alpha} \tag{3.2}$$

Where, ρ_w is the density of water, ρ_r is the density of rock mass and α is the inclination of shaft.

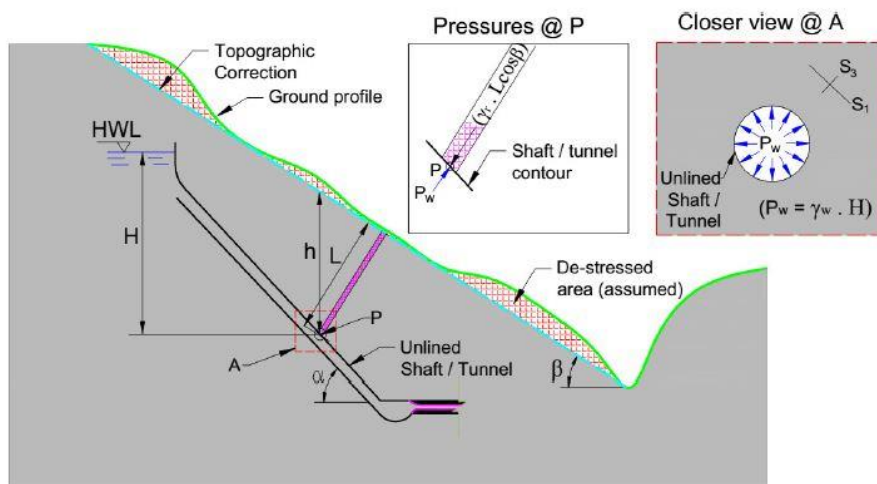


Figure 3-5 Different parameters for different design criteria for unlined pressure tunnels/shafts (Note: S_1 and S_3 are major and minor principal stress and HWL is head water level) (Basnet 2018)

According to (Halseth 2018), in Bjørlykke and Selmer-Olsen (1972) this formula is only applicable to shafts up to 60°. In addition, they state that the formula is only valid up to 35°, and for valley sides steeper than that it is validate only within several restricting conditions. Another formula presented by Bergh-Christiansen and Dannevig 1971 incorporates the inclination valley side as;

$$L > \frac{\rho_w \cdot H}{\rho_r \cdot \cos \beta} \tag{3.3}$$

where, L is the shortest distance between surface and point studied and β is the average inclination of valley side.

3.5.1.2 Finite element method and design charts:

The empirical equilibrium rules of thumb presented above mainly covers the gravitational induces stresses in the rock mass. However, the rock stresses in valley sides largely influenced by topography and in some cases tectonic stresses (Nilsen and Broch 2012). According to (Halseth 2018) in Bjørlykke and Selmer-Olsen (1972) equation 3.3 can be applied only at points where the principal stresses are normal to and parallel to valley side. This could be in the middle part of slope, close to the surface. However, due to topography the principal stress will be different than this in areas near the top plateau and the valley bottom. Thus, there are high chances that this equation gives too optimistic or too conservative overburden values at these points. In 1972, after Bjørlykke and Selmer-Olsen (1972) presented a method based on a finite element analysis of two-dimensional models, a better perspective to these types of problems was possible (Halseth 2018).

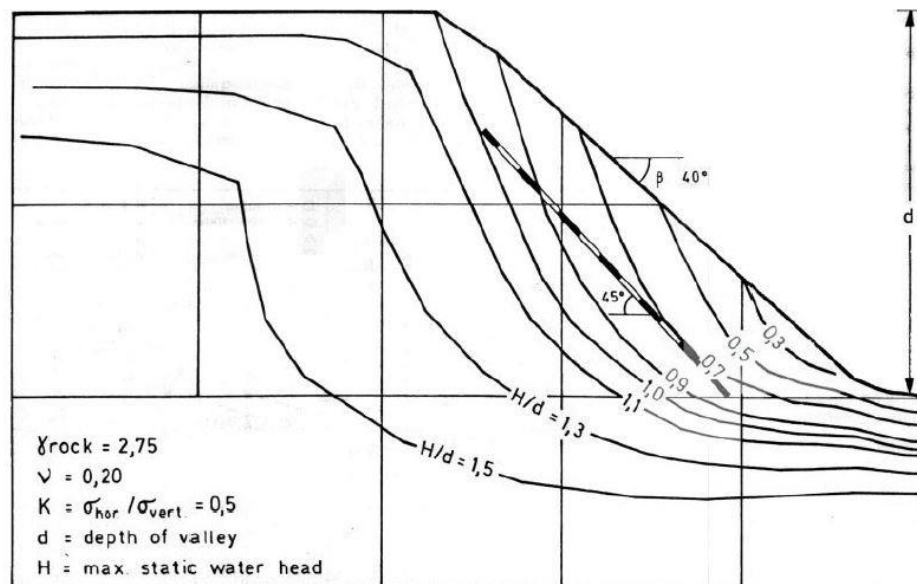


Figure 3-6 Design chart for finite element model. The curves run through points where the internal water pressure equals the minor principal stress in the rock mass. The pressure shaft is placed with sufficient overburden for $H/d=0.7$ (Broch 1984)

This infinite element method is based on strain analysis and can be used with various input for valley inclination (β) and rock properties (γ, ν). As shown in Figure 3-6, a result from such analysis is presented as a chart. Both gravitational and tectonic stresses are responsible for horizontal stress, which is defined by factor k , a ratio of σ_h/σ_v in a distance $5d$ from the valley. H/d is defined as the static water head where, H is the maximum static head and d is the depth of valley. From the calculation of model, a design chart can be obtained showing lines running through points where the water head is equal to the minor principal stress in the surrounding rock. The least overburden required at the given conditions of H/d is represented by the line. At points where the internal water pressure does not exceed the minor principal stress in the rock mass, the tunnel or shaft can thus be placed inside the model.

3.5.1.3 Stress Criteria:

Both the ‘rule of thumb’ formulas and finite element method for design should be used carefully because these are based on two dimensional considerations and a simplified geometry. Especially in areas where the topography forms a ridge, giving a convex shape to the valley side and stress relieve of the rock mass, more attention should be given. Broch (2000) suggests that the ridges should be accounted for the design, which is done by making a revised topographical profile where extra overburden is ignored.

Today, the criterion of enough confinement is often expressed in such a way that the maximum water pressure should never exceed the minor in-situ stress in the rock mass (Panthi 2014) expressed mathematically as:

$$\sigma_3 > H \cdot \gamma_w \quad 3.4$$

where, σ_3 is the minor in situ stress.

Rock stress measurement can be done by hydraulic fracturing and use of numerical modelling to check this criterion. Depending on the complexity of the geology, degree of pre-investigations, accuracy of stress measurements and knowledge of final water head level, usually a factor of safety is required.

3.5.2 Leakage Analysis:

In presence of permeable rock mass, leakage is inevitable even if necessary overburden is provided. Probability of leaking depends on the properties of discontinuities and material infill in the faults and joints. Overburden may become unstable when surface spring is formed, or pressure is created within the rock mass due to large openings and erodible materials like calcite. To make unlined tunnel fully watertight is indeed a costlier task because permeability and discontinuity in rock mass is unavoidable. So, a small amount of leakage must be tolerated, when actual leakage is known from the initially controlled fillings (Nilsen and Thidemann 1993). In-situ test such as hydraulic fracturing must be performed while dealing with high static head in geologically uncertain conditions, for safe positioning of critical sections.

Table 3-1 Recommended factor of safety against hydraulic jacking or uplift (Benson 1989)

Design condition	Normal operating		Water hammer
	static	surge	
The lifting of the rock above horizontal unlined or concrete-lined tunnel.	1.3*	1.1	N/A
Along sloping portion near valleys, and at the end of steel liner, with proper allowance for slope, topography, and possible landslides removing soil cover	1.3	1.1	N/A

*Maybe reduced to 1.2 if geological conditions are well- known.

4 SOLU KHOLA (DUDHKOSHI) HYDRO ELECTRIC PROJECT

4.1 General

The review study report is based on the following documents that has been already conducted:

1. Multi-Channel analysis of surface waves (MASW), Seismic Refraction Tomography (SRT) and Electrical Resistivity Tomography (ERT) conducted by Geophysical Research and Consultancy Pvt. Ltd.
2. Geo Technical Investigation (Drilling) Report conducted by ICGS Pvt. Ltd and
3. Geology Design Project Report conducted by Hydro Consult Engineering Ltd.

4.2 Project Information

Solu Khola (Dudhkoshi) Hydro Electric Project (SKDKHEP) lies in Solukhumbu district of Sagarmatha zone in Eastern Development Region of Nepal. It is an 86 MW Run of River (RoR) type hydroelectric project located at Dudhkaushika and Necha-Salyan Municipalities (former Tingla, Kangel and Panchan V.D.Cs) which extends from latitude of 27°21'53"N to 27°25'15"N and longitude of 86°37'35"E to 86°41'15"E covering about 130 km area (aerial). This project has a design discharge of 17.05 m³/s and utilises gross head of 613.2 m and net head of 598.09 m between proposed intake at Solu Khola and Powerhouse at Dudhkoshi river. Project site is indicated in the map of Nepal as shown in Figure 4-1:

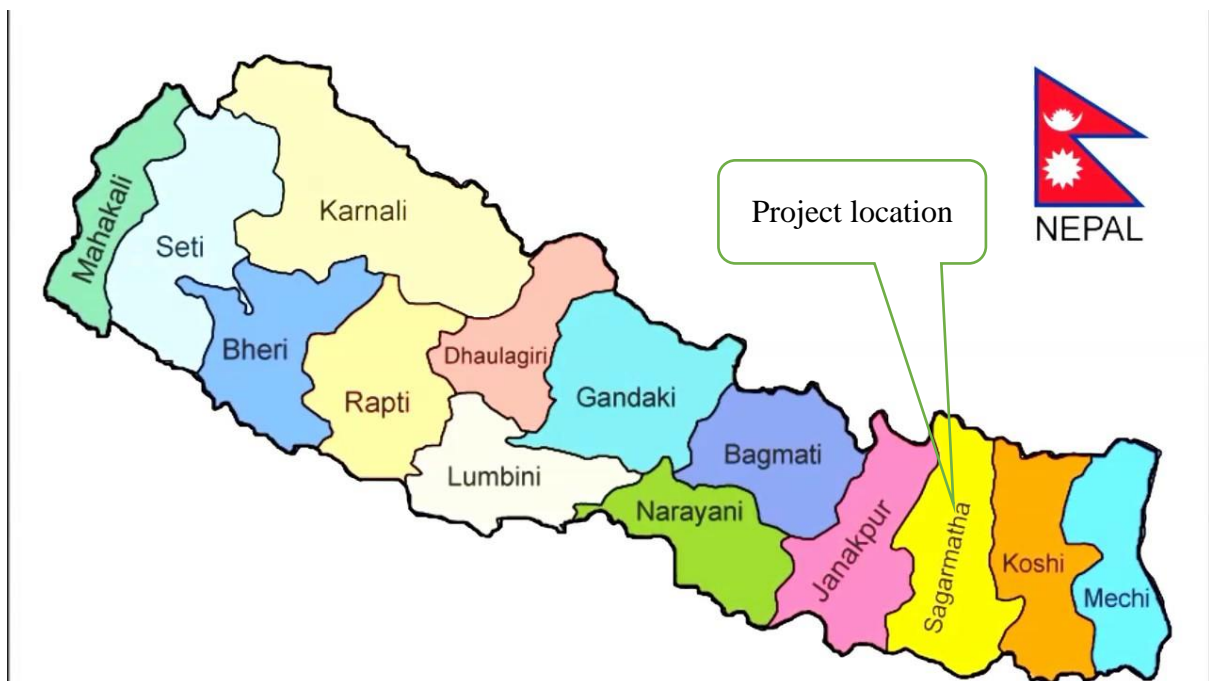


Figure 4-1 Map of Nepal showing project site

The existing design was done by Hydro Venture Pvt. Ltd. and this thesis relies mainly on the raw data provided by them. The main hydraulic structures of the project are; headwork located at Gairigaun village of Necha-Salyan Rural Municipality, approximately 600 m downstream of the suspension bridge over Solu Khola at Sanghutar, Khola at Sangutar (Bhadaure), surface

settling basin, underground headrace tunnel, inclined pressure shaft that passes through different places of Dudhkaushika Rural Municipality, surge shaft, and surface powerhouse. The proposed powerhouse, switchyard and tail race canal are located near Maikubesi of Dudhkaushika Municipality, on the right bank of Dudhkoshi river which is about 3.5 km upstream of the confluence of Solu Khola and Dudhkoshi River which is represented below in Figure 4-2.

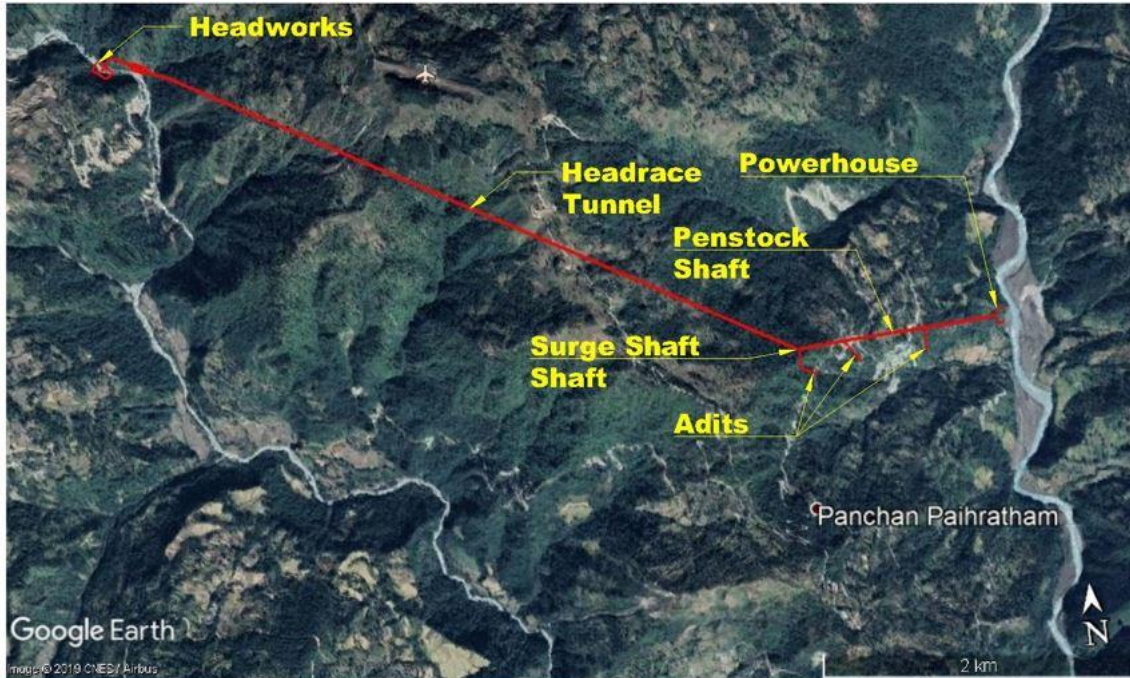


Figure 4-2 Google map showing different proposed components of SKDKHEP

The headrace tunnel has a total length of 4259.0 m among which the penstock pipe is 2085 m which includes drop shaft 1 with length 224.18 m horizontal section 1 of length 715.65, drop shaft 2 of length 199.61 m and horizontal section 2 of length 926.94 m. The tail water will be released at the level of 640.57m in the Dudhkoshi River.

4.3 Geology of Study Area

Most of the hydropower projects and especially the underground structures are situated in lesser Himalayan or lower part of higher Himalayan (Panthi 2006). The Solu Khola Dudhkoshi Hydroelectric project lies in the Lesser Himalaya of Okhaldhunga Window based on the Nepal Geological Map Compiled by Department of Mines & Geology (1996). Augen gneiss of Paleozoic age and the Kuncha formation of green phyllite of Precambrian age are main rock types. The rocks of the area are exposed by Okhaldhunga window and surrounded by the Main Central Thrust (MCT) in north and south.

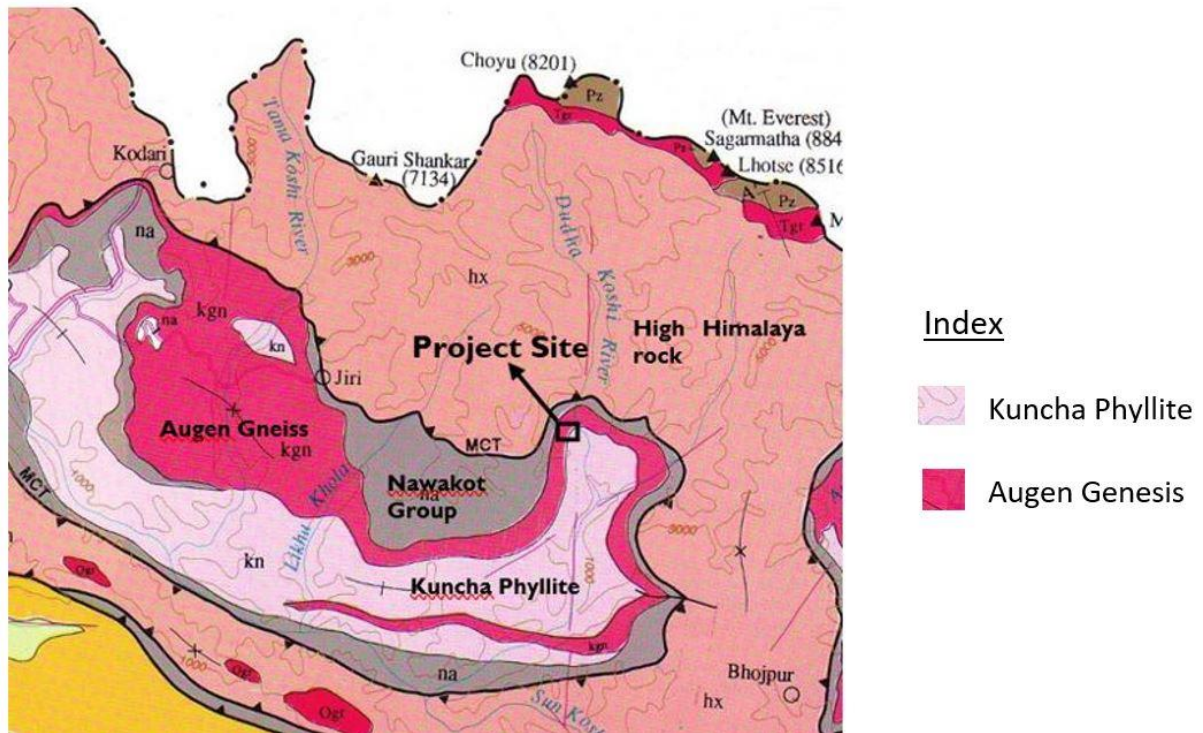


Figure 4-3 Regional Geological map showing project site (Compiled by Department of Mines & Geology, 1996)

Geologically, the project area lies in the lesser Himalayan Zone of the Okhaldhunga window in Eastern Nepal, consisting various lithological units such as gneiss, phyllitic schist, phyllite and slate intercalated with quartzite. The rock unit consisting of medium to very thick bands of light grey to grey augen gneisses with schist partings is extensively encountered throughout headworks, tunnel alignment, and surge tank area. This unit lies within Lesser Himalayan rock unit of the central Nepal and is known as Ulleri Augen Gneiss or locally as Mellung Salleri Augen Gneiss. The lower portion of the project area such as part of surge shaft, penstock and powerhouse is in grey to green grey, foliated, moderately strong to weak schist, phyllite and slate with minor intercalation of quartzite. This rock unit lies within the Seti Formation of Lesser Himalayan Rock unit equivalent to Kuncha Formation of Central Nepal.

4.3.1 Stratigraphy

The rocks of the eastern Nepal divided into following four major groups. These are:

1. Quaternary Deposit
2. Midland Group
3. Kathmandu Group
4. Himal Group

4.3.1.1 Quaternary Deposit

In Solu Khola and Dudhkoshi River basins, within the project area, fluvial terrace and slope terrace deposits are present. They are recognized by their unconsolidated character varying in size from boulders (maximum diameter 10m) and gravel to fine silt and clay.

4.3.1.2 Midland Group

The Midland Group is subdivided into Gondwana Sub-group, Lakharpata Sub-group, Pokhara Sub-group, and Dailekh Sub-group. In the Okhaldhunga area, only the Ghan Pokhara Formation (Gp), Seti Formation (St), Kushma Formation (Ks), and Ulleri Formation (Ul) of the Pokhara Sub-group are exposed. Among them Seti Formation and Ulleri Formation are present in the project area which are described in Table 4-1.

Table 4-1 Litho-stratigraphical sequence of the project area

Lithological Sequence		Name of Formation	Geological Age
Quaternary Deposit		Alluvial and Colluvial Deposits	Recent
Pokhara Sub - Group	GhanPokhara Formation (Gp)	Black carbonaceous phyllites and slates, grey to greenish grey shales with limestone bands.	Upper Precambrian to Late Paleozoic
	Seti Formation (St)	Grey to greenish grey phyllites, gritty phyllites, quartzites, with minor conglomeratic layers, and basic intrusions.	
	Ulleri Formation (Ul)	Augen gneisses with Feldspathicschists, intrusion of granite	
Himal Group	Himal Gneiss (Hg)	Two mica gneisses, granitic gneisses, banded gneisses, kyanite bearing gneisses and migmatites and thin bands of marbles	Precambrian
	Panglema Quartzite (Pg)	Fine-grained compact quartziticschists and quartzites occasionally limestones	
	Dware Khola Schist (Dk)	Medium to coarse-grained quartz muscovite biotiteschists, garnetiferous schistose gneisses and kyaniteschists	
	Hm	Undifferentiated Hg, Pg, Dk	

4.3.1.3 Kathmandu Group

The Kathmandu Group is subdivided into Phulchoki Sub-group and Bhimphedi Sub-group. In the Okhaldhunga area, only Tawa Khola Formation (Ta) and Shirping Khola Formation (Sp) of the Bhimphedi Sub-group are outcropped. The rocks of the Kathmandu Group are not present in the Project area.

Himal-Group

The Himal Group of Precambrian age is divided into 4 formations: Himal Gneiss (Hg), Panglema Quartzite (Gp), Dware Khola Formation (Dk), and Ulleri Formation (Ul).

4.4 Assessment on Rock Engineering Aspects

During the planning phase, investigation of the rock mass quality along the headrace tunnel was done based on surface and few sub surface investigations. The tunnel is yet to be constructed and thus, the actual rock condition is not known. Owing to this, it is hard to predict whether the actual rock mass conditions varies from the predicted one. However, we assume that the actual rock conditions will be similar as predicted and thus, only the rock mass quality that was predicted during planning phase investigation is discussed further.

4.4.1 Rock types and their character:

4.4.1.1 Augen gneiss:

Some part of the headrace tunnel of alternate design will also pass through these rocks. It is commonly known as Ulleri Augen Gneiss and also called Melung Augen gneiss in Tamakoshi valley. This gneiss is extended from Dudhkoshi valley to Tamakoshi valley and bigger body is exposed around Tamakoshi valley. Augen gneiss is grey, coarse to very coarse grained, widely foliated to massive, medium strong to strong porphyroblastic as shown in Figure 4-4 with bands of very weak green chlorite-talcosite schist bands parallel to the foliation. Granitic gneiss bands are also observed. These tectonized schist bands created major georisks during construction of Khimti I Hydropower Project (Sunuwar 2011) and therefore it is very important to identify these tectonized schist bands i.e. shear/weak zones which are considered the source of georisks. The tectonized schist bands characterised by weak, crenulated, sheared, chlorite-sericite-talcosite schist with clay gouge and are major considered as weak and shear zones which are aligned parallel to the foliation plane (15° - 25° / 000° - 010°). They are few centimetres to tens of metre thick and are parallel to the foliation at intervals of 2 to 200 m forming a gentle topography. Augen Gneiss was extended from Tinla, headworks to Panchan, surge shaft area and headrace tunnel and surge shaft was constructed in the gneiss in the existing design.



Figure 4-4 Outcrops and close view of Augen gneiss at headwork (Hydro-Consult 2016)

4.4.1.2 Green Phyllite:

Phyllite was extended from Panchan, penstock shaft to Maiku, powerhouse area. Penstock shaft, penstock tunnel and surface powerhouse in the existing design lies in the phyllite. Major

part of the penstock tunnel in the alternate design will pass through this rock. Green phyllite known as Kuncha) is grey to green, fine to coarse-grained, slightly to moderately weathered, closely to widely foliated, weak to medium strong crenulated with strong green quartzite intercalation and 1 to 20m thick bands as shown in Figure 4-5.



Figure 4-5 Outcrop and close view of green phyllite with quartzite intercalation at Powerhouse (Hydro-Consult 2016)

Mica content in Augen Gneiss varies from 15% to 20% whereas in meta-siltstone is 40% which is high which could reduce strength of rock (Hydro-Consult 2016). Bore holes (BH) 5 and (BH) 6 done at powerhouse site indicates presence of phyllite bedrock only after 41.5 m onwards and 37m onwards respectively.

Table 4-2 Summary of second phase Uniaxial Compression test near powerhouse location

Sample No	Depth	Sample			Failure Load (kN)	Unconfined compressive strength(N/mm ²)
		Diameter mm	Height mm	Weight gm		
1	15.33-15.44	44.3	122.7	528.8	14.3	9.3
2	16.42-16.65	44.3	116.5	501.7	53.5	34.7
3	19.52-19.64	44.3	133.0	568.2	20.7	13.4
4	22.00-22.48	44.4	124.3	529.9	33.6	21.7

Construction of underground structures in green phyllite is challenging due to low strength, low deformation modulus properties and closely spaced with jointed nature. The UCS values near powerhouse from second phase are low as presented in Table 4-2 ranging from 9.32 MPa to 34.7 MPa. Large size cavern may not be constructible in this weak phyllite. (ICGS 2017) Thus, possibility of underground power house has been dropped.

4.4.2 Joints

Most serious geological problems in development of infrastructure are generated by faults and shear zones (Sunuwar 2011). Fault, shear and weak zones ranging from few centimeters to few meters were identified in the project area based on the field evidences and geomorphologic features on the Google Earth, as mentioned in the DPR. There are 2 types of shear/weak zones and faults. Major shear zone is 1 to 20 m thick and oriented parallel to the foliation plane (NEE-SWW) dipping ($<20^\circ$) towards north. Similarly, another steep fault is few centimeters to 2m thick and oriented E-W direction and dips ($>65^\circ$) towards south. According to the DPR report huge wedge failures and rockslides in Dudhkoshi river is a due to combination of shear/weak zones along the foliation and steep faults.

The shear/weak zone parallel to the foliation plane is expected to be Clayey brittle shear zone (Sunuwar 2011) containing sheared blocks with majority of clay gouge and holding ground water above. This shear zone is likely to cross the headrace tunnel almost parallel and oblique. These shear zones are gently dipping ($<20^\circ$) which will be more problematic during construction due to continuous exposure of shear zone in long distance. Other small shear/weak zones of few centimeters thick along the foliation plane were also present.

Table 4-3 Properties of joints in Phyllite near powerhouse

Properties	Foliation (F1)	Joint (J2)	Joint (J3)
Dip/dip direction	28-40°/340-345°	60-70°/030-040°	50°/155-160°
Spacing (cm)	2 - 20	5 - 50	20-200
Aperture (mm)	0-1	Tight-open	0-5
Roughness	Smooth	Rough undulating	Rough planar
Filling	Clay, Sericite	Silt-open	Silt open
Weathering	Fresh-Slightly	Slightly	Slightly
Persistence (m)	> 20	0.5-3	0.5-10
Water	Dry	Dry	Dry

4.4.3 Rock mass condition along penstock alignment and powerhouse

The rock mass quality was rated based on the surface rock mass outcrop along the tunnel alignment and interpolating data from surrounding rock outcrop. In addition, according to DPR Geological report, knowledge of geomorphologic features, aerial photo and topographic features were considered to estimate the quality of rock mass in poor rock outcrop areas. During surface geological mapping RQD, joint number, joint roughness, joint spacing, joint filling, joint alteration number, ground water condition and stress condition were rated for rock mass classification. RQD, in the report has been estimated by empirical formula ($RQD = 115 - 3.3 \times J_v$) by finding number of joints per 1 m^3 (J_v) which resulted RQD value in range due to minimum and maximum joint number. In average joint number varies from 10 to 20. However deeper at tunnel level joint number are expected to be decreased. So, it is expected that RQD could be greater than 40% except in shear/weak zones and fractured rock. Similarly, 3 sets of joint number are prominent except some places. However steep joint was found filled by thin clay based on tunneling experience in Nepal. Finding the filling material at surface was difficult due to washing of filling materials. Joint alteration number was found sensitive for downgrading and upgrading of Q-value. Major weak/shear zones were rated in extremely to exceptionally poor rock mass. Q-value was estimated in close range like 1 to 4. RMR and GSI values were also taken into consideration for tunnel design. The rock mass along the tunnel alignment are divided into six classes based on Q system for purposed of rock support design. Rock Mass Distribution in the headrace tunnel is presented in Table 4-5.

However, this preliminary predicted rock mass may not be 100% precise due to limited rock outcrop, limited site investigation and interpolation of rock mass quality from surface observation down to more than 300m tunnel level. Nonetheless, identification of shear/weak zones would surely help to propose the new alignments of penstock. While doing so, the joints are assumed to move parallel deeper into the surface and does not changes in geometry and size.

4.5 Engineering Geological Conditions

4.5.1 Weir Site:

The surface material in this area can be categorized as medium dense soil. Between depths 2.5 m to 4 m a formation equivalent to very soft or hard soil is located. Soft rock or very hard soil is expected to be located at depths between 6 m to 8 m. High to moderately jointed bedrock is expected to be located at depths about 13 m. The bedrock is overlain by colluvial and alluvial deposits; in the slope on the right bank colluvial deposit and detached blocks are present while alluvial deposits are seen on the left bank. Tomograms indicate that the bedrock is likely to be dissected by several weak zones or sheared zones. The thickness of the colluvial and alluvial cover in the area is expected to vary between 10m to 15 m. However, on the slope of right bank the thickness of the detached blocks and colluvium is lower. The elevation of the top of the bedrock varies between 1240 m to 1250 m in the Weir Site. Allowable bearing capacity of the material at depth between 4 m to 6 m is about 339 KN/m^2 .

4.5.2 Settling Basin

The surface material in this area can be categorized as medium dense soil. Between depths 6 m to 8 m a formation equivalent to very soft or hard soil is located. High to moderately jointed bedrock is expected between depths 13 m to 16 m. Tomograms indicate three-layered subsurface: first layer of very loose material, second layer of consolidated material and the third layer of bedrock. The second layer furthermore have two sub layers: the upper part is relatively compact layer and lies above water table while the lower part below the water table is either cemented deposit or highly weathered and highly fractured bedrock. The elevation of the water table in this area varies between 1250 m to 1255 m. The elevation of the bedrock varies between 1247 m to 1250 m. However, this bedrock is expected to be jointed. Allowable bearing capacity of the material at depth between 10 m to 14 m is about 395 KN/m².

4.5.3 Surge Tank

The surface area is covered by thin loose soil whose thickness varies between 1 m to 5 m, usually thick towards the uphill side. In the uphill side bedrock is not encountered. Bedrock in this area is encountered only in the lower portion (towards downhill side) at the elevation of about 1305 m. Tomogram in this area indicates that the bedrock is highly sheared. At least three sheared zones are expected in this area. Bedrock could have minor sheared zones between surface lengths 0 m to 240 m. Low resistivity zones formed on top of the bedrock. These zones are parallel to the slope mainly due to the formation of moisture circulation zone. The depth until the intact bedrock in the proposed Surge Tank area is about 60 m.

4.5.4 Adit Portal

Thin loose soil layer whose thickness varies between 0.5 m to 2 m covers the area. The depth upto cemented deposit or highly weathered rock varies between 3 m to 6 m along the profile. This could be because of the sheared zones. The bottom part of the section is interpreted as jointed bedrock. Jointed bedrock is located at depth about 12 m from the surface. Tomogram indicates that the lower portion of the section is predominated by low resistivity zones, which is an indication of the sheared zones.

4.5.5 Headrace Tunnel:

In the tunnel alignment upstream of the surge tank the tomogram indicates few steeply dipping low resistivity zones which are likely to be related with sheared zones. Several low resistivity patches formed on top of the bedrock are due to the moisture circulation. These zones are likely to be highly fractured and weathered bedrock from 160 m onwards along the profile. The depth to the intact bedrock varies between 50 m to 60 m along the profile. Tunnel alignment in this area mostly would pass through fair to good rock mass zones with very few sheared zones. Tomogram indicates that the ridge is dissected by several zones of variable resistivity. Furthermore, low resistivity zones encountered could be formed due to the presence of schist bands in the host of less conductive gneiss. All these rock masses are covered by colluvium and eluvium along with displaced and open jointed rock mass. The thickness of the cover varies between 5 m to 45 m; thinner towards the downhill side and thicker towards the uphill side.

4.5.6 Powerhouse

Surface material in this area is categorized as very loose deposit. The thickness of the deposit is about 2 m. Medium dense soil is overlain by this loose layer. A formation which can be categorized as very soft rock or hard soil is located at depth about 7 m. Soft rock or very hard soil is expected to be located at depth about 16 m. Seismic Refraction Tomography (SRT) done in this area does not indicate any trace of bedrock within the range of investigated depth. However, in another SRT done nearby the previous SRT, bedrock is encountered in the upper and central part of the profile. Both sections indicate that the area is covered by thick loose soil. Maximum thickness of the overburden in the area is towards the valley and minimum towards the uphill side. Bedrock encountered was considered to be jointed. A formation similar to high to moderately jointed rock mass is expected to be located at depth about 21 m. This could also be related with highly cemented material. Bearing capacity of the formation at depths between 18 m to 21 m is about 462 KN/m².

4.6 Present Design Review

Figure 4-6 is the existing layout and longitudinal section showing all the major components of SDKHEP. It is characterized by two vertical shafts at chainage 4+259 and 5+000 respectively and a sub-surface powerhouse with tailrace culvert.

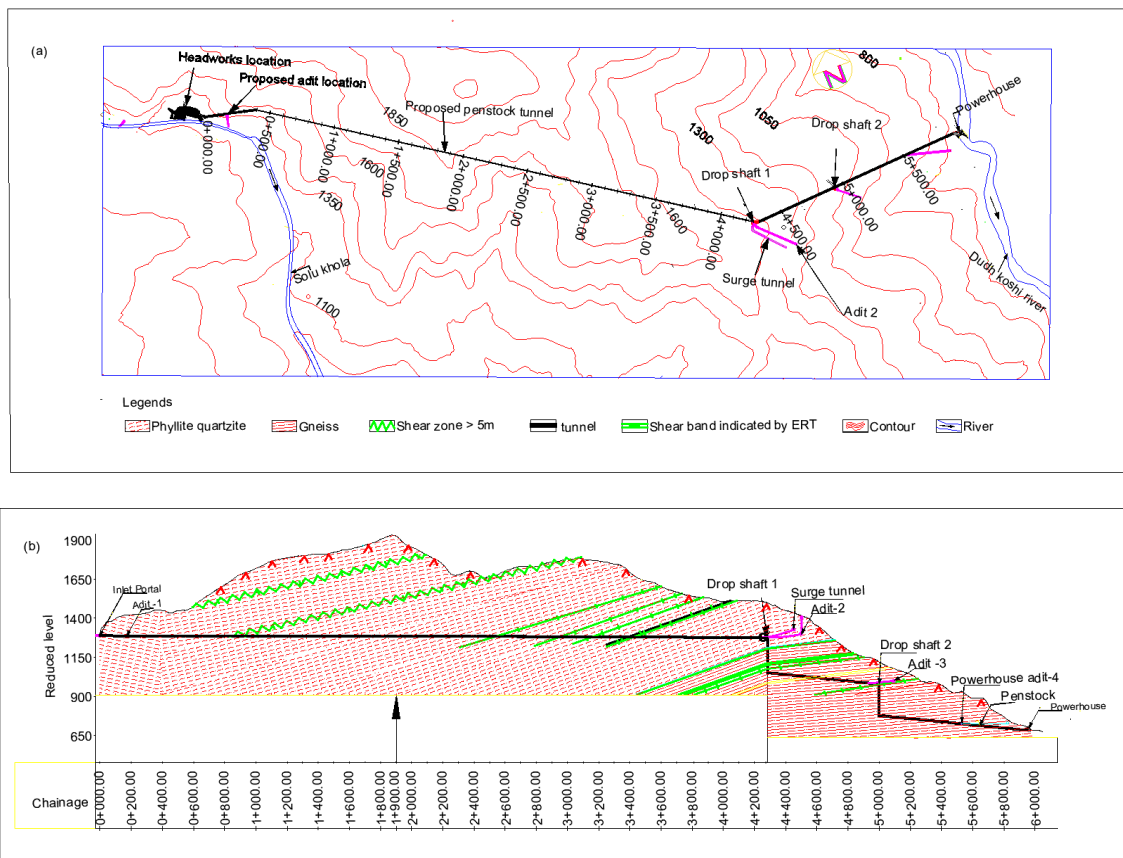


Figure 4-6 a) Layout and b) Longitudinal section of existing Headrace Tunnel (Original), Not to scale

Although our main focus would be on pressurized waterways, general design review of major components in brief is presented here;

4.6.1 Diversion Weir

Approximately, minimum 2 m to maximum 6 m excavation (depending on undulating ground topography) is necessary for construction of the diversion weir based on the design. In this depth, weir foundation will be on the alluvial origin boulder mixed heterogeneous soil. In addition, water seepage will be risk. Cut off wall from the bedrock level will be considered for the protection of seepage instead of clay blanket upstream. Gravity type weir is being proposed having total length of 31.8m and the weir crest level being at elevation 1260.50 masl.

4.6.2 Surface Settling Basin

Surface settling basin is being proposed on the left bank in gently dipping loose alluvial deposit of boulder mixed soil overlain by debris flow deposit. About 12 to 13 m excavation will be necessary for settling basin construction according to design. Hence, foundation of surface settling basin will be on the weathered rock soil and cemented compacted soil. Number of bays in the settling basin is proposed as four and dimensions are (Lx Bx H) 85.0 m x 9.5 m x 4.5 m. It will have an efficiency of 90 % and the nominal size of the trapped particle of 0.15mm.

4.6.3 Headrace Tunnel

This project has intake at Solu Khola and Powerhouse at Dudhkoshi River and in between these two lies Kangel-Panchan hill. Therefore, headrace tunnel (HRT) seemed to be only obvious option for waterway to cross Kangel-Panchan hill. HRT option without Adit at intermediate was considered due to unavailability of suitable place to introduce adit at middle. Two adits in Inlet and outlet will be considered for excavation of HRT. In this option HRT length will be around 4,500m and excavation distance from one face will be 2,250 m which may not be so convenient if more shear/weak zones may encounter. However, it has been planned to make it constructible by using mechanized tunneling equipment like boomer drilling machine, robot shotcrete machine with efficient mucking and ventilation system. Invert D shaped HRT with total length of 4259m has been proposed with a finished dimension of 4.0 m x 4.25 m (B x H). Height of tunnel is designed in such a way to accommodate about 0.6m height for ventilation duct with clearance for equipment movement. Green phyllite underlies the gneiss and exposed at around 1300-1400m elevation in Pancham and surge shaft areas which indicates that phyllite will encounter at the end of headrace tunnel and mostly in penstock tunnel. In addition, total 15 numbers of identified shear/weak zones thicknesses ranging from 1 m to 20 m aligned parallel to the foliation plane with gently dipping at 15°-20° which will continue for long distance if encounter. However, only few shear/weak zones could cross the tunnel alignment due to low angle dipping nature.

4.6.4 Surge Shaft/Surge Tunnel

Geophysical investigations (SRT-4, SRT-5, DDERT-7 & DDERT-8) showed that about 30 to 60m thick soil deposit and surge shaft will not be feasible to construct in such thick soil.

Likewise, for 8m diameter surge tank design, surge tank location needs to be pushed deep inside to keep minimum cover of 130m (50m soil + 30m weathered rock + 50m rock) and aeration tunnel will be greater than 200m. In addition, starting of penstock shaft requires minimum 130m cover (50m soil +30m weathered rock + 50m rock).

Consequently, it was considered better to construct surge tunnel surge tank with multiple chambers due to thick soil cover and long aeration tunnel. Access was not considered to be necessary. Inverted D shaped Surge Tunnel was designed to be of length 342.72 m and finished dimension of 4.0 m x 4.0 m (B x H).

4.6.5 Penstock

This is the main area where this thesis will put focus on. Based on the topography of the project area underground option was chosen. Penstock will be divided into two stages by introducing adit at middle for construction purposes. Inclined shaft was considered to be risky due to less rock cover and hence combination of vertical shaft and horizontal tunnel was considered. The penstock alignment is planned to pass through weak to medium strong, closely to widely foliated green phyllite with 3 sets of joints. Total 8 numbers of shear/weak zones thicknesses ranging from 5m to 14m have been detected by 2D ERT (DDERT-7, DDERT-8 & DDERT-9) along the penstock slope. These shear/weak zones are expected to cross the proposed penstock.

From tunneling point of view this phyllite weak rock and is not suitable for big size tunnel due to risk of deformation and over break. However, small size tunnel is constructible but risk of over break during construction of inclined (45°) penstock tunnel as compare to vertical shaft. By considering probable geo-risks during construction and available rock cover, underground penstock is considered as vertical shaft and 10-12% gradient penstock tunnel.

The total length of 2085.00 m penstock until trifurcation has been further divided into four parts as: drop shaft 1 with length 224.18 m horizontal section 1 of length 715.65, drop shaft 2 of length 199.61 m and horizontal section 2 of length 926.94 m. The steel pipe having internal diameter of 2.5 m for 1121 m length (pipe including 22.55 m length up to surge tunnel), 2.25 m internal diameter for 546 m length and 2.10 m diameter for 418 m length has been designed.

4.6.6 Surface Powerhouse

A powerhouse having dimensions 54.6 m x 16.2 m x 19.45 m has been proposed in bedrock ridge of green medium strong to weak phyllite with strong quartzite interactions and bands. Bedrock observed around the powerhouse area is thinly to widely foliated, light grey to green, weak to medium strong phyllite intercalated with quartzite and three sets of joints. Estimated RQD is 20-30%. Powerhouse has been designed to be constructed in bedrock by excavating steeply dipping rock ridge from elevation 670 m down to the design level of elevation 640.57 m. Critical foliation joint is moderately dipping due north which is inside hill and favorable for stability. However, stress relief joint (50°/145°) which controlled the dip slope of the ridge by making 50° angle may be critical for slope stability towards upslope and hence slope stabilization work is necessary in upslope cutting section. Bedrock exposed from north to west side whereas small shallow colluvium deposit present in SW side. Cut slope design in rock will be 80° to 84° angle with 1m wide bench in every 8-10m length supported by 5-8 cm thick wire

mesh or fiber shotcrete with pattern of 3m long rock bolts in 1.5-2 m spacing. Similarly, in colluvium deposit cut slope design will be 45° angle with 1m wide bench in each 8-10m length supported by 10-12cm thick wire mesh shotcrete with pattern of 3m long soil anchor in 1.5m spacing. Weep holes has been considered at 1.5 to 2m² spacing in shotcrete to release pore water pressure. In addition, rock anchoring with shotcrete has been considered to be necessary in remaining rock portion towards north i.e. river side.

4.6.7 Tailrace Canal

It is an RCC conduit of length 75m. Tailrace area consists of flat alluvial deposits about 2m high from the river bed level. It contains about 60-70% rounded shaped gravels, cobbles, boulders and about 30-40% silt-sand.

4.7 Critical Comments

Underground structures of this projects are headrace tunnel, surge shaft/surge tunnel, drop shafts and horizontal pressure tunnels. The penstock alignment after the surge tunnel will be considered for the possibility of alternative design which will be described in Chapter 5. Though the possibility of Underground Cavern was supposed to investigate, the geology and the rock mass properties did not let do so thus, the originally proposed surface option was considered to be fine.

The location and properties of expected shear zones are summarized in the Table 4-4 and the rock mass distribution in headrace tunnel is presented in Table 4-5.

Table 4-4 Properties and location of expected shear zones

No	Location, tunnel	Shear/weak zone	Orientation	Thickness in tunnel (m)	Remarks
			(Strike/dip)		
1	Expected to cross from Ch. 620-625m	Steep fault with fault gouge.	E-W/ $>70^\circ$ S	< 5	Crosses oblique to the strike.
2	Expected to cross from Ch.1884-1856m	Steep fault with fault gouge and charged with ground water.	E-W/ $>70^\circ$ S	< 10	Crosses perpendicular to the strike.
3	Expected to cross from Ch.865-891m	Shear/weak zone with thick clay gouge and holding ground water above it.	E-W/ $<18^\circ$ N	< 26	Crosses oblique to the strike.

4	Expected to cross from Ch.1700-1722m	Shear/weak zone with thick clay gouge and holding ground water above it.	E– W/>18°N	< 22	Crosses oblique to the strike.
5	Expected to cross from Ch.2535-2557m	Shear/weak zone with thick clay gouge and holding ground water above it.	E– W/>18°N	< 22	Crosses oblique to the strike.
6	Expected to cross from Ch.2944-2963m	Shear/weak zone with thick clay gouge and holding ground water above it.	N– S/>70°E	<19	Crosses oblique to the strike.

Table 4-5 Rock Mass distribution in headrace tunnel (Hydro-Consult 2016)

Support class	Rock class	Q - value	Percentage
I	Fair to Good rock	>4	15%
II	Poor rock	1 – 4	36%
III	Very poor rock	0.5 – 1	28%
IV	Very poor rock	0.1 – 0.5	13%
V	Extremely poor rock	0.1 – 0.01	2%
VI	Exceptionally poor rock	< 0.01	6%

Based on the geological data and interpretation, it has been expected that only four shear/weak zone of 1-20 m would cross headrace tunnel. Certainly, the shear/weak zones will induce squeezing problem where they cross. Hence, the DPR report suggests that special treatment like flexible support system will have to consider if overburden exceeds 200m and squeezing condition is severe.

5 ALTERNATIVE DESIGN OF WATERWAY

5.1 Layout Design

Two alternative options of the penstock tunnel have been proposed on the basis of available geological information. Basic difference between these two options is the placement of the cavern. Further cost and stability analysis of these both options are needed to conclude the better one.

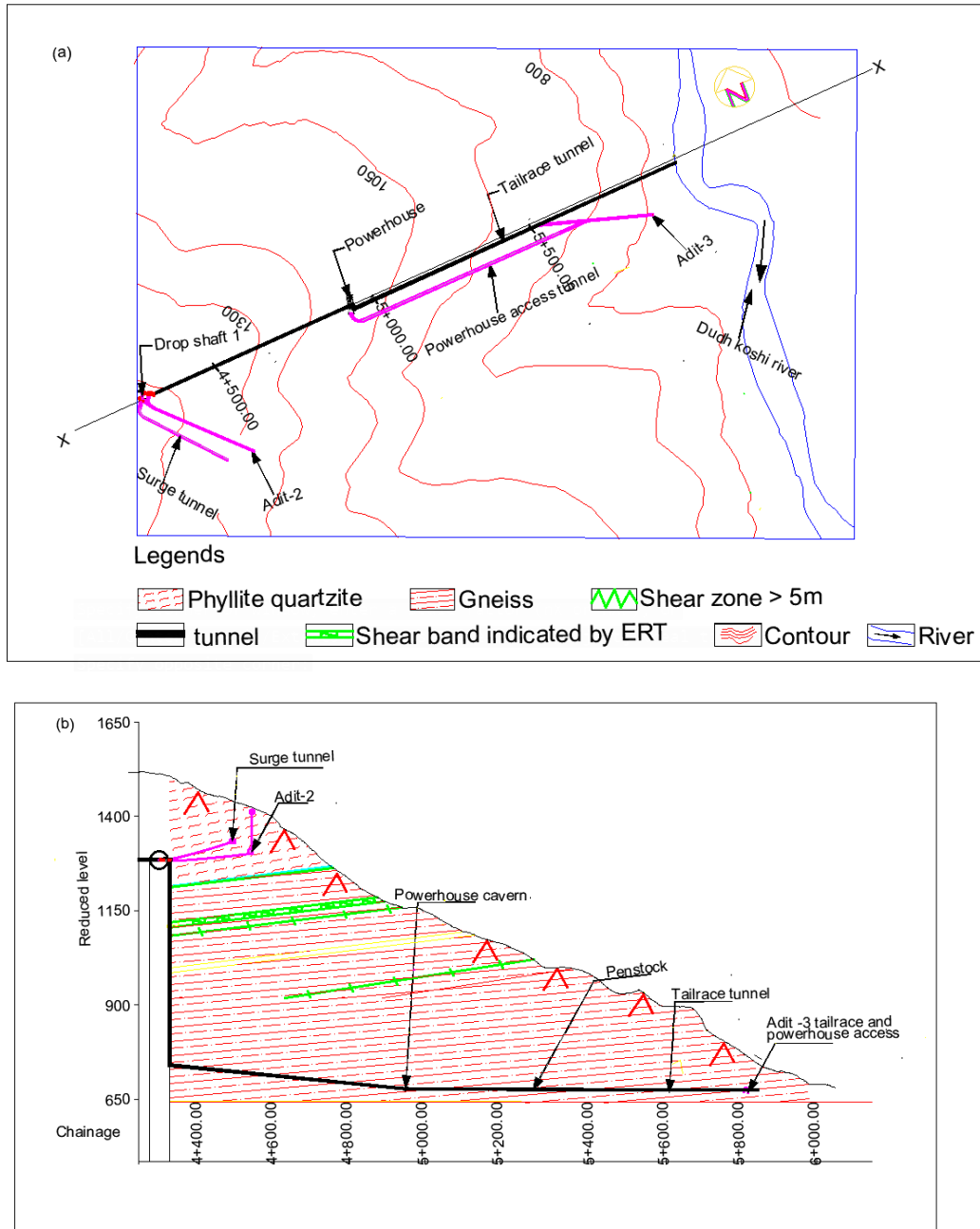


Figure 5-1 Penstock alignment (a) Layout; (b) Longitudinal section along X-X (Alternative 1)

Figure 5-1 is the layout and longitudinal of alternative 1, where an underground powerhouse has been introduced at chainage 4+490. The vertical drop shaft is kept longer than that of existing layout, so that it clearly passes all the shear zones that else could have had affect the underground structure. The presence of multiples shear and weakness zones causes the instabilities in the tunnel periphery. The degree of weakness leads to roof collapses and squeezing of the walls and invert if severe. Penstock tunnel already has to carry higher hydraulic pressure, so it is better to omit the weakness zones in the penstock tunnel alignment during the design period. The most remarkable feature of this first alternative is that the powerhouse is kept underground, a new tailrace tunnel and adit 3 has been introduced. The elevation of the tailrace level would be the same as original one. The construction processes will be eased on doing so.

From Figure 5-2, it can be seen that not only the number of drop shaft has been reduced (from 2 to 1) but also the length of drop shaft is shorter in alternative 2 than the existing one. On doing so, it has been marked that the vertical drop shaft alone has crossed all the weakness zones and the new alignment of the penstock does not cross any of the shear zones.

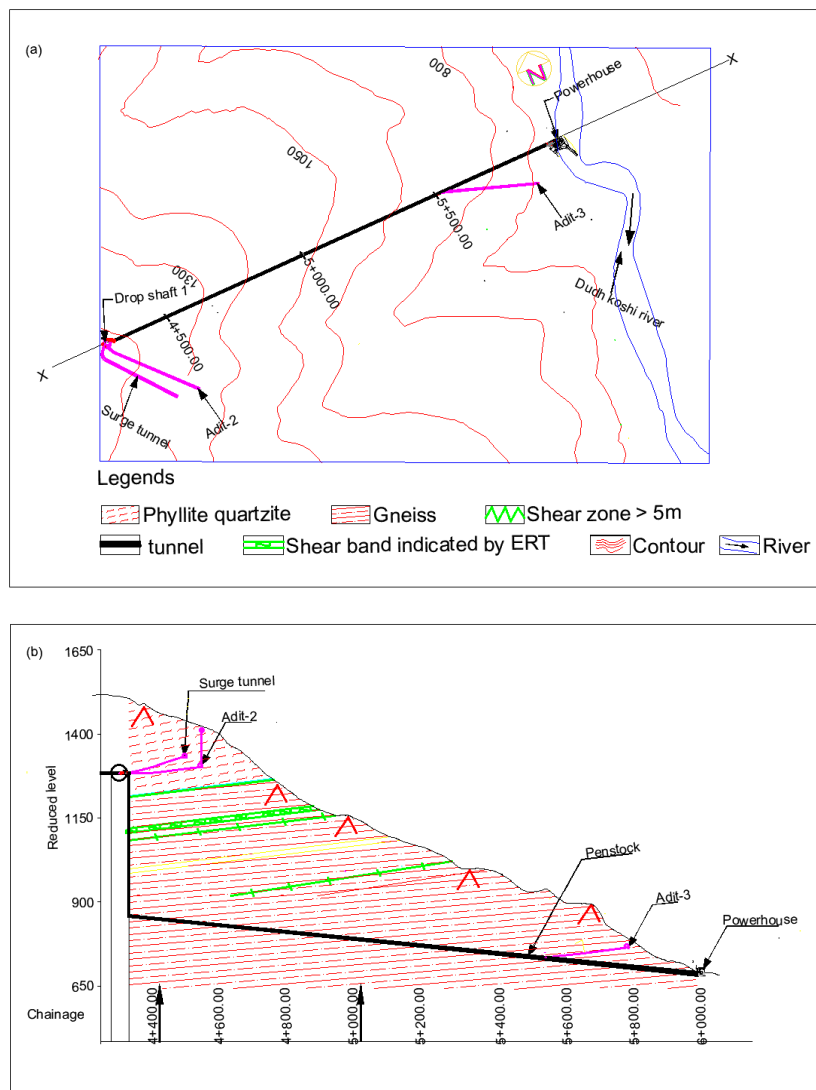


Figure 5-2 Penstock alignment a) Layout; b) Longitudinal section along X-X (Alternative 2)

Moreover, possibility of the underground powerhouse cavern in alternative 2 was not done because it needs larger underground opening which may lead to instability around the opening or the support required for the opening will be increased in larger amount making the construction uneconomic. So, powerhouse cavern is being decided to be kept at its original position which overrides the limitation of proposed alternative 1.

5.2 Comparison

The characteristics difference between the prevailing and the proposed design are summarized as:

Table 5-1 Comparison of salient features of original design with new alternatives

	Option 1	Option 2	Existing Design
Vertical shaft length (m)	513.6	340.5	413.79
Inclined shaft length (m)	650.8	1651.9	1654.68
Total shaft length (m)	1164.4	1992.4	2068.47
Inclined shaft gradient (%)	12%	10%	
Penstock Branches total length (m)	66.90 m	66.90 m	66.90 m
Tailrace tunnel (m)	1024.5	Tailrace culvert	Tailrace culvert
Tailrace Tunnel Gradient (%)	0.10%	0.10%	NA
length of adit 3	226.5 m	300 m	536.87
Powerhouse access tunnel length	855 m	NA	NA
Powerhouse type	Underground	Surface	Surface
Cavern size (LxBxH)	55 x 25 x 30	NA	54.6x16.2x19.45

5.3 Cost Comparison:

Though detail cost comparison is not within the scope of this thesis, the concern if the new alternatives are costlier than the proposed one remains. Keeping all other parameters constant such as tunneling methods, tunnel size etc. the length of the penstock tunnel and nature of powerhouse cavern will be the main basis for qualitative cost comparison. Table 5-1 indicates that option 1 has longer vertical shaft than the original but option 2 has the shorter vertical shaft length than the original. The total shaft length is shorter in both options compared to the existing design. In option 1, though the length of the inclined shaft is reduced significantly, however, length of the tailrace tunnel cannot be undermined. Length of shaft is considered to be the major determinant in the cost of Hydropower. The construction of shaft requires very capable and skilled manpower. The requirement of mechanized and costly machines will be required if construction is being done by down to up alignment. The construction requires installation of winch machine and more other equipment if done from up to down alignment. Moreover, shaft construction requires additional equipment making it a costly business to deal with. With this perspective alternative 2 seems to be most economical.

Another perspective is the placement of powerhouse caverns. Underground powerhouse caverns are considered to have several advantages over surface powerhouse like; land cost,

safety reasons, stability and seismic reasons. Due to presence of underground cavern in option 1, it may be costlier, but due to safety and seismic reasons it worth the cost. However, the cost of all three cannot be quantized and compared at this stage.

5.4 Conclusion

Both the alternatives provided appear to be better in terms of reduced number of vertical shafts as the number of drop shaft are two in the one originally proposed. The first option provided suggests single shaft making the construction process easier. It develops new idea of underground powerhouse which will be safer in terms of seismic hazards and surficial problems such as flooding and landslides. Though it is not considered attractive as the rock mass around the proposed underground powerhouse cavern has weak phyllite with very low UCS value. The cavern may be prone to collapse and squeezing thus making it unstable during the construction and afterwards. The cost of the cavern construction will be high and introduction of one more adit tunnel for reaching the cavern location makes it further uneconomic. On the other hand, the second alternative is found to be very economic and easier in many senses. The decrease in vertical shaft length and overall shaft length is major attraction. The decrease in total shaft length to that of the proposed one, reduction of number of vertical shafts to one, an increment in the length of only vertical shaft has provided the second alternative to have no weakness and sheared zone in its penstock tunnel. The construction of surface powerhouse is another attraction. The underground excavation and surface powerhouse construction can be done simultaneously, making the second alternative more economical compared to option 1. The further analysis will be done in chapter 6 for penstock tunnel using this option so that it will be representative for whole section.

6 SQUEEZING ANALYSIS AND NUMERICAL MODELING

6.1 Squeezing analysis

The main instability in the headrace tunnel and penstock tunnel can be squeezing or larger deformation with lapse of time. As discussed in chapter 2, different empirical, analytical, semi-analytical and numerical modeling methods can be used for the prediction of squeezing of the tunnel. The approaches of (Singh, Jethwa et al. 1992), (Jethwa, Singh et al. 1984), (Goel 1994) and numerical modeling has been conducted for the prediction of squeezing in the tunnel in this study.

6.1.1 Empirical approach for squeezing

For the assessment of squeezing using empirical approach, Singh approach (1992) and Goel et al. approach (1994) were used as discussed in section 2.3.5. The Q-value required for the assessment were derived from the relation $RMR = 15 \times \log Q + 50$ (Barton, 1995).

Table 6-1 Assessment of squeezing using empirical approach.

Chainage	Overburden (m)	RMR	Q	N	Check!			
					Singh (1992)	Goel (1994)	Singh (1992)	Goel (1994)
1+900	638	70	10	10	754	505.8	Safe	Safe
4+400	511	30	0.02	0.02	95	65.1	Squeeze	Squeeze
5+000	285	30	0.02	0.02	95	65.1	Squeeze	Squeeze

6.1.2 Semi empirical approach for squeezing

For the assessment of squeezing potential of the ground using semi empirical approach, the value of in-situ stress and UCS of rock mass was required along with internal support pressure and coefficient of volumetric expansion. The necessary rock mass parameter σ_{cm} was derived using the Rocdata software and the values obtained can be found in Appendix 3.

Table 6-2 Assessment of squeezing using semi empirical approach.

Chainage	Overburden (m)	RMR	Q	Average σ_{cm} MPa	In Situ Stress $P_o = \gamma H$ MPa	$N_c = \frac{\sigma_{cm}}{P_o}$	Check !
1+900	638	70	10	28.44	17.23	1.65	Mild Squeezing
4+400	511	30	0.02	3.62	14.31	0.25	Highly Squeezing

5+000	285	30	0.02	2.68	14.31	0.19	Highly Squeezing
-------	-----	----	------	------	-------	------	------------------

From the above Table 6-1 and Table 6-2 we can see that there is probability no or mild squeezing in chainages 1+900 m. Despite the presence of very intact rock gneiss in this section the prediction of mild squeezing is because of higher overburden in that chainage. The other two chainages 4+400 m and 5+000 m are likely to undergo squeezing phenomenon due to high overburden and weak rocks. While designing, this must be considered because the area of squeezing requires heavy support and special considerations. The further analysis of probable squeezing or larger displacements are carried using the numerical modeling.

6.2 Numerical modeling

Phase² modeling was conducted for the three sections. The stress analysis, deformation analysis and support system required were obtained and will be discussed later in the chapter.

Different geological and engineering geological condition of Solu Khola (Dudhkoshi) Hydro Electric Project (SKDKHEP) has been already described in previous chapter (chapter 4).

The mechanical properties of the rock mass were evaluated by studying the geological reports of Solu Khola (Dudhkoshi) Hydro Electric Project (SKDKHEP), literature review and reports from the projects having similar geological condition and discussions with supervisor and co-supervisor . The project area comprises of gneiss and phyllite rock types to larger extent throughout the headrace tunnel, surge shaft and penstock tunnel.

Compressive strength, the intact value of the major rock types, i.e. Gneiss and Phyllite presented by DPR conducted by (Hydro-Consult 2016) are tabulated in the preceding sections. The laboratory data for other rock mass parameter testing such as UCS are obtained from drilling report of (ICGS 2017).

6.2.1 Elastic parameters

The elastic parameters of the Gneiss and Phyllite can be derived using the GSI calculator using the Rocscience software. The intact deformation modulus of the rocks is, Gneiss 20 GPa and for siliceous phyllite 14 GPa. The Poisson's ratio has been found to be 0.2 (Thapa 2018) for siliceous phyllite and 0.1 (Panthi 2006).

6.2.2 Hoek-Brown parameters

Hoek-brown failure criteria require different parameters such as GSI, m_i , and D. These parameters can be used in Rocdata to estimate the Mohr-Coulomb parameters. The material constant for Gneiss ranges from 23 to 33 and the Disturbance factor is taken as 0.8. The material constant for siliceous phyllite ranges from 4 to 10. GSI values are taken from the engineering geological mapping data (Hydro-Consult 2016) which are around 65 for Gneiss and 25 for phyllite.

6.2.3 Dilation Parameter

The dilatancy of the material is a measure of how much volume increase occurs when the material is sheared. A dilation parameter can be defined for Mohr-Coulomb and Hoek-Brown for plastic material. For a Mohr-Coulomb material, dilatancy is an angle that generally varies between zero (non-associative flow rule) and the friction angle (associative flow rule). For Hoek-Brown materials, dilatancy is defined using a dimensionless parameter that generally varies between zero and m . Low dilation angles/parameters are generally associated with soft rocks while high dilation angles/parameters are associated with hard brittle rock masses. The value of the dilation parameter is suggested to start from $0.333*m$ or $0.333*\phi$ for soft rocks and $0.666*m$ or $0.666*\phi$ for hard rocks. (Rockscience 2019)

6.3 Estimation of in-situ stress at different sections

The estimation of the stress at these locations for further stability is the most. The stress components in these locations are the overburden and tectonic stress. These stresses were used to estimate the direction and magnitude of the in-situ stresses.

6.3.1 Model setup

The in-situ stresses were calculated by constructing a 2D valley-slope model of the different sections with different sets of parameters. The model is provided with rollers at the side boundaries and bottom with a roller. The surface boundary is not restrained, and the four corners of the model were restrained to move at x and y -direction. For the analysis, the gravity type field stress was chosen, and the actual ground surface was used because of the variable elevation profile of the model. The tectonic stress was used from (Neupane and Panthi 2012). The direction of the tectonic stress from the world stress map was resolved to in-plane and out plane directions as done in (Basnet and Panthi 2017). In this model, the material is assumed to be elastic as to capture the maximum stress without failure. The rock mass is assumed to be isotropic and consist of Gneiss and phyllite with their particular specific weight. The model was run multiple times for each analysis as described in further section with minimum, mean and maximum value set with slight changes to the Poisson's ratio, elastic modulus and rock mass quality in each section. The existing field stress i.e. σ_1 , σ_3 and σ_z were obtained from valley slope model and used in box model for further stability analysis.

6.4 Stability analysis of tunnel at different sections

After obtaining in-situ stress from the topographic model, the values from the topographic model were used for further stability analysis of the tunnel.

6.4.1 Selection of tunnel sections for stability analysis

The stability analysis of headrace tunnel was conducted using numerical analysis at three different chainages i.e. 1+900 m, 4+400 m and 5+000 m. The first section 1+900 m has the

maximum overburden amongst all the other section throughout the tunnel alignment and is peculiar to other analyzed section due to presence of gneiss rock type with excellent geological condition. The other section lies in the siliceous phyllite rock type and lies immediately after the proposed surge shaft. The third section 5+000 m has similar geology to that of 4+400 m but has less vertical cover (only 285 m). These sections are representative chainage for overall headrace tunnel as they lie in varying geological conditions, varying overburden height and locations. The mechanical properties and stress regime developed around these sections can describe the overall condition that may be encountered during the tunnel excavation.

6.4.2 Model setup

The 2D box-model of the tunnel was set up taking the area 5 times to the excavation width. The in-situ stress from the topographic model has used constant stress. The model was divided into ten stages with excavation at stage 1. The boundary was restrained at both directions on all corners and the rest of the boundary was set to be on roller movement. A uniform distributed load is added to the tunnel in the initial stage. The factor is taken such that it will gradually reduce the magnitude of the pressure. As a result, tunnel deformation will increase as the pressure is lowered to zero. As this stage the internal pressure is removed, simulating the reduction of support due to the advance of tunnel face. Generalized Hoek and Brown failure criterion was used, and the rock mass was assumed to be elastic first of all and plastic analysis was conducted in the strength factor was found to be less than 1 (Phase² tutorial no. 1. The model was studied in different conditions for each set of stress and rock parameters. The model was set up for three different possibilities with minimum, mean and maximum values of rock mass parameters.

Table 6-3 Input parameters for Phase2 analysis for each tunnel sections for elastic and plastic analysis.

Chainage	Rock Type	Field stress type	Initial element loading	Elastic type	Failure criterion	Material type
1+900 m	Gneiss	Gravity	Field stress and body force	Isotropic	Generalized Heok-Brown	Elastic, Plastic
4+400 m	Phyllite	Gravity	Field stress and body force	Isotropic	Generalized Heok-Brown	Elastic, Plastic
5+000 m	Phyllite	Gravity	Field stress and body force	Isotropic	Generalized Heok-Brown	Elastic, Plastic

6.4.3 Chainage 1+900 m

The selected chainage consists of beds of gneiss (Table 6-4). The phyllite is dominant over quartzite. The overburden is high in this chainage and is measured to be 638 m.

6.4.3.1 Rock mass parameters

The uniaxial compressive strength was found to be 91 MPa, Geological strength Index (GSI) is 65 for the gneiss rock type near the headwork area. Young's modulus of Gneiss is taken 20000 MPa from Phase² software and Poisson's ratio that of 0.2 (Thapa 2018)

Hoek-Brown constant m_i is 28. The disturbance factor is taken 0.8 for gneiss and the data are mean value obtained from Phase software. The calculation of input rock mass parameters required in Phase² software was obtained from Roc-Data1 software.

Tectonic stress is taken as 5 MPa of N-S orientation from world stress map shown in Appendix (2-5). Tunnel alignment is on the NW-SE direction, so the angle made by tunnel to the tectonic stress is 56° .

Table 6-4 The average rock mass parameter value set for analysis of chainage 1+900 m.

Chainage	Rock type	Overburden	Density MN/m ³	Poisson's ratio	E_i (MPa)	σ_{ci} (Mpa)	M_i	GSI	σ_1	σ_3	σ_z
1+900 m	Gneiss	638 m	2.7	0.2	20000	91	28	65	20	19	21

Elastic Analysis

As the result shown in Figure 6-1, the strength factor is less than one. Thus, for further analysis of the failure of material more additional information of plastic analysis is needed (Phase² tutorial no. 1). As the strength factor is less than one all along the tunnel periphery plastic analysis is performed.

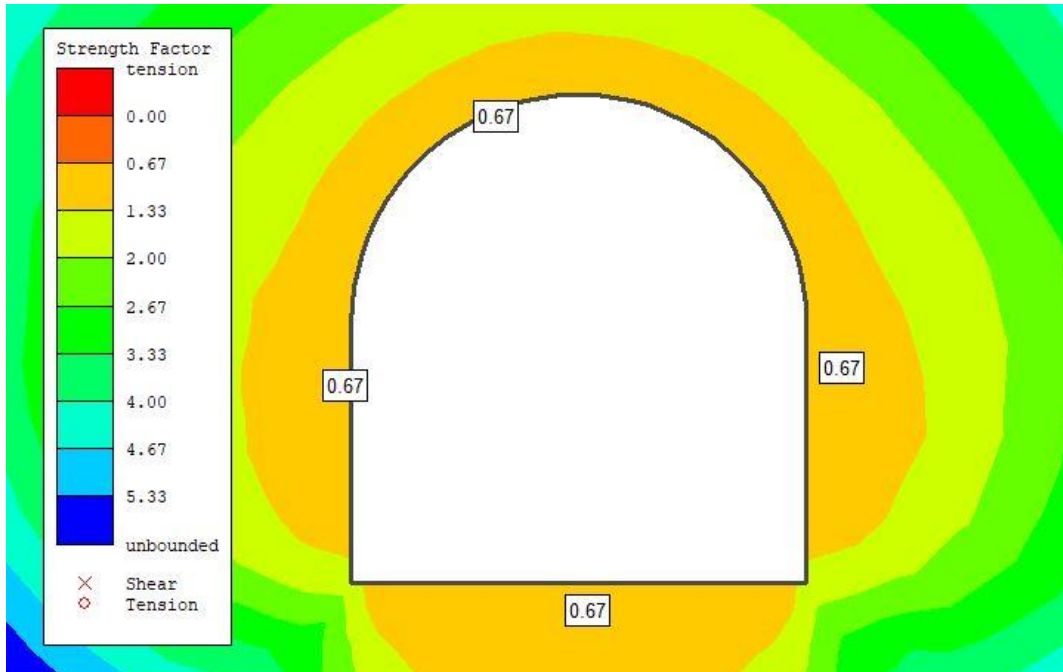


Figure 6-1 Strength factor at chainage 1+900 m (Elastic analysis).

Plastic Analysis

The total displacement (u_{max}) of the tunnel is 5 mm. This is about the 0.1% of tunnel span. The extent of plastic zone (R_p) 4.1 m as shown in Figure 6-2.

The unsupported section (X) will be maximum of 2 m distance from the tunnel face. The ratio of the distance from the tunnel face to tunnel radius (X/R_t) is 0.83 and the plastic zone to tunnel radius (R_p/R_t) is 2.1. By using Vlachopoulos and Diederichs method, the above values are plotted gives ratio of closure to maximum closure equal to 0.76. Therefore, the closure equals to 3.8 mm which mean 76% of total deformation will already take place before support is installed. Internal pressure factor of 0.01 yields the tunnel wall displacement computed above for the point of support installation.

There was significant role topography in the stress distribution while checking the valley slope model which is given in Appendix 3. The distribution of major principle stress is inclined towards the hill section. Thus, the further analysis was conducted with the actual ground surface rather than constant field stress. Low value of stress is developed around the tunnel periphery after excavation without support and increased after the tunnel excavation. The stress values are particularly high in left and right inverts. The stress value is constant around both the walls and increased in the crown after support installation (Figure 6-3, left and right respectively).

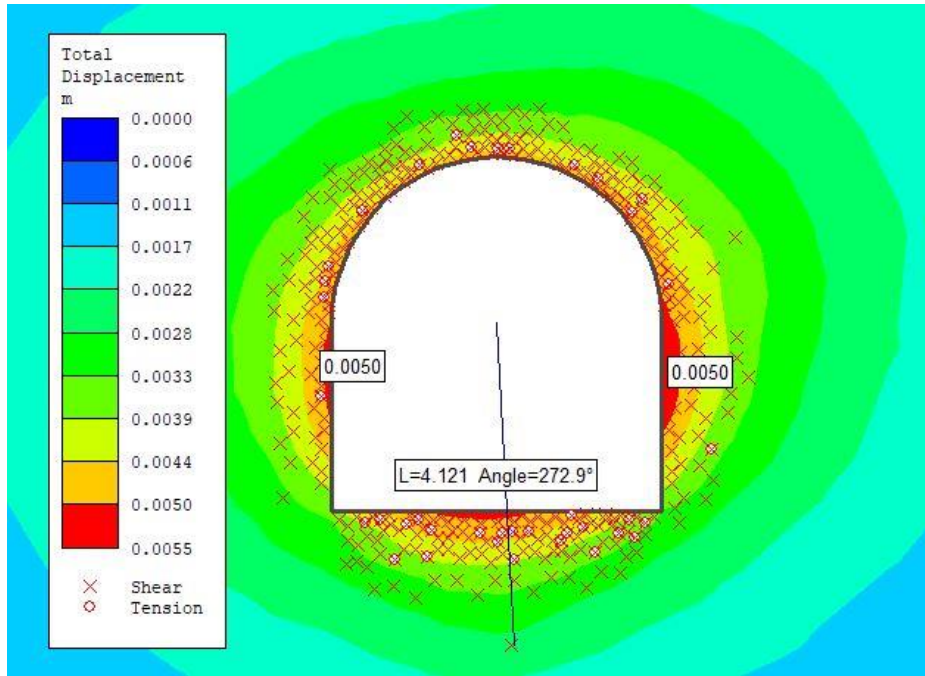


Figure 6-2 Result showing displacement of 5 mm and radius of plastic zone 4 m in unsupported tunnel in chainage 1+900 m.

The total displacement is reduced by few margins after the installation of the support. The total displacement is very low due to the presence of intact gneiss rock.

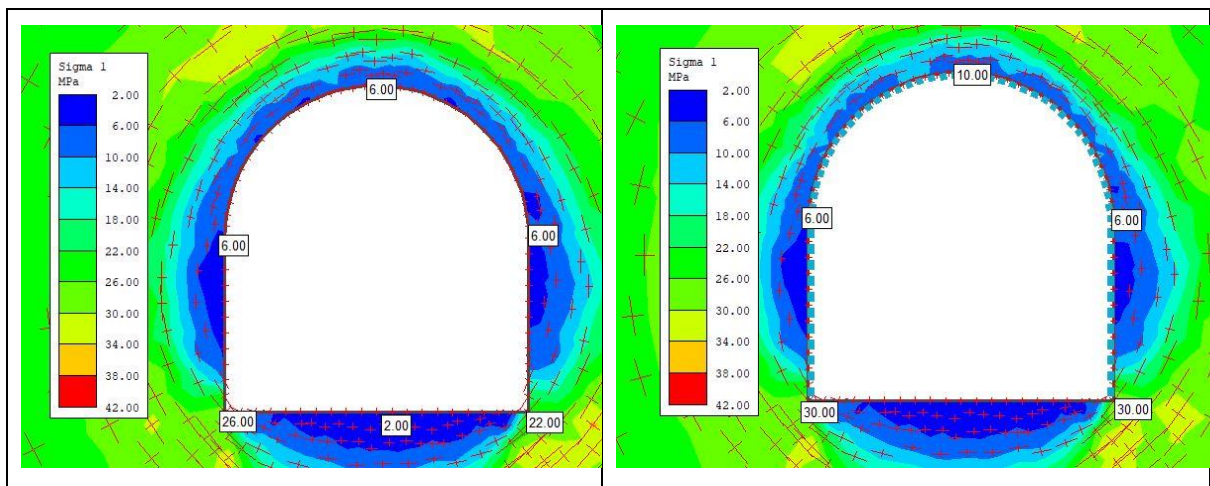


Figure 6-3 Major principal stress distribution before and after support installation at chainage 1+900 m (plastic analysis).

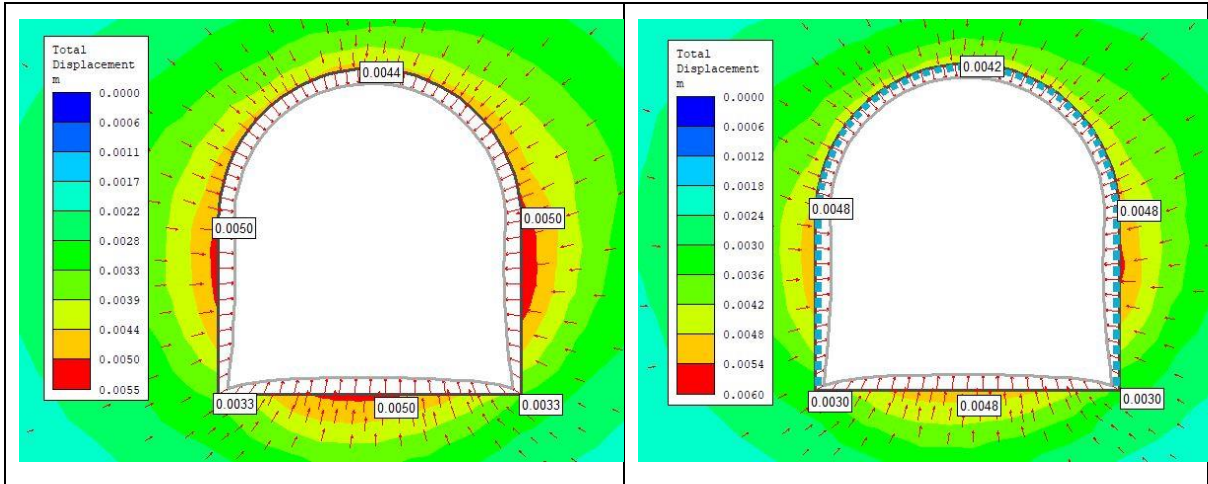


Figure 6-4 Total displacement before and after support installation for chainage 1+900 m (plastic analysis).

The support is installed as suggested by DPR of the project for Rock Support I (Appendix 3). While conducting the modeling the support capacity seems adequate. The support capacity plot is generated for the support considered.

As suggested by Figure 6-5, we can see the liner support scattered inside the designed factor of safety envelope 1.4.

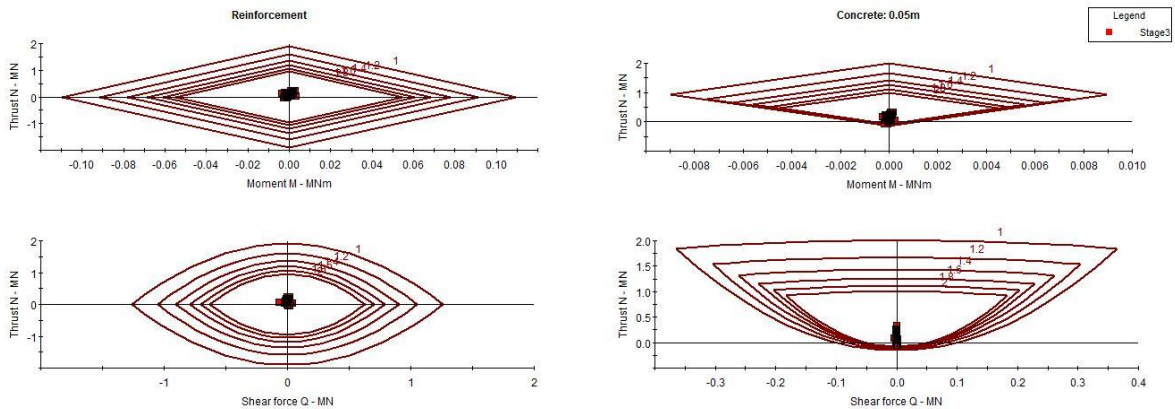


Figure 6-5 Support capacity plot for chainage 1+900 m (mean values) with obtained factor of safety.

The similar modeling was conducted decreasing the value of rock mass parameter as increasing the value is meaningless because average value is stable with minimum of the support.

The actual conditions of observed rock mass were considered to be mean of probable rock mass conditions and the following value were used as minimum to analyze the condition of chainage 1+900 m.

Table 6-5 The taken rock mass parameter value for further analysis according to the decrement of rock mass properties value.

The probable values	Overburden	Density MN/m ³	Poisson's ratio	E _i (MPa)	σ _{ci} (Mpa)	M _i	GSI	σ ₁	σ ₃	σ _z
Minimum	638 m	2.7	0.15	10000	65	28	45	22	16.5	19.5

Minimum Value

The total displacement (u_{max}) of the tunnel is 17.3 mm. This is about the 1.7% of tunnel span. The extent of plastic zone (R_p) is about 5.09 m.

The unsupported section (X) will be maximum of 2 m distance from the tunnel face. The ratio of the distance from the tunnel face to tunnel radius (X/R_t) is 0.83 and the plastic zone to tunnel radius (R_p/R_t) is 2.1. By using Vlachopoulos and Diederichs method, the above values are plotted gives ratio of closure to maximum closure equal to 0.67. Therefore, the closure equals to 11.59 mm which mean 67% of total deformation will already take place before support is installed. Internal pressure factor of 0.1 yields the tunnel wall displacement computed above for the point of support installation.

There was no significant role topography in the stress distribution while checking the valley slope model (Appendix 3). Thus, the further analysis was conducted in the box model with external boundary 5 times the excavation and the constant field stress was used.

Low value of stress is developed around the tunnel periphery after excavation without support and a higher value of stress is developed after the support installation especially in the crown and invert parts

The total displacement is reduced after the installation of the support. The total displacement is reduced significantly after the support application indicating the appropriate choice of the support elements. The increase in the displacement in the invert part is because of lack of support in that section.

The support is installed as suggested by DPR of the project for Rock Support II (Appendix 3). The support capacity plot is generated for the support considered. The support seemed inadequate thus the model with increasing concrete thickness was run multiple times.

As suggested by Figure 6-6, we can see the liner support all lying in the factor of safety envelope of 1.4 after increasing the concrete lining up to 15 cm. We can conclude the adequacy of the support according to the design of the project.

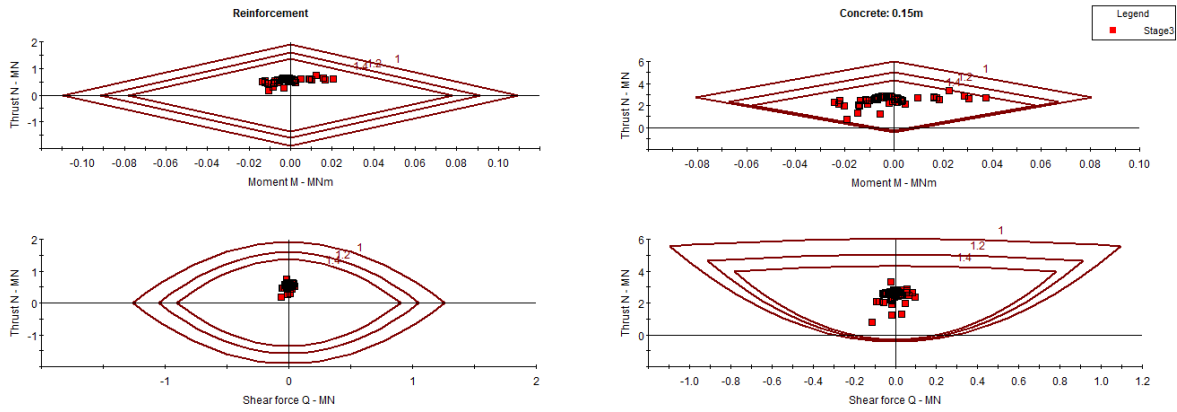


Figure 6-6 Support capacity plot for chainage 1+900 m (minimum values) with obtained factor of safety.

The above analysis also concludes the presence of rock with high strength requires minimum support pressure for the stability of the tunnel due to deformation. The rock support provided by the DPR report also seems to be inadequate for Rock Class II according to the numerical modeling.

6.4.4 Chainage 4+400m

The selected chainage consists of alternating beds of phyllite and quartzite (Figure 5-2). The phyllite is dominant over quartzite. The overburden is high in this chainage and is measured to be that of 511 m.

6.4.4.1 Rock mass parameters

The uniaxial compressive strength was found to be 25 MPa, Geological strength Index (GSI) is 35 (DPR) for the phyllite rock type near the powerhouse area. Young’s modulus of phyllite with quartzite (siliceous phyllite) is taken 14000 MPa from Phase² software and Poisson’s ratio that of 0.05 (Panthi 2006).

Hoek-Brown constant m_i is 7. The disturbance factor is taken 0.5 for phyllite and the data are mean value obtained from Phase software. The calculation of input rock mass parameters required in Phase² software was obtained from Roc-Data1 software.

Tectonic stress is taken as 5 MPa of N-S orientation. Tunnel alignment is on the NW-SE direction, so the angle made by tunnel to the tectonic stress is 87° .

Table 6-6 The average rock mass parameter value set for analysis of chainage 4+400 m.

Chainage	Rock type	Overburden	Density MN/m ³	Poisson’s ratio	E _i (MPa)	σ _{ci} (Mpa)	M _i	GSI	σ ₁	σ ₃	σ _Z
4+ 400 m	Phyllite	511 m	2.86	0.05	14000	35	7	25	12	9	4.9

Elastic Analysis

As the result shown in Figure 6-7, the strength factor is less than one. Thus, for further analysis of the failure of material more additional information of plastic analysis is needed (Phase² tutorial no. 1). As the strength factor is less than one all along the tunnel periphery plastic analysis is performed.

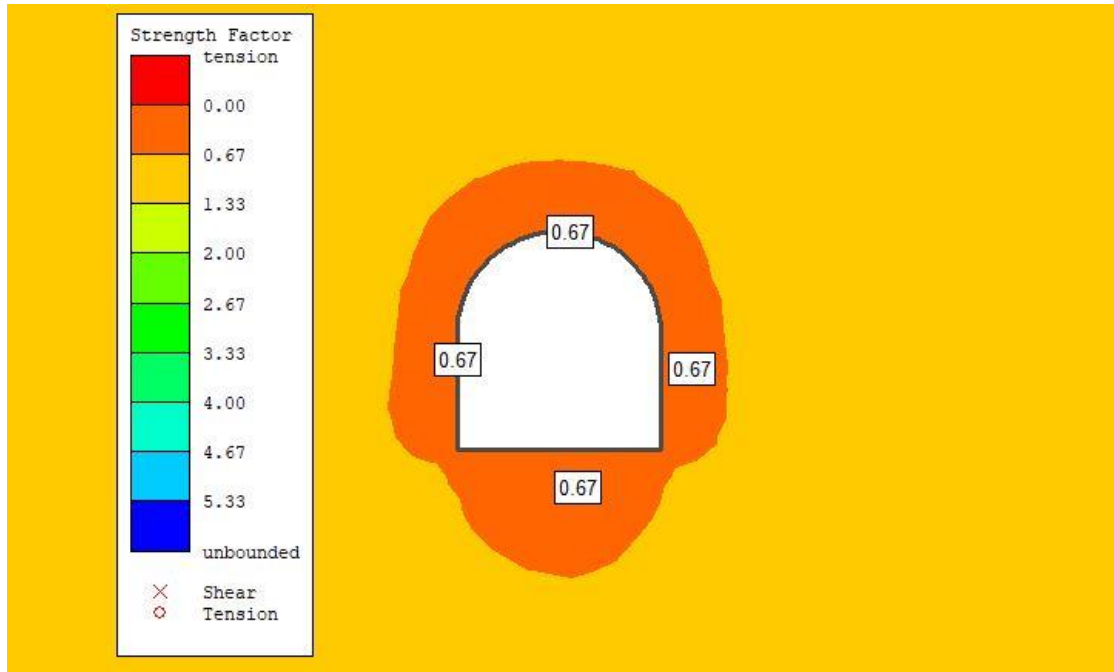


Figure 6-7 Strength factor at chainage 4+400 m (Elastic analysis).

Plastic Analysis

The total displacement (u_{\max}) of the tunnel is 36 mm. This is about the 0.8% of tunnel span. The extent of plastic zone (R_p) is throughout the section from tunnel periphery to external boundary up to the ground surface as shown in Figure 6-8. Therefore, the support was installed in stage 2, i.e. immediately after the excavation was done.

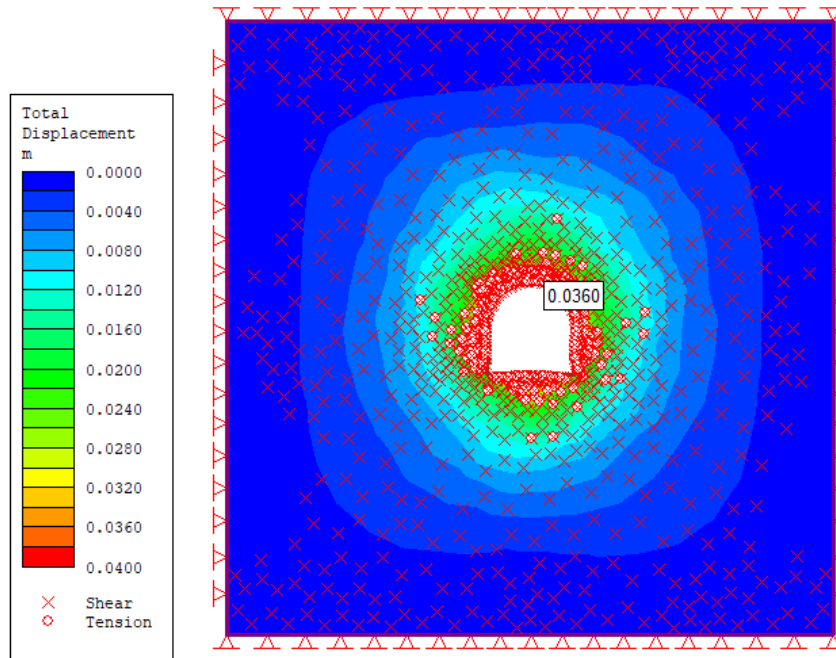


Figure 6-8 Result showing displacement of 36 mm and radius of plastic zone throughout the external boundary in unsupported tunnel in chainage 4+400 m.

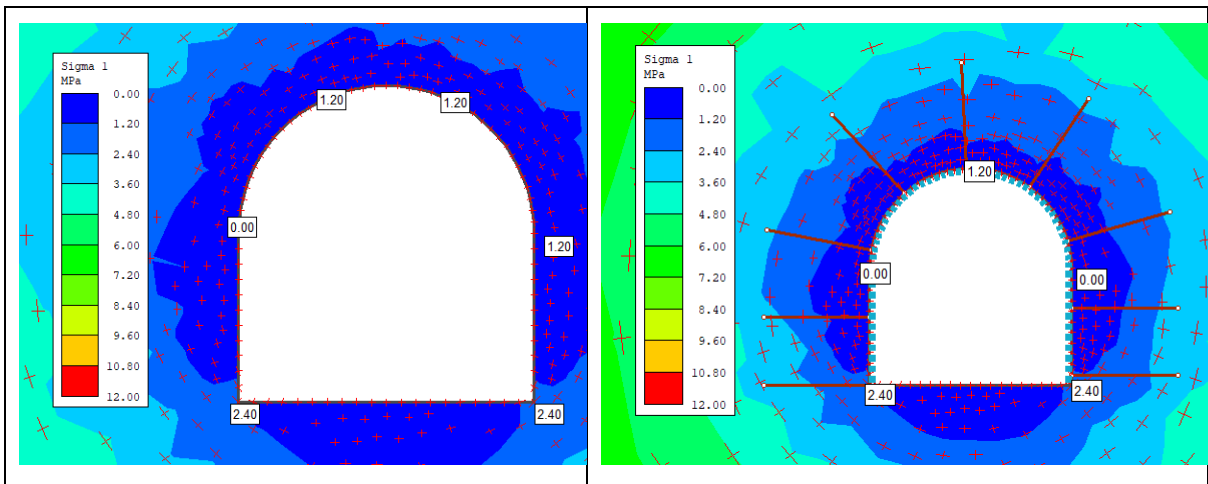


Figure 6-9 Major principal stress distribution before and after support installation at chainage 4+400 m (plastic analysis).

There was no significant role topography in the stress distribution while checking the valley slope model (Appendix 3). Thus, the further analysis was conducted in the box model with external boundary 5 times the excavation and the constant field stress was used. Low value of stress is developed around the tunnel periphery after excavation without support and remained constant even after support installation. The stress value is decreased around both the walls after support installation. (Figure 6-9 left and right respectively).

The total displacement is reduced after the installation of the support. The total displacement is reduced significantly after the support application indicating the appropriate choice of the support elements. Nevertheless, the displacement seems increased in the invert part of the tunnel where support is not provided.

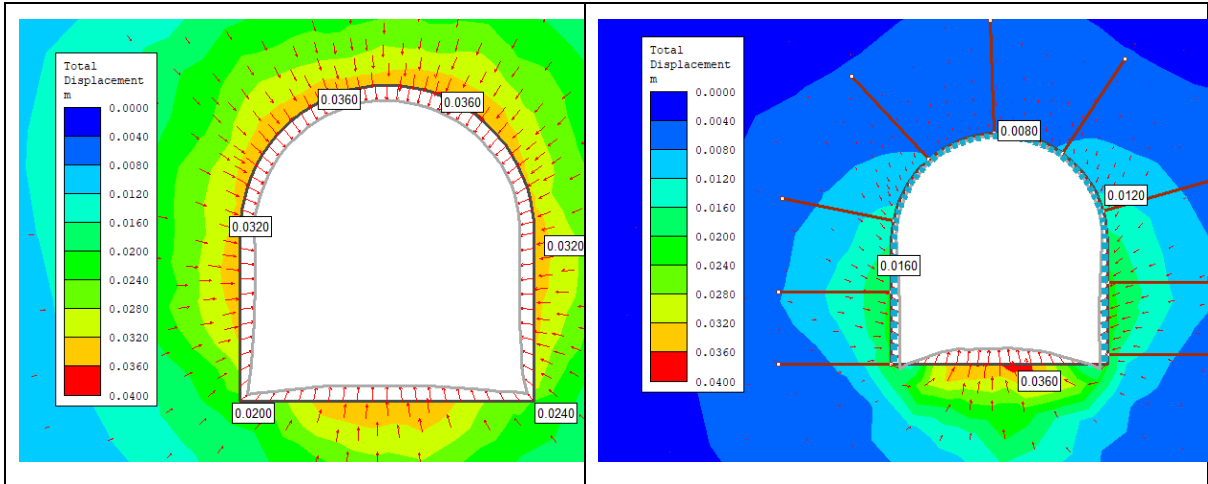


Figure 6-10 Total displacement before and after support installation for chainage 4+400 m (plastic analysis).

The support is installed as suggested by DPR of the project for Rock Support IV (Appendix 3). While conducting the modeling the support capacity seems inadequate, so the model was run many times increasing the thickness of concrete in each model. The support capacity plot is generated for the support considered.

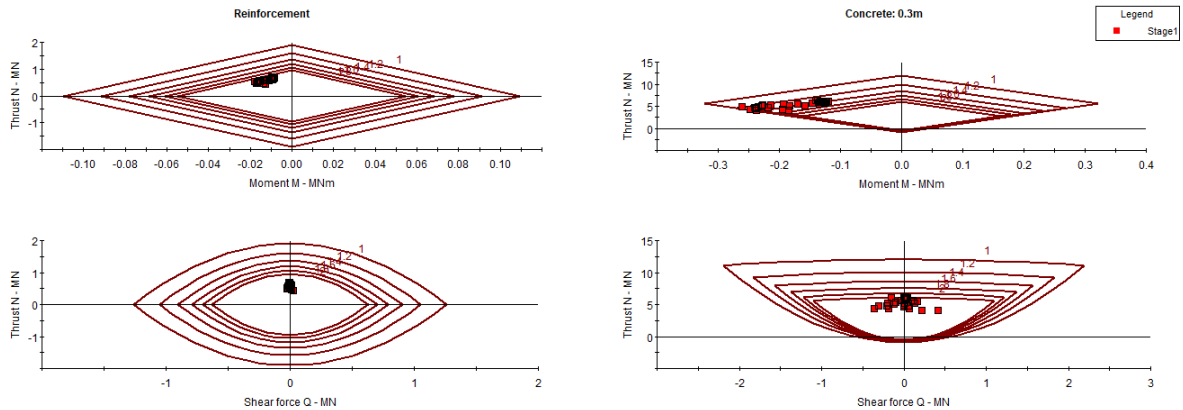


Figure 6-11 Support capacity plot for chainage 4+400 m (mean values) with obtained factor of safety.

As suggested by Figure 6-11, we can see the liner support scattered equally inside the factor of safety envelope of 1.4 while increasing the concrete thickness up to 0.3 m.

The similar modeling was conducted increasing and decreasing the value of rock mass parameter. The main objective was to find out the change in the support capacity required for each condition. One cannot directly conclude the projected rock mass in the tunnel alignment from surface data satisfies the actual condition. So, an approach was made to understand the stress condition, displacement after the excavation and probable support required according to the changing geological conditions.

The actual conditions of observed rock mass were considered to be mean of probable rock mass conditions and the following value were used as minimum and maximum to analyze the condition of chainage 4+400 m.

Table 6-7 The taken rock mass parameter value for further analysis according to the increment and decrement of rock mass properties value.

The probable values	Overburden	Density MN/m ³	Poisson's ratio	E _i (MPa)	σ _{ci} (Mpa)	M _i	GSI	σ ₁	σ ₃	σ _Z
Maximum	511 m	2.86	0.1	16000	45	7	40	17.5	12.5	14
Minimum	511 m	2.86	0.05	10000	25	7	20	25	14	2.4

Maximum Value

The total displacement (u_{max}) of the tunnel is 24 mm. This is about the 0.5% of tunnel span. The extent of plastic zone (R_p) is about 7.59 m as shown in Figure 6-12.

The unsupported section (X) will be maximum of 2 m distance from the tunnel face. The ratio of the distance from the tunnel face to tunnel radius (X/R_t) is 0.83 and the plastic zone to tunnel radius (R_p/R_t) is 3.2. By using Vlachopoulos and Diederichs method, the above values plotted gives ratio of closure to maximum closure equal to 0.46. Therefore, the closure equals to 11.09 mm which mean 46% of total deformation will already take place before support is installed. Internal pressure factor of 0.04 yields the tunnel wall displacement computed above for the point of support installation.

There was no significant role topography in the stress distribution while checking the valley slope model (Appendix 3). Thus, the further analysis was conducted in the box model with external boundary 5 times the excavation and the constant field stress was used. Low value of stress is developed around the tunnel periphery after excavation without support and a higher value of stress is developed after the support installation especially in the crown and invert parts.

The total displacement is reduced after the installation of the support. The total displacement is reduced significantly after the support application indicating the appropriate choice of the support elements. The increase in the displacement in the invert part is because of lack of support in that section.

The support is installed as suggested by DPR of the project for Rock Support IV. The support capacity plot is generated for the support considered.

As suggested by Figure 6-12, we can see the liner support all lying in the factor of safety envelope of 2. We can conclude the adequacy of the support according to the design of the project.

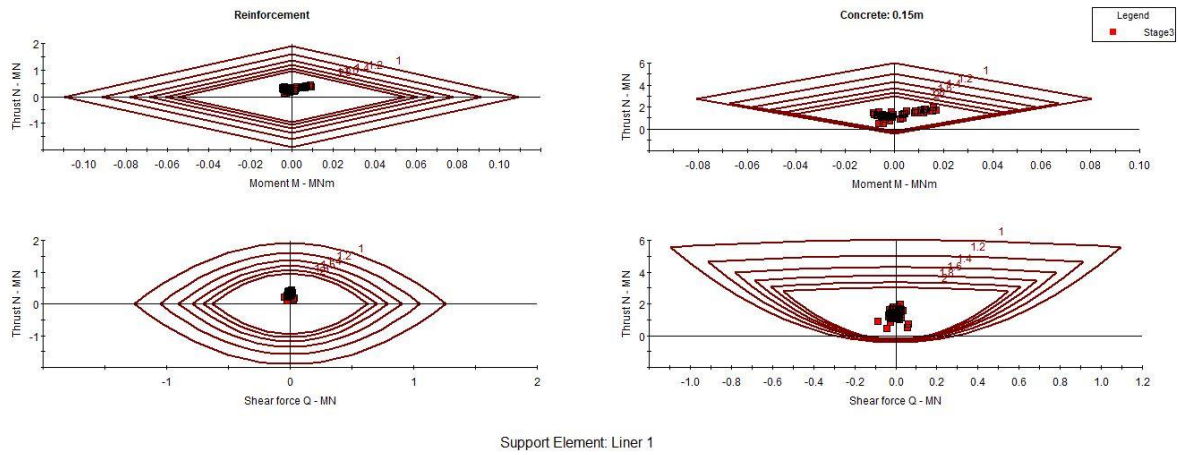


Figure 6-12 Support capacity plot for chainage 4+400 m (maximum values) with obtained factor of safety.

Minimum values

A uniform distributed load is added to the tunnel in the initial stage. The factor is taken such that it will gradually reduce the magnitude of the pressure. As a result, tunnel deformation will increase as the pressure is lowered to zero. As this stage the internal pressure is removed, simulating the reduction of support due to the advance of tunnel face.

The total displacement (u_{max}) of the tunnel is 101.5 mm. This is about the 2.26% of tunnel span. The extent of plastic zone (R_p) is throughout the section from tunnel periphery to external boundary. Therefore, the support was installed in stage 2 i.e. immediately after the excavation was done.

There was no significant role topography in the stress distribution while checking the valley slope model. Thus, the further analysis was conducted in the box model with external boundary 5 times the excavation and the constant field stress was used. Low value of stress is developed around the tunnel periphery after excavation without support and increased after the support installation.

The total displacement is reduced after the installation of the support. The total displacement is reduced significantly after the support application indicating the appropriate choice of the support elements. Nevertheless, the displacement seems increased in the invert part of the tunnel where support is not provided.

The support is installed as suggested by DPR of the project for Rock Support IV. While conducting the modeling the support capacity seems inadequate, so the model was run many times increasing the thickness of concrete in each model. The support capacity plot is generated for the support considered.

As suggested by Figure 6-13, we can see the liner support still scattered outside the factor of safety envelope of 1.4 for concrete moment capacity while increasing the concrete thickness even up to 0.5 m. This section will thus require the installation of steel ribs for withstanding the failure.

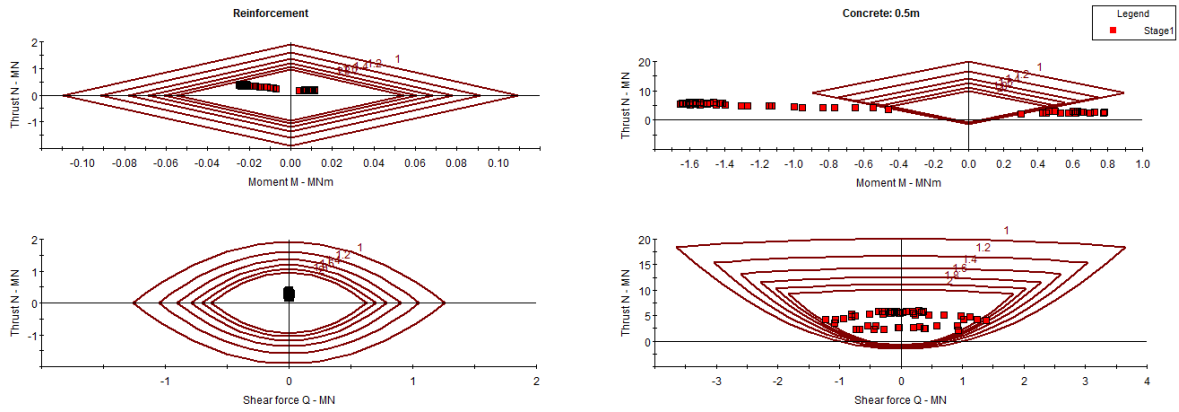


Figure 6-13 Support capacity plot for chainage 4+400 m (minimum values) with obtained factor of safety.

As suggested by the above three conditions of rock mass properties in the chainage 4+400 m, we can conclude the displacements around the tunnel periphery increases with reduction in the strength of surrounding rock mass. The higher value of rock mass suggests the lesser requirement of the support for the stability against the stress and displacement.

6.4.5 Chainage 5+000m

The selected chainage consists of alternating beds of phyllite and quartzite (Figure 5-2). The phyllite is dominant over quartzite. The overburden is high in this chainage and is measured to be 285 m.

6.4.5.1 Rock mass parameters

The uniaxial compressive strength was found to be 25 MPa, Geological strength Index (GSI) is 35 (Hydro-Consult 2016) for the phyllite rock type near the powerhouse area. Young’s modulus of phyllite with quartzite (siliceous phyllite) is taken 14000 MPa from Phase² software and Poisson’s ratio that of 0.05 (Panthi 2006).

Hoek-Brown constant m_i is 7. The disturbance factor is taken 0.5 for phyllite and the data are mean value obtained from Phase software. The calculation of input rock mass parameters required in Phase² software was obtained from Roc-Data1 software.

Tectonic stress is taken as 5 MPa of N-S orientation. Tunnel alignment is on the NW-SE direction, so the angle made by tunnel to the tectonic stress is 87° .

Table 6-8 The average rock mass parameter value set for analysis of chainage 5+000 m.

Chainage	Rock type	Overburden	Density MN/m ³	Poisson’s ratio	E _i (MPa)	σ _{ci} (Mpa)	M _i	GSI	σ ₁	σ ₃	σ _Z
5+ 000 m	Phyllite	285 m	2.86	0.05	14000	35	7	25	13.5	8.5	9

Elastic Analysis

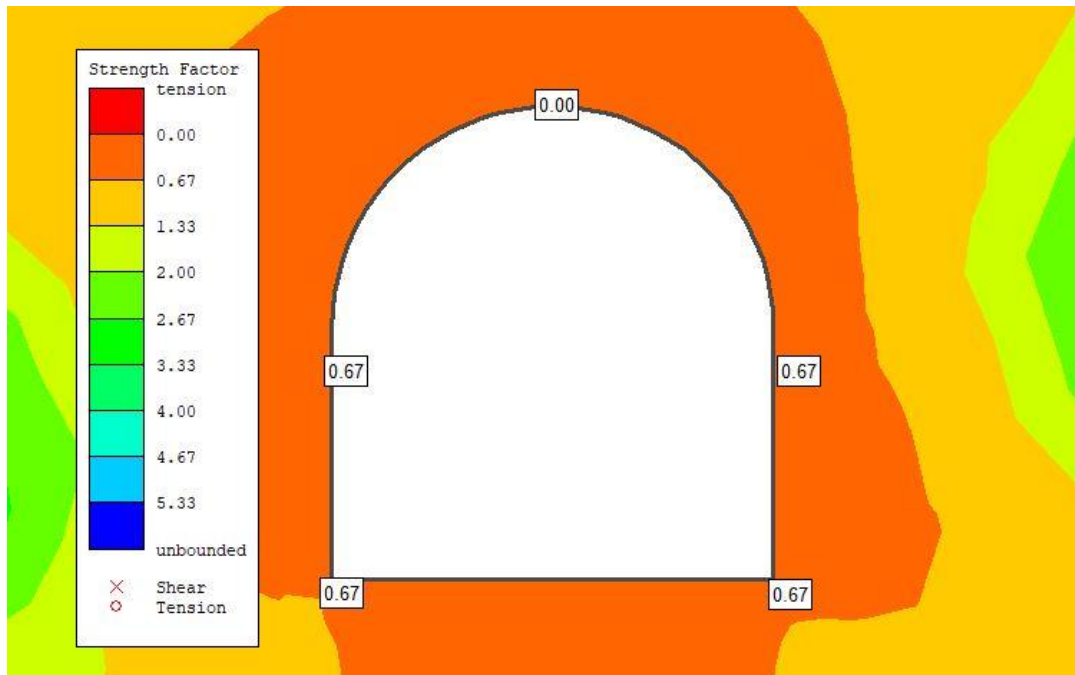


Figure 6-14 Strength factor at chainage 5+000 m (Elastic analysis).

As the result shown in Figure 6-14, the strength factor is less than one. Thus, for further analysis of the failure of material more additional information of plastic analysis is needed (Phase² tutorial no. 1). As the strength factor is less than one all along the tunnel periphery plastic analysis is performed.

Plastic Analysis

The total displacement (u_{max}) of the tunnel is 11.04 mm. This is about the 0.2% of tunnel span. The extent of plastic zone (R_p) is 10.24 m from center of the tunnel (Figure 6-15). The unsupported section (X) will be maximum of 2 m distance from the tunnel face. The ratio of the distance from the tunnel face to tunnel radius (X/R_t) is 0.83 and the plastic zone to tunnel radius (R_p/R_t) is 4.3. By using Vlachopoulos and Diederichs method, the above values are plotted gives ratio of closure to maximum closure equal to 0.4. Therefore, the closure equals to 4.42 mm which mean 40% of total deformation will already take place before support is installed. Internal pressure factor of 0.1 yields the tunnel wall displacement computed above for the point of support installation.

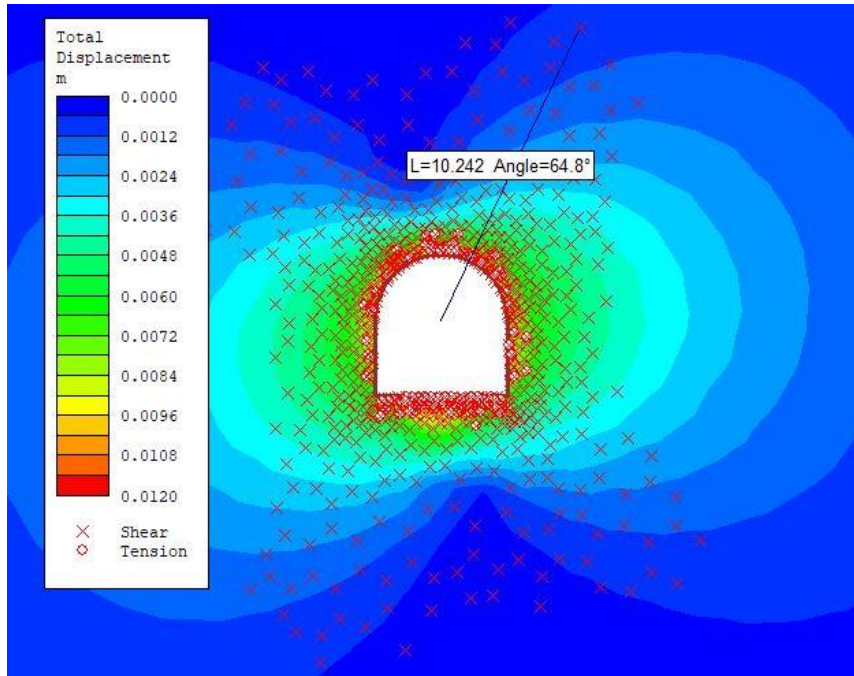


Figure 6-15 Result showing displacement of 11.04 mm and radius of plastic zone throughout the external boundary in unsupported tunnel in chainage 5+000 m.

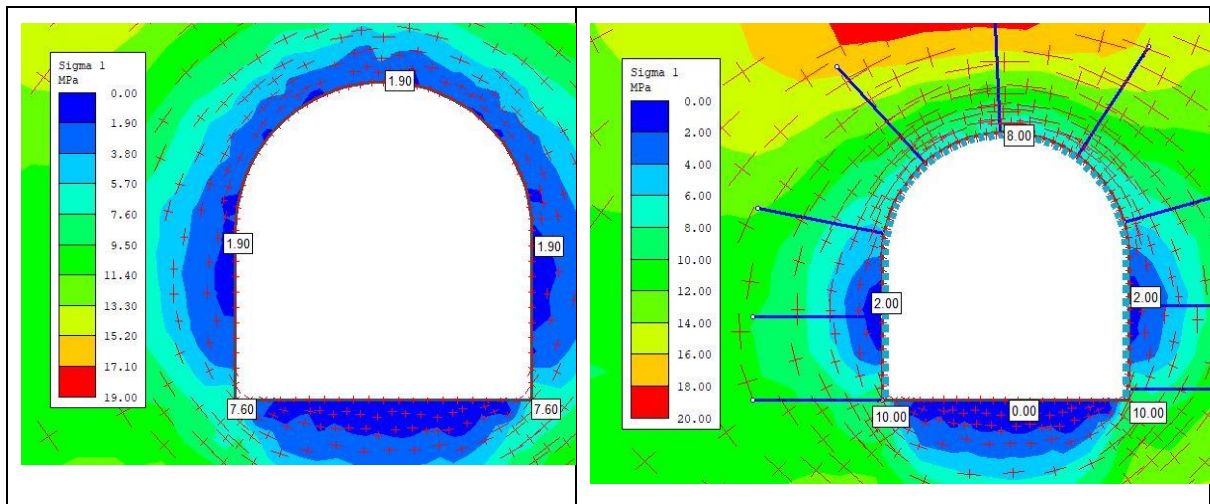


Figure 6-16 Major principal stress distribution before and after support installation at chainage 5+000 m (plastic analysis).

There was no significant role topography in the stress distribution while checking the valley slope model (Appendix 3). Thus, the further analysis was conducted in the box model with external boundary 5 times the excavation and the constant field stress was used. Low value of stress is developed around the tunnel periphery after excavation without support and increased at the crown and invert after support installation. The stress value is increased around both the walls after support installation. (Figure 6-16, left and right respectively).

The total displacement is reduced after the installation of the support. The total displacement is reduced significantly after the support application indicating the appropriate choice of the

support elements. Nevertheless, the displacement seems constant in the invert part of the tunnel where support is not provided.

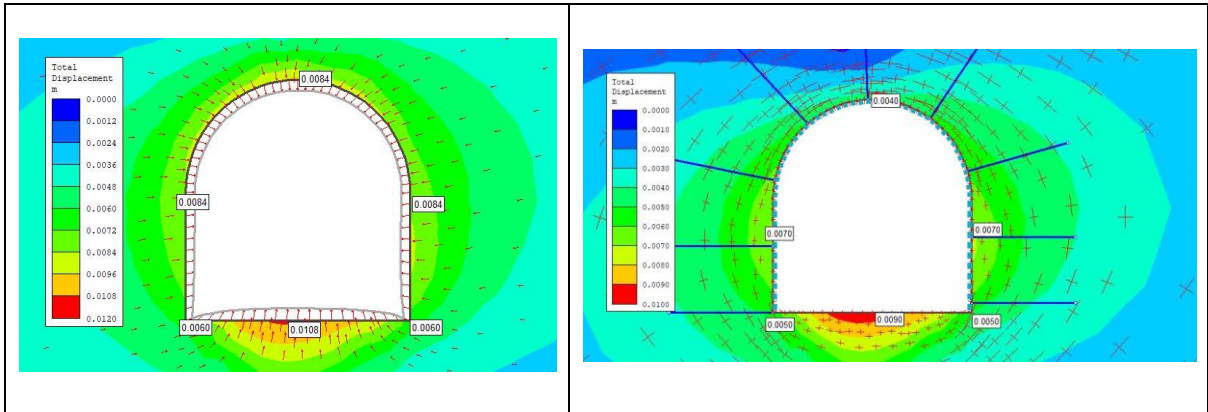


Figure 6-17 Total displacement before and after support installation for chainage 5+000 m (plastic analysis).

The support is installed as suggested by DPR of the project for Rock Support IV. While conducting the modeling the support capacity seems adequate. As suggested by Figure 6-18, we can see the liner support scattered equally inside the factor of safety envelope of 1.4 while lining the tunnel periphery with the concrete thickness of 10 cm.

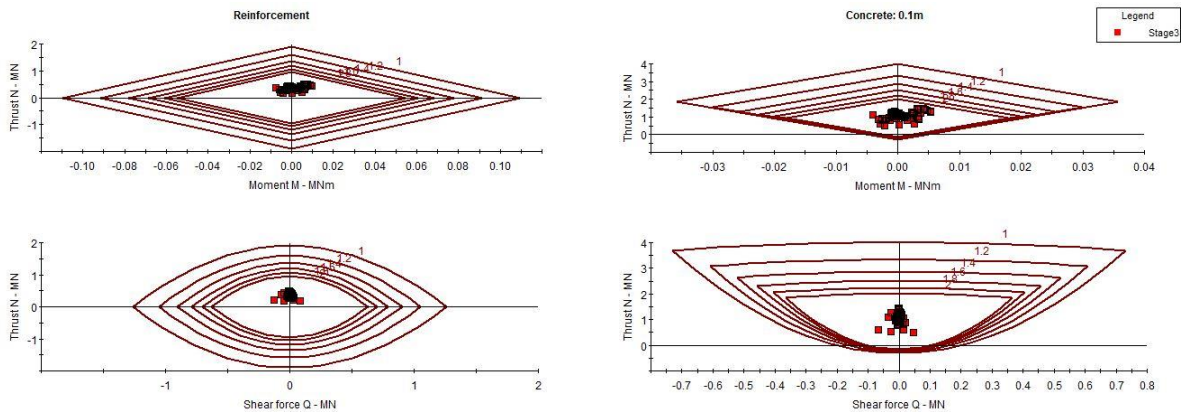


Figure 6-18 Support capacity plot for chainage 5+500 m (mean values) with obtained factor of safety.

The similar modeling was conducted by increasing and decreasing the value of rock mass parameter. The main objective was to find out the change in the support capacity required for each condition. One cannot directly conclude the projected rock mass in the tunnel alignment from surface data satisfies the actual condition. So, an approach was made to understand the stress condition, displacement after the excavation and probable support required according to the changing geological conditions.

The actual conditions of observed rock mass were considered to be mean of probable rock mass conditions and the following value were used as minimum and maximum to analyze the condition of chainage 5+500 m.

Table 6-9 The taken rock mass parameter value for further analysis according to the increment and decrement of rock mass properties value.

The probable values	Overburden	Density MN/m ³	Poisson's ratio	E _i (MPa)	σ _{ci} (Mpa)	M _i	GSI	σ ₁	σ ₃	σ _Z
Maximum	285 m	2.86	0.1	16000	45	7	40	12	7.2	7.8
Minimum	285 m	2.86	0.05	10000	25	7	20	12	7.9	7.8

Maximum Value

The total displacement (u_{max}) of the tunnel is 7.5 mm. This is about the 0.2% of tunnel span. The extent of plastic zone (R_p) is about 6.15 m.

The unsupported section (X) will be maximum of 2 m distance from the tunnel face. The ratio of the distance from the tunnel face to tunnel radius (X/R_i) is 0.83 and the plastic zone to tunnel radius (R_p/R_i) is 2.6. By using Vlachopoulos and Diederichs method, the above values are plotted gives ratio of closure to maximum closure equal to 0.52. Therefore, the closure equals to 3.9 mm which mean 52% of total deformation will already take place before support is installed. Internal pressure factor of 0.08 yields the tunnel wall displacement computed above for the point of support installation.

There was no significant role topography in the stress distribution while checking the valley slope model. Thus, the further analysis was conducted in the box model with external boundary 5 times the excavation and the constant field stress was used. Low value of stress is developed around the tunnel periphery after excavation without support and a higher value of stress is developed after the support installation especially in the crown and invert parts.

The total displacement is reduced after the installation of the support. The total displacement is reduced significantly after the support application indicating the appropriate choice of the support elements. The increase in the displacement in the invert part is because of lack of support in that section.

The support is installed as suggested by (Hydro-Consult 2016) of the project for Rock Support II. The support capacity plot is generated for the support considered.

As suggested by Figure 6-19, we can see the liner support all lying in the factor of safety envelope of 1.4. We can conclude the adequacy of the support according to the design of the project.

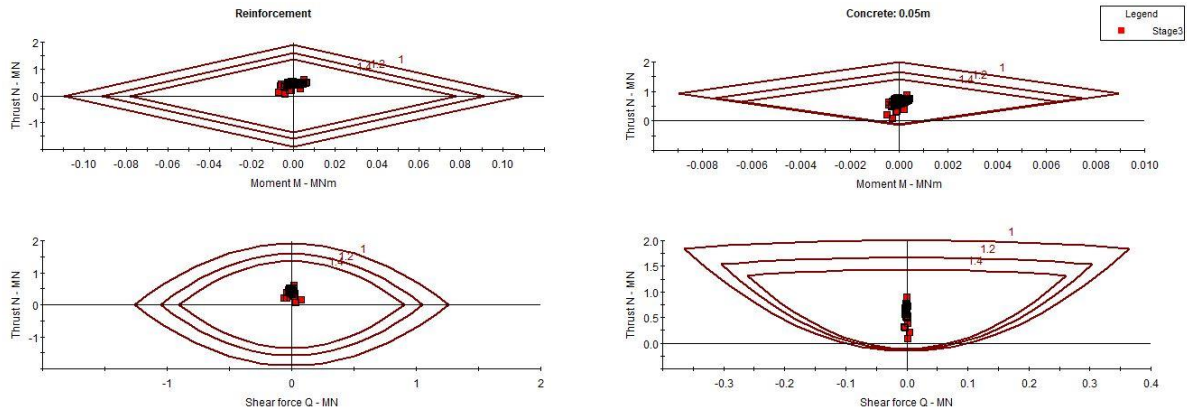


Figure 6-19 Support capacity plot for chainage 4+400 m (maximum values) with obtained factor of safety.

Minimum values

A uniform distributed load is added to the tunnel in the initial stage. The factor is taken such that it will gradually reduce the magnitude of the pressure. As a result, tunnel deformation will increase as the pressure is lowered to zero. As this stage the internal pressure is removed, simulating the reduction of support due to the advance of tunnel face.

The total displacement (u_{max}) of the tunnel is 26 mm. This is about the 0.6% of tunnel span. The extent of plastic zone (R_p) is throughout the section from tunnel periphery to external boundary. Therefore, the support was installed in stage 2 i.e. immediately after the excavation was done.

There was no significant role topography in the stress distribution while checking the valley slope model. Thus, the further analysis was conducted in the box model with external boundary 5 times the excavation and the constant field stress was used. Low value of stress is developed around the tunnel periphery after excavation without support and increased after the support installation.

The support is installed as suggested by DPR of the project for Rock Support IV. While conducting the modeling the support capacity seems inadequate, so the model was run many times increasing the thickness of concrete in each model. The support capacity plot is generated for the support considered.

As suggested by Figure 6-20, we can see the liner support still scattered equally inside and outside the factor of safety envelope of 1.4 for concrete moment capacity while increasing the concrete thickness even up to 0.5 m. This section will thus require the installation of steel ribs for withstanding the failure.

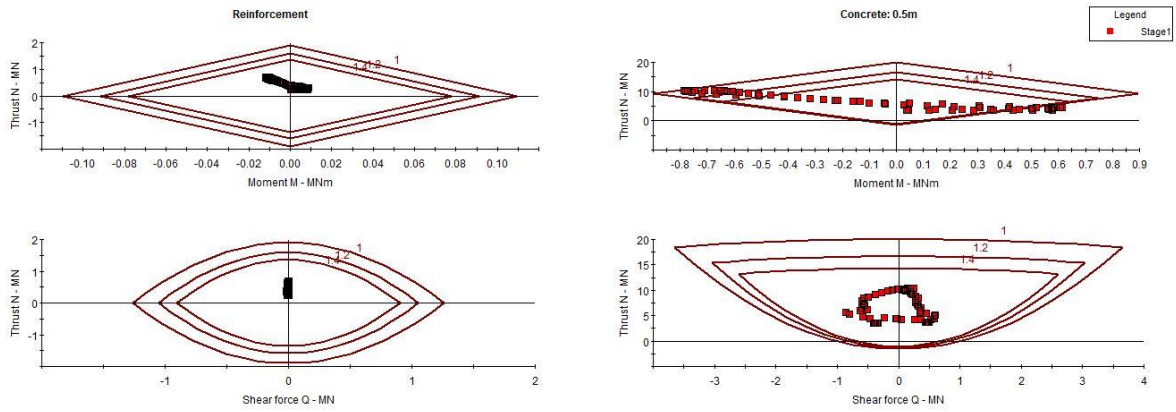


Figure 6-20 Support capacity plot for chainage 5+000 m (minimum values) with obtained factor of safety.

As suggested by the above three conditions of rock mass properties in the chainage 5+000 m, it is concluded that the displacements around the tunnel periphery increases with reduction in the strength of surrounding rock mass. The higher value of rock mass suggests the lesser requirement of the support for the stability against the stress and displacement.

7 DISSCUSION

The analyzed three sections of the tunnel lies in varying geological conditions and locations showed the varying stability as well. The need of support to reduce the deformation on each section was different as well. The approach was made to understand the behavior of tunnel stability with varying geological conditions which may be encountered during the excavation process even peculiar to the one suggested by actual condition.

Chainage 1+900 m

The chainage consists of gneiss rock type. The rock mass parameters used for this section particularly suggest the strong and self-supporting nature of the rock mass. Very minimal total displacement of 5 mm only was obtained around the tunnel periphery during the numerical analysis. The deformation was only 0.1% of total tunnel span. The support provided to this section was using the Rock Class I according to the Detail Geological Report (Appendix 3) of the tunnel and the displacement was reduced by only single millimeter even after the analysis as well. As the support capacity plot (Figure 7-4) gives the plot of applied thickness of concrete lying within factor of safety 1.4, the provided support is considered adequate to overcome the further instability. Although being the section with highest overburden height, no any signs of squeezing was seen while keeping the mean data value set Table 7-1. The comparisons of maximum total displacement values according to the changing rock mass parameters are tabulated below.

Table 7-1 Total displacement values of different data set along with displacement percentage of chainage 1+900 m.

	Minimum values		Mean values	
	Displacement (mm)	%	Displacement (mm)	%
Before Support	17.3	0.38	5	0.1
After Support	15	0.33	4	0.09

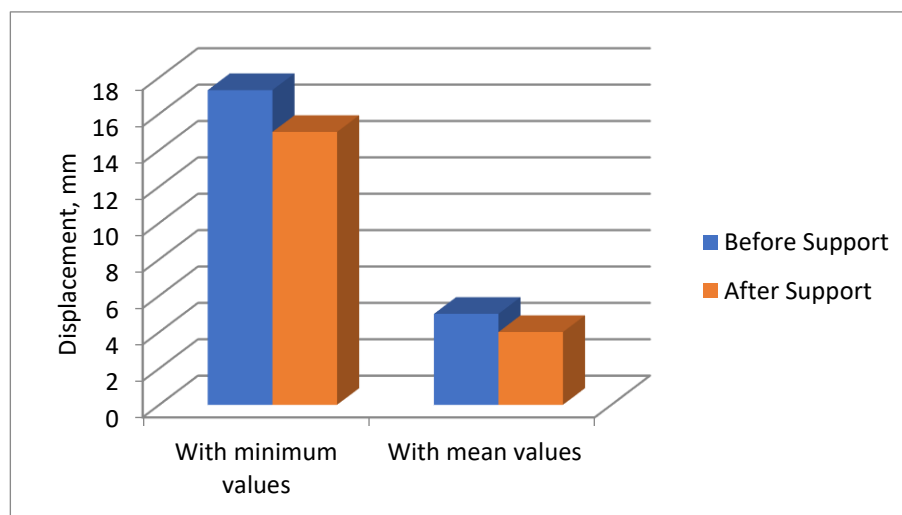


Figure 7-1 Comparisons of maximum total displacement values according to the changing rock mass parameters at chainage 1+900 m.

Chainage 4+400 m

The chainage consists of siliceous phyllite rock type. The rock mass parameters used for this section particularly suggest the weak nature of the rock mass. Total displacement of 36 mm was obtained around the tunnel periphery during the numerical analysis. The deformation was only 0.8% of total tunnel span. The support provided to this section was using the Rock Class IV according to the Detail Geological Report (Appendix 3) but as the thickness of concrete was inadequate, the thickness of concrete was increased up to 30 cm. As the support capacity plot (Figure 7-4) gives the plot of applied thickness of concrete lying within factor of safety 1.4, the provided support is considered adequate to overcome the further instability. The total displacement reduced significantly after the analysis as well. The comparisons of maximum total displacement values according to the changing rock mass parameters are tabulated below.

Table 7-2 Total displacement values of different data set along with displacement percentage of chainage 4+400 m.

	Minimum values		Mean values		Maximum values	
	Displacement (mm)	%	Displacement (mm)	%	Displacement (mm)	%
Before	101.5	2.26	36	0.80	24	0.53
After	84	1.87	19	0.42	17	0.38

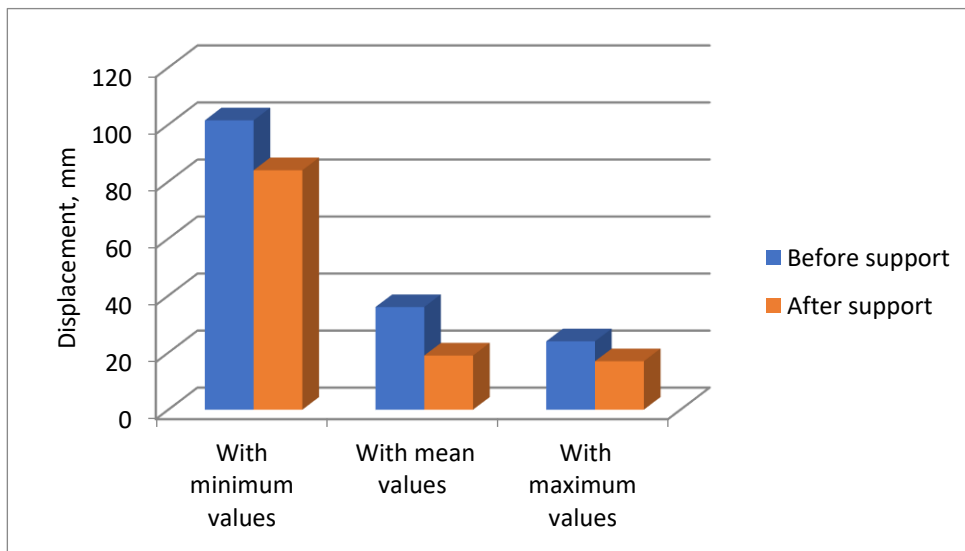


Figure 7-2 Comparisons of maximum total displacement values according to the changing rock mass parameters at chainage 4+400 m.

Chainage 5+000 m

The chainage consists of siliceous phyllite rock type. The rock mass parameters used for this section particularly suggest the weak nature of the rock mass. Total displacement of 11 mm was obtained around the tunnel periphery during the numerical analysis. The deformation was only 0.8% of total tunnel span. The support provided to this section was using the Rock Class IV according to the Detail Geological Report (Appendix 3). As the support capacity plot

(Figure 7-4) gives the plot of applied thickness of concrete lying within factor of safety 1.4, the provided support is considered adequate to overcome the further instability. The total displacement reduced significantly after the analysis as well. The comparisons of maximum total displacement values according to the changing rock mass parameters are tabulated below.

Table 7-3 Total displacement values of different data set along with displacement percentage of chainage 5+000 m.

	Minimum values		Mean values		Maximum values	
	Displacement (mm)	%	Displacement (mm)	%	Displacement (mm)	%
Before	26	0.58	11	0.24	7.5	0.17
After	19.6	0.44	9.6	0.21	8.5	0.19

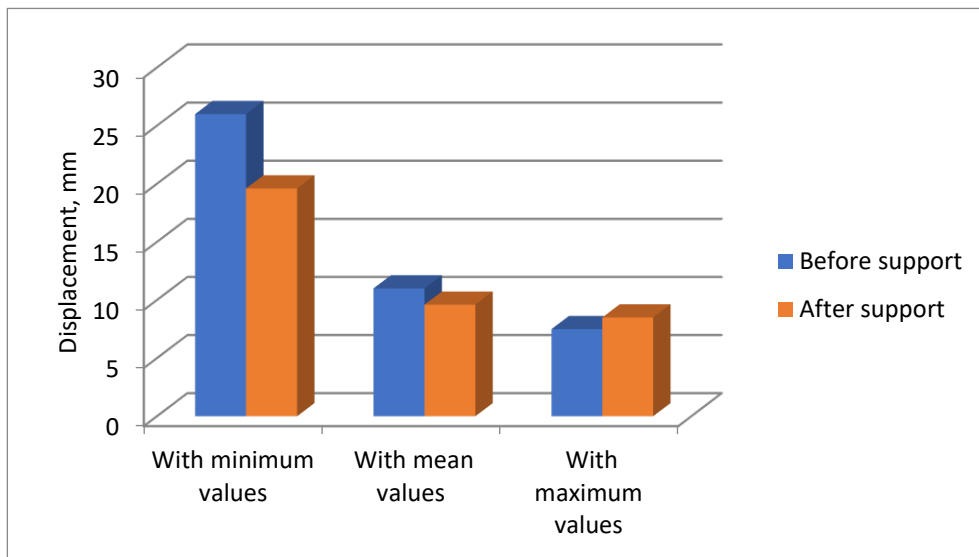


Figure 7-3 Comparisons of maximum total displacement values according to the changing rock mass parameters at chainage 5+000 m.

The thickness of lining of concrete required was different at different section according to the displacement occurring around the tunnel periphery. The comparably weaker section 4+400 m and 5+000 m required more thickness of concrete to obtain the factor of safety of 1.4. The Table 7-4 compares the thickness of concrete at different sections.

Table 7-4 Comparisons of required thickness of concrete to obtained factor of safety 1.4 at different chainages.

Chainage	Required thickness of concrete lining (cm)		
	With minimum values	With mean values	With maximum values
1+900 m	15	5	-
4+400 m	50	30	15
5+000 m	50	10	5

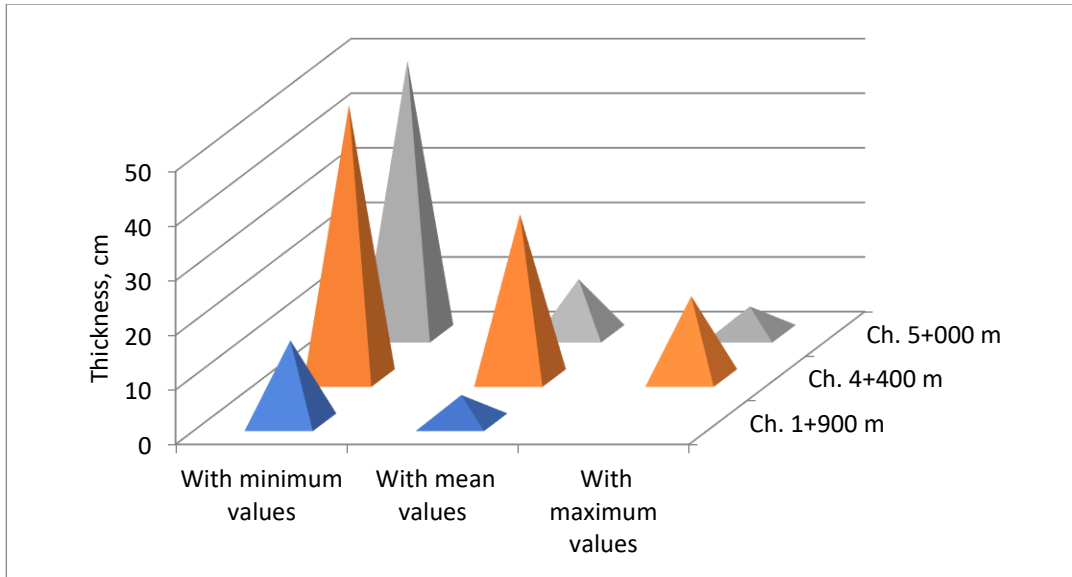


Figure 7-4 Comparisons of required thickness of concrete to obtained factor of safety 1.4 at different chainages.

The tunnel seems to need large quantity of support in all three sections if encountered with poor rock mass than predicted. The section 1+900 m requires least concrete thickness compared to other, because of presence of self-supporting intact gneiss rock with good rock mass parameters despite this section having highest overburden. This section if encountered with mean value of rock mass parameter requires comparatively very less concrete (5 cm). The other two sections require more support (nearly 50 cm) concrete if encountered with minimum values of rock mass parameters because these sections lie in the poor rock mass of phyllite rock. The section 4+400 m requires more support if encountered with mean values rock mass than other section 5+500 m with similar rock type. This is because of greater overburden in 4+400 m than that of 5+500 m which has comparatively lesser overburden value.

The possibilities of support requirement (minimum, mean and maximum) were analyzed at whole tunnel section according to the geological cross-section of the tunnel alignment of the project as shown by symbol “arrow” in Figure 4-6 and Figure 5-2

Table 7-5 Possible support requirement at different section of tunnel alignment.

	Ch.0+000 m to 0+830 m	Ch.0+830 m to 2+500 m	Ch.2+500 m to 4+200 m	Ch.4+200 m to 5+100 m	Ch.5+100 m to 5+800 m
Rock Type	Gneiss	Gneiss	Gneiss	Phyllite	Phyllite
Overburden	73 m – 370 m	364 m – 581 m	227 m – 490 m	305 m – 511m	25 m – 305 m
Possibility of rock	Minimum rock mass	Mean rock mass values	Minimum rock mass	Mean rock mass values	Minimum rock mass

mass and support required	values (15 cm concrete)	(5 cm concrete)	values (15 cm concrete)	(30 cm concrete)	values (50 cm concrete)
Percent of tunnel length	14.31%	28.79%	29.31%	15.52%	12.07%

The headrace tunnel section 0+000 m to 0+830 m may require more support as this section is predicted to have comparatively less strong rock mass. The overburden height ranges from 70 to 370 m. The surface weathering effect may reach the tunnel and seepage can be a major problem due to less overburden. The presence of sheared rock mass at chainage 0+800 m may have caused the surrounding rocks weak as well. The section is supposed to require support of 15 cm concrete.

The headrace tunnel section 0+830 m to 2+500 m is supposed to require very less support (5 cm concrete). This section consists of gneiss rock mass which will be intact in nature. The overburden height ranges from 409 to 581 m. Seepage and surface weathering will have no effect in this section. Only single sheared band is present at chainage 1+700 m and absence of any other weakness zones also suggests the stability of this section.

The headrace tunnel section 2+500 m to 4+200 may require more support as this section of many sheared bands and weakness zones. The overburden height ranges from 227 m to 490 m which also indicates the minor seepage possible as most of the extension of tunnel lies at around only 227 m below the surface.

The penstock tunnel section 4+200 m to 5+100 m may require average support (30 cm concrete). This section will have poor rock, squeezing is likely as rock condition is worst. The requirement of higher support is due to presence of higher overburden in loose rock mass. The overburden height ranges from 305 m to 511 m.

The penstock tunnel section 5+100 m to 5+200 m is supposed to require heavy support due to presence of very weak phyllite rock type and less overburden height of 25 m to 305 m. The surface weathering and seepage is predicted to be high and deep to the tunnel alignment causing heavy support requirement.

The support requirement as suggested by design report of the project suggest similar or quite higher than the one proposed by the numerical modeling. The requirement of concrete at first section 0+000 m – 0+830 m suggest 15 cm concrete which is similar to this study analysis. The section 0+830 m – 0+2500 m requires 5 cm concrete whereas the projects report suggests concrete up to 15 cm. The other section requires 15 cm concrete according to numerical modeling in this study whereas the project reports suggest 5 -15 cm concrete in various sections. This difference is due to more detailed approach of empirical study in project report whereas this study comprises representative sections only.

8 CONCLUSION AND RECOMMENDATION

The headrace tunnel and penstock tunnel section analyzed at different chainage have different geological conditions. The adequacy of the support provided for those chainages during design using Q-System was checked and was found to be less in multiple locations. The presence of varying rock mass properties was included in the study using varying values less and more than suggested by surface engineering geological mapping.

8.1 Conclusion

The presence of highly weathered, fractured and jointed rock mass creates the unpredictability of the presence of rock properties as suggested by surface study. This may cause the increase in time and cost of the project lying in surprising geological condition like in Nepal Himalaya. The estimation of the support required to stable the weak sections of underground water way system needs intense care and knowledge for the engineers.

The analysis of the waterways system of the headrace and penstock tunnel suggests the moderate stability of those tunnels. An approach was made to understand the stability of tunnel and safety provided by the support installed using different data value sets. The tectonic stress has been taken 5 MPa in NS orientation. Following conclusions were drawn from the study:

- The project reports, literature and books can be very essential tools for the planning and design of the waterway system. Different lab testing data, drilling and field study reports are important documents before and during construction and it also helps in further analysis.
- The orientation of joint sets with respect to alignment of waterways system, size, method and shape of excavation plays an important role in stability of underground openings. Valley slopes, overburden should be considered with equal importance during design period.
- The rock mass parameters play important role in stability. The choice of the correct parameters during analysis should be done using correct number of test locations, accuracy of the field and laboratory so that they don't mislead the designer.
- The condition of underground rock mass may not be similar to the predicted one from surface study, so it is better to analyze the best and worst case scenario as suggested by this study.
- The use of the Q system (Grimstad and Barton 1993) gives a primary knowledge of support required based on the input parameters. It helps in cost estimation and time period of construction during very first phase of the tunnel construction.
- The alternative design studies help in renewing the ideas and generating the facts for increasing the stability of the designed alignment for waterway system. The alternative analysis of penstock tunnel has helped to overcome the stability problems that might have occurred and also to think from new dimension by introducing underground powerhouse in this study as well. However, the original design is also concluded to be safe in terms of stability, based on numerical modelling done because the original design has less overburden and almost similar

rock mass condition compared to alternative 2. Moreover, alternative 2 is considered to be optimized in terms of stability and economy.

- The Phase2 software is a necessary and modern tool in designing underground openings and slopes. In this study, it was used to analyze total displacement and stress conditions in varying sections with varying rock mass parameters value. It has been used to estimate the support, to be provided in order to obtain the desired factor of safety.
- The requirement of support at different tunnel can be predicted using the numerical modeling. This helps to define the project in terms of cost and time in early phase before excavation. The requirement of support to that of predicted are found quite different from the numerical modeling analysis. Generally, the support required are found to be similar or less from the analysis in the numerical models done compared to that of proposed by using empirical approach.

8.2 Recommendation

As being the study for academic purpose there could be many limitations in this study, the following recommendations are made for further studies:

- In-situ stress measurement should be done with proper instrumentation for obtaining accurate values.
- Groundwater has important role in stability. It is better to use the groundwater effect in further analysis.
- The detail rock mass jointing properties should be used in the numerical analysis which gives more realistic stability of the openings.
- The presence of pointed corner has given higher yielding of tunnel sections in crown and wall, this could be decreased with using smoother corners or circular shape which will help in reducing the support required for the tunnel.
- The stability analysis of the surge shaft and any other sections of original design was not carried in this study (except chainage 1+900).
- (Hoek and Marinos 2000) and (Panthi and Shrestha 2018) approach can also be used to carry out squeezing analysis in further study.

References

- Authority, N. E. (1997). "Upgraded Feasibility Study." Chameliya Hydroelectric Project, Nepal: 1-98.
- Authority, N. E. (2000). "Completion report for headrace tunnel and surge tank." Modi Khola Hydroelectric Project, Parbat, Nepal.
- Barton, N. (1995). The influence of joint properties in modelling jointed rock masses. 8th ISRM Congress, International Society for Rock Mechanics and Rock Engineering.
- Barton, N., et al. (1974). "Engineering classification of rock masses for the design of tunnel support." Rock mechanics **6**(4): 189-236.
- Basnet, C. B. (2013). Evaluation on the Squeezing Phenomenon at the Headrace Tunnel of Chameliya Hydroelectric Project, Nepal, Institutt for geologi og bergteknikk.
- Basnet, C. B. (2018). "Applicability of Unlined/Shotcrete Lined Pressure Tunnels for Hydropower Projects in the Himalaya."
- Basnet, C. B. and K. K. Panthi (2017). "3D in-Situ Stress Model of Upper Tamakoshi Hydroelectric Project Area." Hydro Nepal: Journal of Water, Energy and Environment **21**: 34-41.
- Benson, R. (1989). "Design of unlined and lined pressure tunnels." Tunnelling and Underground Space Technology **4**(2): 155-170.
- Bieniawski, Z. (1993). Classification of rock masses for engineering: the RMR system and future trends. Rock Testing and Site Characterization, Elsevier: 553-573.
- Broch, E. (1984). "Development of Unlined Pressure Shafts And Tunnels in Norway. Hydropower tunnelling, Publication No.3. Norwegian Soil and Rock Engineering Association."
- Broch, E. (2013). "Underground hydropower projects-Lessons learned in home country and from projects abroad." Norwegian Tunneling Society: 11-19.

Carranza-Torres, C. and C. Fairhurst (2000). "Application of the convergence-confinement method of tunnel design to rock masses that satisfy the Hoek-Brown failure criterion." Tunnelling and Underground Space Technology **15**(2): 187-213.

Chern, J., et al. (1998). An empirical safety criterion for tunnel construction. Proceedings of the regional symposium on sedimentary rock engineering, Taipei, Taiwan.

Edvardsson, S. and E. Broch (2002). "Underground powerhouses and high pressure tunnels. Hydropower Development No. 14, Dept." Hydraulic and Environmental Engineering, NTNU, Trondheim.

Encalada, J. (2018). "Tunneling aspects of the waterway system and stability assessment of the powerhouse cavern for the Minas-San Francisco HP."

FAMA, M. E. D. (1993). Numerical modeling of yield zones in weak rock. Analysis and design methods, Elsevier: 49-75.

Freeze, R. and J. A. Cherry (1979). "Groundwater. Prentice-Hall." Inc., Englewood Cliffs, NJ.

Goel, R. (1994). "Correlations for predicting support pressures and closures in tunnels." Nagpur University, Nagpur, India.

Goodman, R. E. (1989). Introduction to rock mechanics, Wiley New York.

Grimstad, E. and N. Barton (1993). "Updating of the q-system for NMT. I proceedings: International Symposium on Sprayed Concrete." Modern Use of Wet Mix Sprayed Concrete for Underground Support, Fagernes, Norwegian Concrete Association, Oslo.

Grimstad, E. and N. Barton (1993). Updating of the Q-system for NMT. Int. Symposium on Sprayed Concrete-Modern use of wet mix sprayed concrete for underground support, Fagernes (Editors Kompen, Opshall and Berg, Norwegian Concrete Association, Oslo).

Halseth, R. T. (2018). Stability assesment of the headrace tunnel system at Brattset Hydropower Project, NTNU.

HH, H. H. (2001). "Construction report, Modi Khola hydroelectric project, Nepal."

Hoek, E. (1990). Estimating Mohr-Coulomb friction and cohesion values from the Hoek-Brown failure criterion. Intl. J. Rock Mech. & Mining Sci. & Geomechanics Abstracts.

Hoek, E. (2007). "Practical rock engineering. 2007." Online. ed. Rocscience.

Hoek, E. and E. Brown (1980). "Underground excavations in rock. Inst." Mining and Metallurgy, London: 156.

Hoek, E. and E. T. Brown (1980). Underground excavations in rock, CRC Press.

Hoek, E. and E. T. Brown (1997). "Practical estimates of rock mass strength." International journal of rock mechanics and mining sciences **34**(8): 1165-1186.

Hoek, E., et al. (2002). "Hoek-Brown failure criterion-2002 edition." Proceedings of NARMS-Tac **1**(1): 267-273.

Hoek, E. and J. A. Hudson (1993). Comprehensive rock engineering: principles, practice & projects. 5. Surface and underground case histories, Pergamon Press.

Hoek, E. and P. Marinos (2000). "Predicting tunnel squeezing problems in weak heterogeneous rock masses." Tunnels and tunnelling international **32**(11): 45-51.

Hydro-Consult (2016). "Geology design project report- SKDKHEP."

ICGS (2017). "Geotechnical Investigation (Drilling) Final Report for SKDKHEP."

ISRM (1975b). "Commission report on terminology."

ISRM, I. (1978). "Suggested methods for the quantitative description of discontinuities in rock masses." Commission on the standardization of Laboratory and Field Tests in Rock Mechanics, ISRM.

Jethwa, J., et al. (1984). 28 Estimation of ultimate rock pressure for tunnel linings under squeezing rock conditions—a new approach. Design and Performance of Underground Excavations: ISRM Symposium—Cambridge, UK, 3–6 September 1984, Thomas Telford Publishing.

Kaiser, P. K., et al. (1986). "Evaluation of rock classifications at BC Rail tumbler ridge tunnels." Rock mechanics and rock engineering **19**(4): 205-234.

Karlsruud, K. and V. Kvelsvik (2002). Control of water leakage when tunnelling under urban areas in the Oslo region. Planning and Engineering for the Cities of Tomorrow. Second International Conference on Soil Structure Interaction in Urban Civil Engineering Swiss Federal Inst of Technology, Zurich; European Commission COST; Swiss Federal Office for Education and Sciences; Swiss Society for Soil and Rock Mechanics; Norwegian Geotechnical Inst; CDM Consult AG; Mott MacDonald; SKANSKA; Bilfinger Berger; Alpine.

Kassana, L. and B. Nilsen (2003). Analysis of water leakage at Lower Kihansi Hydropower Plant System in Tanzania, East Africa. Waterpower XII–HCI Publications. Proceedings of the Waterpower XIII Conference.

KC, R. K. (2016). Assessment on the potential use of shotcrete lined high pressure tunnel at Rasuwagadhi hydroelectric project, Nepal, NTNU

Li, C. (2015). "Applied rock mechanics." Trondheim: Norwegian University of Science and Technology, NTNU.

NEA, N. E. A. (1992). "Detailed feasibility study. Kaligandaki “A” hydroelectric project, volume I – main report and volume III – appendices."

Neupane, B. and K. K. Panthi (2012). "Evaluation on the potential use of shotcrete lined high pressure tunnel at Upper Tamakoshi Hydroelectric Project."

Nilsen, B. and E. Broch (2012). "Ingeniørgeologi–Berg." Lecture notes-Videregående kurs, Norwegian University of.

Nilsen, B. and A. Palmström (2000). "Engineering geology and rock engineering, handbook no. 2." Norwegian Group for Rock Mechanics (NMG), Norway.

Nilsen, B. and A. Thidemann (1993). "Rock Engineering, Hydropower Development Vol. 9." Norwegian Institute of Technology (NTH), 156p.

Palmström, A. and R. Singh (2001). "The deformation modulus of rock masses—comparisons between in situ tests and indirect estimates." Tunnelling and Underground Space Technology **16**(2): 115-131.

Panet, M. (1996). "Two case histories of tunnels through squeezing rocks." Rock mechanics and rock engineering **29**(3): 155-164.

Panthi, K. (2012). Probabilistic Approach In Assessing Tunnel Squeezing-a Discussion Based On Tunnel Projects From Nepal Himalaya. 46th US Rock Mechanics/Geomechanics Symposium, American Rock Mechanics Association.

Panthi, K. and B. Nilsen (2005). Significance of grouting for controlling leakage in water tunnels: A case from Nepal. Proceedings of ITA-AITES 2005 world tunnelling congress and 31st ITA General Assembly, Istanbul, Turkey.

Panthi, K. K. (2006). "Analysis of engineering geological uncertainties related to tunnelling in Himalayan rock mass conditions."

Panthi, K. K. (2012). "Evaluation of rock bursting phenomena in a tunnel in the Himalayas." Bulletin of Engineering Geology and the Environment **71**(4): 761-769.

Panthi, K. K. (2014). "Norwegian design principle for high pressure tunnels and shafts: its applicability in the Himalaya." Hydro Nepal: Journal of Water, Energy and Environment **14**: 36-40.

Panthi, K. K. (2017). "Engineering Geological Uncertainties Related to Tunneling. Lecture Notes."

Panthi, K. K. and B. Nilsen (2008). Uncertainty and risk assessment of leakage in water tunnels-a case from Nepal Himalaya. Proceedings: World Tunnel Congress 2008, Central Board of Irrigation and Power New Delhi.

Panthi, K. K. and P. K. Shrestha (2018). "Estimating Tunnel Strain in the Weak and Schistose Rock Mass Influenced by Stress Anisotropy: An Evaluation Based on Three Tunnel Cases from Nepal." Rock mechanics and rock engineering **51**(6): 1823-1838.

Paudel, T., et al. (1998). "Construction phase engineering geological study in Modi Khola hydroelectric project, Parbat district, western Nepal." Jour. Nepal Geol. Soc **18**: 343-355.

Selmer-Olsen, R. (1969). Experience with unlined pressure shafts in Norway. Proc. Int. Symposium on large permanent underground openings, Oslo.

Shrestha, G. L. (2006). "Stress induced problems in Himalayan tunnels with special reference to squeezing."

Shrestha, P. K. (2014). "Stability of tunnels subject to plastic deformation-a contribution based on the cases from the Nepal himalaya ".

Singh, B., et al. (1992). "Correlation between observed support pressure and rock mass quality." Tunnelling and Underground Space Technology 7(1): 59-74.

Singh, T. D. and B. Singh (2006). Elsevier Geo-Engineering Book 5: Tunnelling In Weak Rocks, Elsevier.

Sunuwar, S. C. (2011). "Faults and shear zones: A geological challenges in Hydropower development of Nepal, Proceedings of World Tunnelling Congress, Helsinki, Finland, 2011, pp. 406."

Thapa, B. (2018). "Optimization and Stability Analysis of Waterway System and Underground Powerhouse Cavern for Himchuli Dordi HPP, Nepal."

Ulusay, R. and J. Hudson (2012). Suggested methods for rock failure criteria: general introduction. The ISRM Suggested Methods for Rock Characterization, Testing and Monitoring: 2007-2014, Springer: 223-223.

Vlachopoulos, N. and M. Diederichs (2009). "Improved longitudinal displacement profiles for convergence confinement analysis of deep tunnels." Rock mechanics and rock engineering 42(2): 131-146.

WEPA (2019). "state of water resources Nepal." from <http://www.wepa-db.net/policies/state/nepal/state.htm>.

Appendix 1

Salient features

The salient features of the project are presented below:

1 Project Location	
Latitude	27°21'53"N to 27°25'15"N
Longitude	86°37'35"E to 86°41'15"E
Development Region	Eastern Development Region
Zone	Sagarmatha
District	Solukhumbu
Intake Site	Tinla and Kagel VDC
Powerhouse Site	Panchan VDC
2 General	
Name of River	Solu Khola
Type of Scheme	Run-of-river
Gross Head	613.2 m
Net Head	598.09 m
Design Discharge	17.05 m ³ /sec
Installed Capacity	86.0 MW
Dry Season Energy	101.27 GWh
Wet Season Energy	419.94 GWh
Total Energy	520.20 GWh
3 Hydrology	
Catchment Area	454 km ²
Design Discharge	17.05 m ³ /sec
Design Flood Discharge (1 in 100 yr. flood)	475 m ³ /s

4 Diversion Weir	
Type of Weir	Gravity Type
Length	31.8 m
Weir Crest Level	El. 1260.50 masl
Foundation Level	El. 1253.10 masl
5 Undersluice	
No. of Openings	2 No. of 2.0 m (w) X3.0 m (h)
Invert Level	El. 1254.60 masl
Length	20.00 m
6 Trash passage	
Opening Size	1.0 m (w) X2.0 m (h)
Length	23.05 m
7 Fish Ladder	
Opening Size	1.0 m (w) X1.0 m (h)
Length	42.15 m
8 Intake Structure	
Type of Intake	Side intake
No. of Intake Openings	4 Nos. of 2.8 m (w) X 2.3 m (h)
Invert Level of Intake	El. 1257.60 masl
9 Gravel Trap	
Size	2 nos 6.15 m x 6.6 m
Bed load size to trap	5 mm
Flushing	Pipe 1.0 m dia, Length: 44 m
10 Approach Culvert	
No.	4
Size	2.20 m (w) X 2.20 m (h)

11 Settling Basin	
No of Bays	4
Inlet Transition	20.70 m
Outlet Transition	15.20 m
Dimension (L x B x H)	85.0 m x 9.5 m x 4.5 m
Nominal Size of Trapped Particle	0.15 mm
Trap Efficiency	90%
12 Headrace Box Culvert	
Length	50.0 m
Dimension (B x H)	1 nos 4.5 m x 4.5 m
13 Headrace Tunnel	
Length	4259.0 m
Type and shape	Inverted D- shape
Finished Dimension (B x H)	4.0 m x 4.25 m
14 Adit 1, Adit 2	
Length	93.93 m, 363.87 m
Type and shape	Inverted D- shape
Finished Dimension (B x H)	4.0 m x 4.25 m
15 Adit 3, Adit 4	
Length	204.64 m, 332.23 m
Type and shape	Inverted D- shape
Finished Dimension (B x H)	3.8 m x 3.8 m
16 Surge Tunnel	
Length	342.72 m
Type and shape	Inverted D- shape
Finished Dimension (B x H)	4.0 m x 4.0 m

17 Penstock Pipe	
Drop Shaft 1	224.18 m
Horizontal section 1	715.65 m
Drop Shaft 2	199.61 m
Horizontal section 2	926.94 m
Total length up to trifurcation	2085.00 m
Internal diameter and length of pipe	2.5 m for 1121 m length (pipe including 22.55 m length up to surge tunnel)
	2.25 m for 546 m length
	2.10 m for 418 m length
Thickness and grade of steel	10 mm to 44 mm, Grade 450 MPA
18 Powerhouse	
Type	Surface
Dimension(L x B x H)	54.6 m x 16.2 m x 19.45 m
Turbine setting level	El 647.30 masl
No. and Type of turbine	3 nos. Pelton Turbine (Vertical axis)
Installed capacity	86.0 MW
Generators	Three phase, Synchronous, 34.6 MVA
Speed of Turbine	600 RPM
19 Tailrace Canal	
Type	RCC Conduit
Length	75 m
20 Transmission Line	
Type	132 kV
Length	10.5 km

Power Evacuation	Proposed Tingla substation
21 Switchyard	
Size	80 m x 40 m

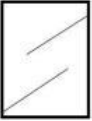
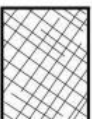




Appendix 2

STANDARD CHARTS AND FIGURES






1. Hoek and Brown Constant, m_i

Rock type	Class	Group	Texture			
			Coarse	Medium	Fine	Very fine
SEDIMENTARY	Clastic		Conglomerates (21 ± 3)	Sandstones 17 ± 4	Siltstones 7 ± 2	Claystones 4 ± 2
			Breccias (19 ± 5)		Greywackes (18 ± 3)	Shales (6 ± 2) Marls (7 ± 2)
	Non-Clastic	Carbonates	Crystalline Limestone (12 ± 3)	Sparitic Limestones (10 ± 2)	Micritic Limestones (9 ± 2)	Dolomites (9 ± 3)
		Evaporites		Gypsum 8 ± 2	Anhydrite 12 ± 2	
	Organic				Chalk 7 ± 2	
METAMORPHIC	Non Foliated		Marble 9 ± 3	Hornfels (19 ± 4) Metasandstone (19 ± 3)	Quartzites 20 ± 3	
	Slightly foliated		Migmatite (29 ± 3)	Amphibolites 26 ± 6	Gneiss 28 ± 5	
	Foliated*			Schists 12 ± 3	Phyllites (7 ± 3)	Slates 7 ± 4
IGNEOUS	Plutonic	Light	Granite 32 ± 3	Diorite 25 ± 5	Granodiorite (29 ± 3)	
		Dark	Gabbro 27 ± 3 Norite 20 ± 5	Dolerite (16 ± 5)		
	Hypabyssal		Porphyries (20 ± 5)		Diabase (15 ± 5)	Peridotite (25 ± 5)
	Volcanic	Lava	Rhyolite (25 ± 5) Andesite 25 ± 5		Dacite (25 ± 3) Basalt (25 ± 5)	
		Pyroclastic	Agglomerate (19 ± 3)	Breccia (19 ± 5)	Tuff (13 ± 5)	

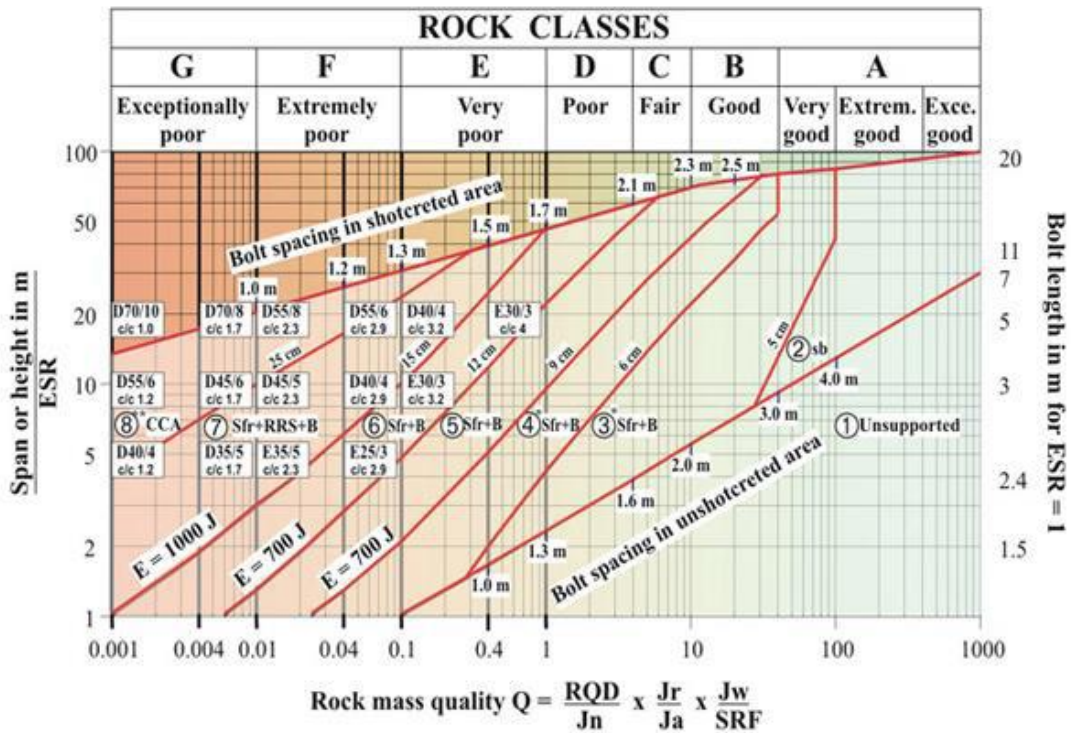
2. Geological Strength Index, GSI

<p>GEOLOGICAL STRENGTH INDEX FOR JOINTED ROCKS (Hoek and Marinos, 2000)</p> <p>From the lithology, structure and surface conditions of the discontinuities, estimate the average value of GSI. Do not try to be too precise. Quoting a range from 33 to 37 is more realistic than stating that GSI = 35. Note that the table does not apply to structurally controlled failures. Where weak planar structural planes are present in an unfavourable orientation with respect to the excavation face, these will dominate the rock mass behaviour. The shear strength of surfaces in rocks that are prone to deterioration as a result of changes in moisture content will be reduced if water is present. When working with rocks in the fair to very poor categories, a shift to the right may be made for wet conditions. Water pressure is dealt with by effective stress analysis.</p>		<p>SURFACE CONDITIONS</p> <p>VERY GOOD Very rough, fresh unweathered surfaces</p> <p>GOOD Rough, slightly weathered, iron stained surfaces</p> <p>FAIR Smooth, moderately weathered and altered surfaces</p> <p>POOR Slickensided, highly weathered surfaces with compact coatings or fillings or angular fragments</p> <p>VERY POOR Slickensided, highly weathered surfaces with soft clay coatings or fillings</p> <p>STRUCTURE DECREASING SURFACE QUALITY →</p>				
 <p>INTACT OR MASSIVE - intact rock specimens or massive in situ rock with few widely spaced discontinuities</p>	90	80	70	60	N/A	
 <p>BLOCKY - well interlocked undisturbed rock mass consisting of cubical blocks formed by three intersecting discontinuity sets</p>	80	70	60	50	40	
 <p>VERY BLOCKY- interlocked, partially disturbed mass with multi-faceted angular blocks formed by 4 or more joint sets</p>	70	60	50	40	30	
 <p>BLOCKY/DISTURBED/SEAMY - folded with angular blocks formed by many intersecting discontinuity sets. Persistence of bedding planes or schistosity</p>	60	50	40	30	20	
 <p>DISINTEGRATED - poorly interlocked, heavily broken rock mass with mixture of angular and rounded rock pieces</p>	50	40	30	20	10	
 <p>LAMINATED/SHEARED - Lack of blockiness due to close spacing of weak schistosity or shear planes</p>	N/A	N/A	30	20	10	

3. Disturbance factor, D

Appearance of rock mass	Description of rock mass	Suggested value of <i>D</i>
	<p>Excellent quality controlled blasting or excavation by Tunnel Boring Machine results in minimal disturbance to the confined rock mass surrounding a tunnel.</p>	<p><i>D</i> = 0</p>
	<p>Mechanical or hand excavation in poor quality rock masses (no blasting) results in minimal disturbance to the surrounding rock mass.</p> <p>Where squeezing problems result in significant floor heave, disturbance can be severe unless a temporary invert, as shown in the photograph, is placed.</p>	<p><i>D</i> = 0</p> <p><i>D</i> = 0.5 No invert</p>
	<p>Very poor quality blasting in a hard rock tunnel results in severe local damage, extending 2 or 3 m, in the surrounding rock mass.</p>	<p><i>D</i> = 0.8</p>
	<p>Small scale blasting in civil engineering slopes results in modest rock mass damage, particularly if controlled blasting is used as shown on the left hand side of the photograph. However, stress relief results in some disturbance.</p>	<p><i>D</i> = 0.7 Good blasting</p> <p><i>D</i> = 1.0 Poor blasting</p>
	<p>Very large open pit mine slopes suffer significant disturbance due to heavy production blasting and also due to stress relief from overburden removal.</p> <p>In some softer rocks excavation can be carried out by ripping and dozing and the degree of damage to the slopes is less.</p>	<p><i>D</i> = 1.0 Production blasting</p> <p><i>D</i> = 0.7 Mechanical excavation</p>

4. Q-system chart and various excavation support ratio categories (Grimstad and Barton 1993)



REINFORCEMENT CATEGORIES

- | | |
|---|--|
| <ul style="list-style-type: none"> 1) Unsupported 2) Spot bolting, sb 3) Systematic bolting, (and unreinforced shotcrete, 5-6 cm), B(+S) | <ul style="list-style-type: none"> 4) Fibre reinforced shotcrete and bolting, 6-9 cm, Sfr+B 5) Fibre reinforced shotcrete and bolting, 9-12 cm, Sfr+B 6) Fibre reinforced shotcrete and bolting, 12-15 cm, Sfr+B 7) Fibre reinforced shotcrete > 15 cm + reinforced ribs of shotcrete and bolting, Sfr+RRS+B 8) Cast concrete lining, CCA or Sfr+RRS+B |
|---|--|

E) Energy absorption in fibre reinforced shotcrete at 25 mm bending during plate testing

$\left[\begin{array}{l} D45/6 \\ c/c 1.7 \end{array} \right]$ = RRS with 6 reinforcement bars in double layer in 45 cm thick ribs with centre to centre (c/c) spacing 1.7 m. Each box corresponds to Q-values on the left hand side of the box. (See text for explanation)

*) Up to 10 cm in large spans

) Or **Sfr+RRS+B

5. Horizontal Compressional Stress from world stress map

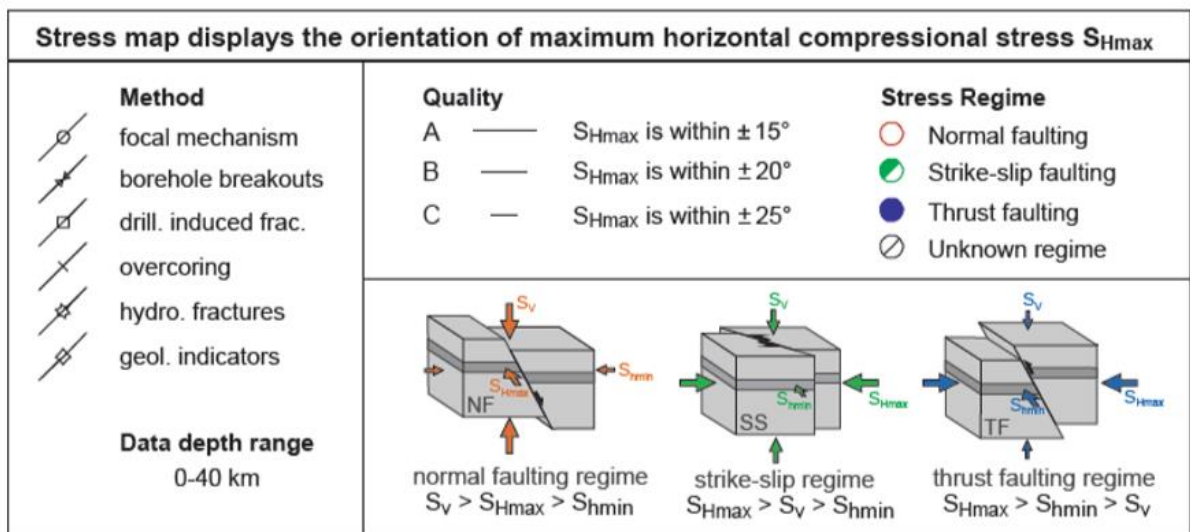
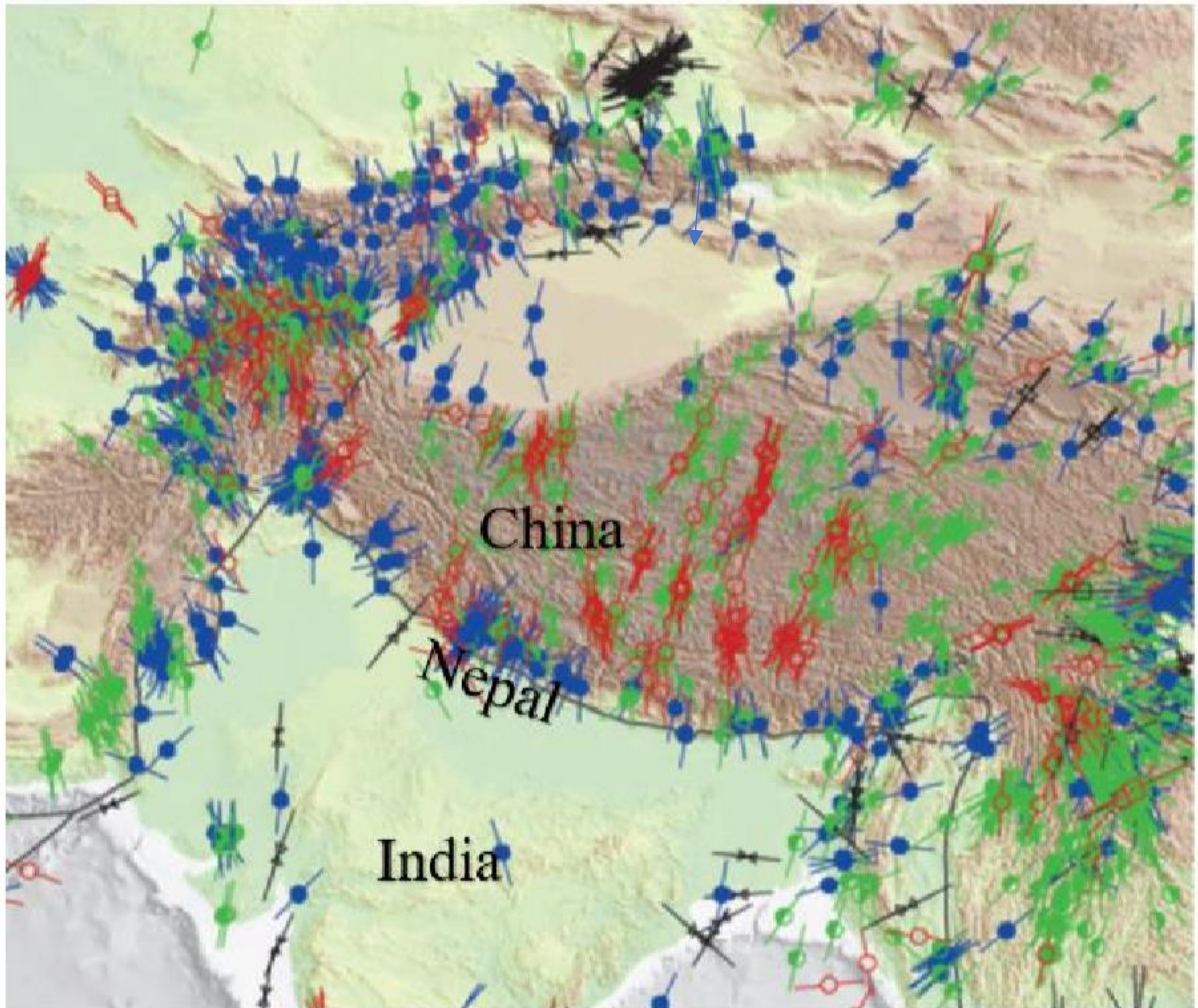


Figure i: A World stress map for the Himalayan region (WSM, 2016)

Appendix 3

Table 9- 1 Recommended Rock Support for the Headrace Tunnel (Width = 4.5m, ESR = 1.6)
(Detail Geological Report, Hydro-consult Engineering, 2016)

Rock Support Class	Q-value RMR	Support amount and type
I FAIR TO GOOD ROCK	>4 >50	Spot bolting or unsupported. Invert concrete lining.
II POOR ROCK	1 – 4 44 – 50	Bolts in pattern 1.8 m spacing. Apply 5cm plain shotcrete at crown and jointed area. Invert concrete lining.
III VERY POOR ROCK	0.5 – 1 38 – 44	Bolts in pattern 1.6 m spacing. 5cm fiber shotcrete at crown and walls. Invert concrete lining.
IV VERY POOR ROCK	0.1 – 0.5 23 – 38	Bolts in pattern 1.4 m spacing. Fiber shotcrete: Crown = 10cm, Walls = 5cm. Invert concrete lining.
V EXTREMELY POOR ROCK	0.01 – 0.1 < 23	Bolts in pattern 1.2m spacing. Fiber shotcrete: Crown = 15cm, Walls = 10cm. Spiling c/c = 40cm in crown, L = 6m. Spiling shall be inclined at 10° to 15°. L = 6m or pull +1.5m. End of spiling to be fixed with straps/re-bars and bolts. Final support: Additional 5-8cm thick fiber shotcrete only in cracked sections. Invert concrete lining.
VI EXCEPTION- ALLY POOR ROCK	<0.01	Bolts in pattern 1 x 1m spacing. Fiber shotcrete: Crown = 15cm, Wall = 15cm. i) Steel sets (ISMB175mm) in 1m spacing (If overburden less than 200m). ii) Steel sets ISMB175mm) with sliding joints and slots in shotcrete along the joints in severe squeezing sections (If overburden exceeds 200m) Spiling c/c = 20-40cm in crown, L = 6m. Spiling shall be inclined at 10° to 15°. L = 6m or pull +1.5m. End of spiling to be fixed with straps/re-bars and bolts. Final support: a) 8 - 10cm thick additional fiber shotcrete in stable with minor cracks and smooth sections. b) 20cm thick reinforced concrete lining only at walls and 10cm fiber shotcrete at crown in very rough surface with wide cracks and critical sections. c) 25cm thick reinforced concrete lining with back filling only in high overbreak sections to avoid air trapping and hydraulically smoothness. Invert concrete lining.

Table 9- 2 Rock mass parameters for different set of values generated by RocData

Ch. 1+900 m			Ch. 4+400 m			Ch. 5+500 m		
Mean Values			Mean Values			Mean Values		
Hoek-Brown Classification			Hoek-Brown Classification			Hoek-Brown Classification		
Sig ci	91	MPa	Sig ci	45	MPa	Sig ci	25	MPa
GSI	65		GSI	40		GSI	50	
mi	28		mi	7		mi	7	
D	0.5		D	0.5		D	0.5	
Hoek-Brown Criterion			Hoek-Brown Criterion			Hoek-Brown Criterion		
mb	5.28852		mb	0.402028		mb	0.647237	
s	0.00940356		s	0.000335463		s	0.00127263	
a	0.501975		a	0.511368		a	0.505734	
Failure Envelope			Failure Envelope			Failure Envelope		
Range			Range			Range		
Application	Tunnels		Application	Tunnels		Application	Tunnels	
sig3max	8.34353	MPa	sig3max	6.31735	MPa	sig3max	3.58368	MPa
Unit Weight	0.027	MN/m3	Unit Weight	0.0286	MN/m3	Unit Weight	0.0286	MN/m3
Tunnel Depth	638	m	Tunnel Depth	511	m	Tunnel Depth	285	m
Mohr-Coulomb Fit			Mohr-Coulomb Fit			Mohr-Coulomb Fit		
c	3.37944	MPa	c	0.893411	MPa	c	0.631059	MPa
phi	48.6455	degrees	phi	23.4293	degrees	phi	27.1104	degrees
Rock Mass Parameters			Rock Mass Parameters			Rock Mass Parameters		
Sig t	-0.161808	MPa	Sig t	-0.0375491	MPa	Sig t	-0.0491564	MPa
Sig c	8.74348	MPa	Sig c	0.752552	MPa	Sig c	0.858403	MPa
Sig cm	28.443	MPa	Sig cm	3.62202	MPa	Sig cm	2.6805	MPa
Em	16966.1	MPa	Em	2829.23	MPa	E m	3750	MPa
Ch. 1+900 m			Ch. 4+400 m			Ch. 5+000 m		

Minimum Values			Minimum Values			Minimum Values		
Hoek-Brown Classification			Hoek-Brown Classification			Hoek-Brown Classification		
sigci	65	MPa	sigci	25	MPa	sigci	25	MPa
GSI	45		GSI	20		GSI	20	
mi	28		mi	7		mi	7	
D	0.5		D	0.5		D	0.5	
Hoek-Brown Criterion			Hoek-Brown Criterion			Hoek-Brown Criterion		
mb	2.04042		mb	0.155111		mb	0.155111	
s	0.00065339		s	2.33E-05		s	2.33E-05	
a	0.508086		a	0.543721		a	0.543721	
Failure Envelope Range			Failure Envelope Range			Failure Envelope Range		
Application	Tunnels		Application	Tunnels		Application	Tunnels	
sig3max	7.92507	MPa	sig3max	5.84611	MPa	sig3max	3.3768	MPa
Unit Weight	0.027	MN/m3	Unit Weight	0.0286	MN/m3	Unit Weight	0.0286	MN/m3
Tunnel Depth	638	m	Tunnel Depth	511	m	Tunnel Depth	285	m
Mohr-Coulomb Fit			Mohr-Coulomb Fit			Mohr-Coulomb Fit		
c	2.04005	MPa	c	0.381116	MPa	c	0.269539	MPa
phi	38.2785	degrees	phi	13.0817	degrees	phi	15.8497	degrees
Rock Mass Parameters			Rock Mass Parameters			Rock Mass Parameters		
sigt	-0.0208146	MPa	sigt	-0.00375684	MPa	sigt	-0.0037568	MPa
sigc	1.56584	MPa	sigc	0.0757125	MPa	sigc	0.0757125	MPa
sigcm	12.0651	MPa	sigcm	0.994991	MPa	sigcm	0.994991	MPa
Em	4534.38	MPa	Em	666.855	MPa	Em	666.855	MPa

Ch. 4+400 m			Ch. 5+000 m		
Maximum Values			Maximum Values		
Hoek-Brown Classification			Hoek-Brown Classification		
sigci	45	MPa	sigci	45	MPa
GSI	40		GSI	40	
mi	7		mi	7	
D	0.5		D	0.5	
Hoek-Brown Criterion			Hoek-Brown Criterion		
mb	0.402028		mb	0.402028	
s	0.000335463		s	0.00033546	
a	0.511368		a	0.511368	
Failure Envelope			Failure Envelope		
Range			Range		
Application	Tunnels		Application	Tunnels	
sig3max	6.31735	MPa	sig3max	3.64899	MPa
Unit Weight	0.0286	MN/m3	Unit Weight	0.0286	MN/m3
Tunnel Depth	511	m	Tunnel Depth	285	m
Mohr-Coulomb Fit			Mohr-Coulomb Fit		
c	0.893411	MPa	c	0.632519	MPa
phi	23.4293	degrees	phi	27.5639	degrees
Rock Mass Parameters			Rock Mass Parameters		
sigt	-0.0375491	MPa	sigt	-0.0375491	MPa
sigc	0.752552	MPa	sigc	0.752552	MPa
sigcm	3.62202	MPa	sigcm	3.62202	MPa
Em	2829.23	MPa	Em	2829.23	MPa

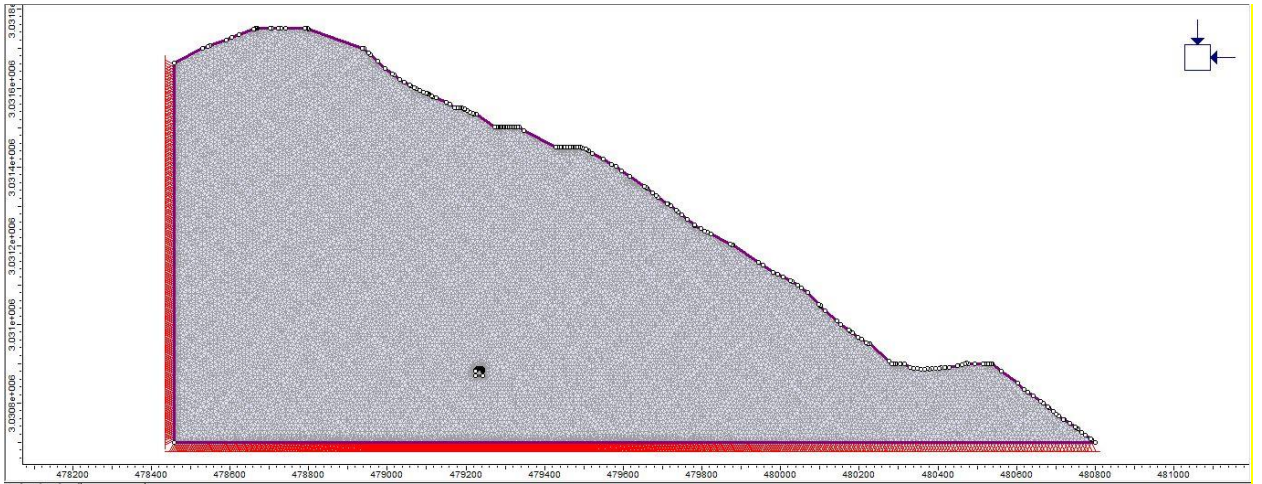


Figure ii: Finished valley slope model at chainage 1+900 m.

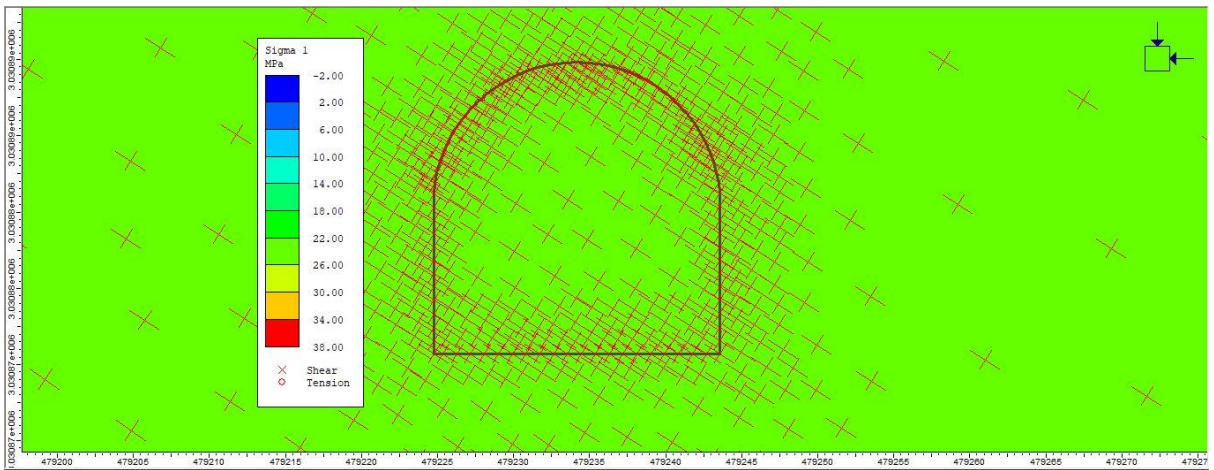


Figure iii: Inclination of major principle stress towards hill section at chainage 1+900m.

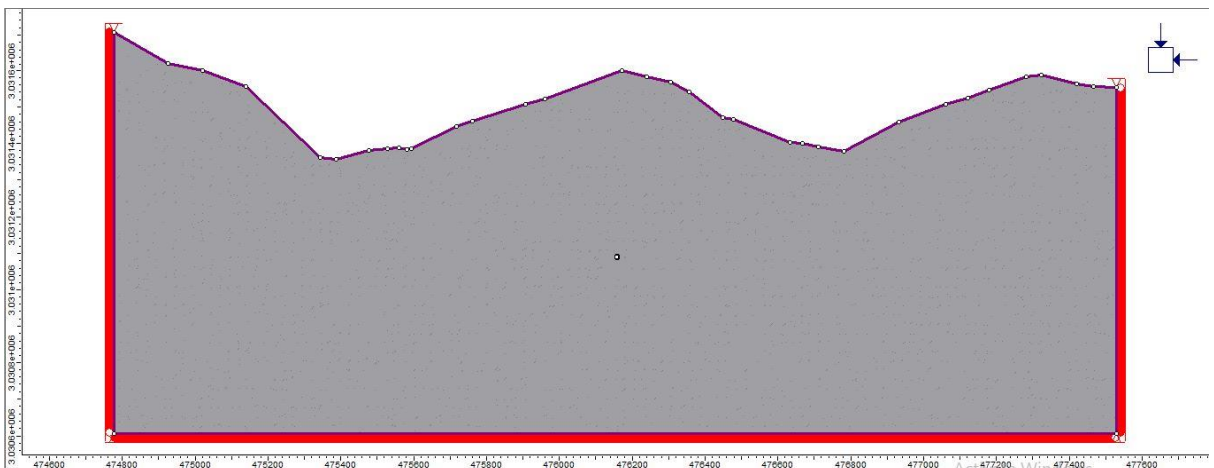


Figure iv: Finished valley slope model at chainage 4+400 m.

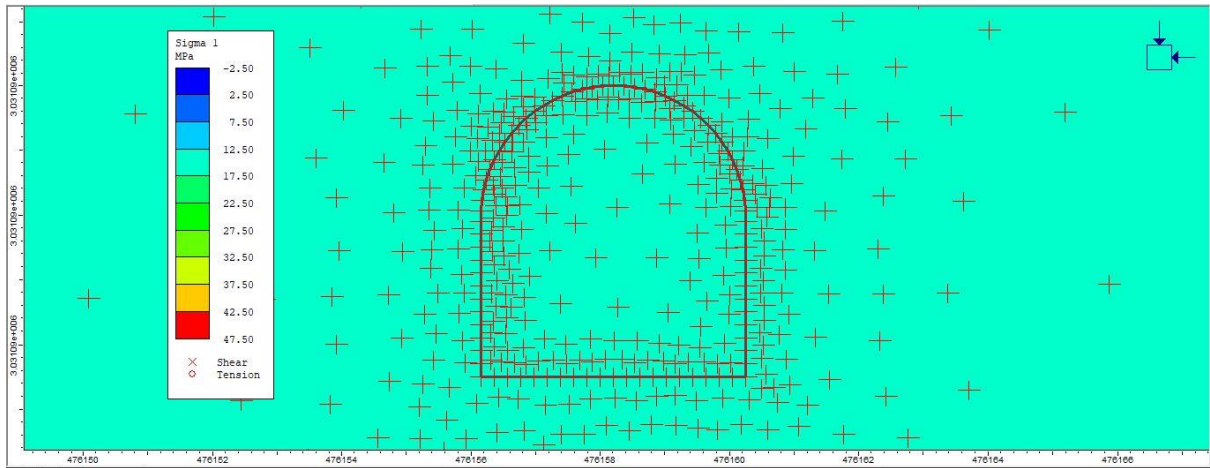


Figure v: Major principle stress distribution at chainage 4+400 m (Valley slope model).

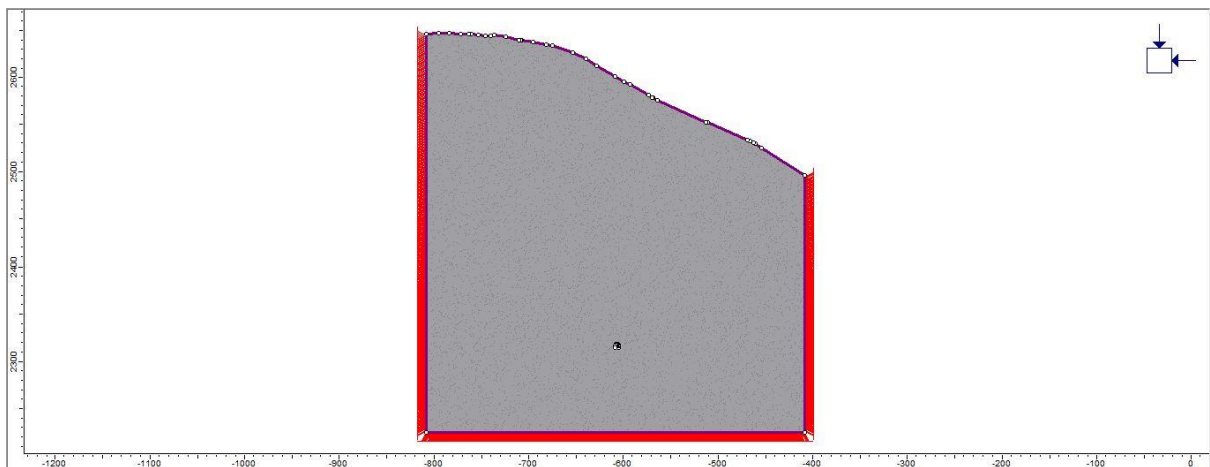


Figure vi: Finished valley slope model at chainage 5+000 m.

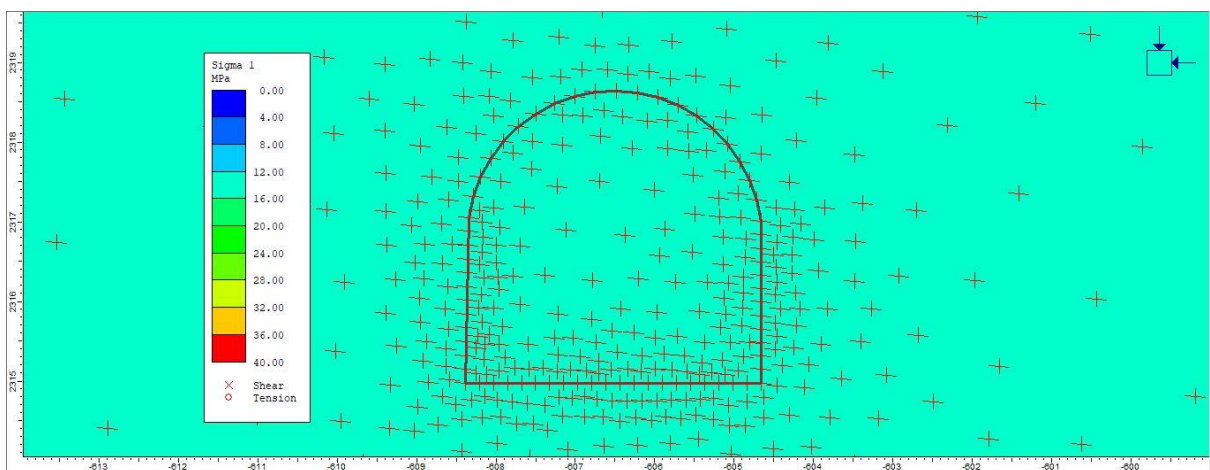


Figure vii: Major principle stress distribution at chainage 5+500 m (Valley slope model).

